Master's Thesis of Engineering

Seismic Design of Wall-Column Transfer Structure in RC Building

철근콘크리트 구조물의

벽기둥 전이구조 내진설계

February 2023

Graduate School of Enginerring

Seoul National University

Architercture and Archterctural Engineering

Ja Hyung Koo

Seismic Design of Wall-Column Transfer Structure in RC Building

Advisor: Hong Gun Park

Submitting a Master's thesis of
Architecture and Architectural Engineering

January 2023

Graduate School of Engineering
Seoul National University
Architecture and Architectural Engineering

Ja Hyung Koo

Confirming the Master's thesis written by
Ja Hyung Koo

February 2023

Chair	**Sung Gul Hong**	**(Seal)**
Vice Chair	**Hong Gun Park**	**(Seal)**
Examiner	**Cheol Ho Lee**	**(Seal)**

Abstract

Seismic design of wall-column transfer structure in RC buildings

Ja Hyung Koo
Department of Architecture and Architectural Engineering
College of Engineering
Seoul National University

In high-rise RC buildings, transfer structures are used to secure openness and public space. The existing transfer structure used a large section of members on the transfer floor. Recently, a simplified transfer structure has been developed to enhance constructability and economics. As one of the simplified transfer structures, a method where the load directly passes from the wall to the column was developed. However, there needs to be an optimized seismic design method for the wall-column transfer structure. This study aims to develop economical design methods and guidelines through research and test verification.

The capacity design for the wall-column transfer structure intends to induce the flexural ductility behavior of the wall against the earthquake load. Also, it is to prevent damage to the members on the transfer floor which can occur brittle failure in the system considering the overstrength. Therefore, the seismic

demand for the transfer structure is calculated as the nominal flexural strength of a wall based on the reinforcement. For the transfer structure to secure safety, the members (column, spandrel beam) in the transfer floor should be designed to have sufficient strength by applying an overstrength factor (Ω_0,1.25). Also, since the transfer structure is the 'D' region where stress concentration occurs, analysis and design were conducted based on the strut-and-tie model.

The cyclic loading test aims to verify the strength and deformation capacity of the seismic load by applying a cyclic lateral load under a constant compression force. For the boundary condition of the specimen, two extreme lateral support conditions that may occur on the transfer floor were considered. The one is where the wall-column frame systems are continuous and are supported by the moment resistance on the lateral force. The other case is where the wall-column transfer structure is supported by a highly rigid structure in the transfer floor.

The specimen is a reduced scale of the transfer structure in the RC apartment. The test parameters were boundary condition, re-bar ratio, reduction in width ratio, allowable lateral displacement, and application of an overstrength factor. In addition, details with transverse reinforcement and diagonal re-bar were applied to lower the stress concentration due to the vertical discontinuity.

As a result of the tests, all specimens showed ductile behavior regardless of boundary conditions. Furthermore, damage to members on the transfer floor was prevented, satisfying the intended seismic performance in capacity design. However, some damage, such as flexural cracks, occurred in the columns and spandrel beams where overstrength was not applied. Therefore, the validity of

applying the overstrength factor to the transfer floor was verified. In addition, when flexural tensile force is applied in the discontinuous section where the diagonal re-bars are placed, the design strength of the wall is not satisfied. So, a consideration for the strength degradation was reflected in the design method. In addition, the validity of the proposed re-bar details to prevent local failure of the transfer structure was also confirmed.

Based on the test results, a seismic design method that can be applied to the wall-column transfer structure was proposed. The conventional design procedure of high-rise RC structures was considered for the seismic design method. The seismic design procedure is proposed in the following order: preliminary design, design of wall, calculation design loads for capacity design, strut-tie model analysis, design transfer structure applied to overstrength factor and guidelines for re-bar details. This procedure includes the recommendations and limitations where reduction ratio, member size, material strength, and general strut-tie model for the wall-column transfer structure.

Keywords : High-rise RC building, Wall-column transfer structure, Capacity design, Strut-and-Tie model, Cyclic loading test

Student Number : 2021-27166

Contents

List of Tables

List of Figures

List of Figures

Chapter 1. Introduction

1.1 Background

Through the Pohang earthquake in Korea, significant damage was found in vertically discontinuous buildings among structural damage. In particular, relatively extensive damage occurred on the column in the piloti structure. The piloti structure is a transfer structure to secure openness and space on the lower floor. The shear failure of the column in the piloti structure was shown in Figure 1-1 below.

Figure 1-1 Shear failure of Piloti Structure

In measure to these damages, the Seismic Building Design Code (Korean Building Code) added 'Considerations for columns in piloti structure,' which were not previously included.

In addition, earthquake damage was observed non-seismic RC apartments. It can be seen that shear failure is observed, as shown in Figure 1-2, in the vertical irregular structure where the first floor is partially separated by the vertical member of the pit floor.

Figure 1-2 Shear failure of Apartment

The vulnerability of vertical irregular structures to earthquakes can also be confirmed through the 2010 Maule, Chile earthquakes. The 2010 Maule earthquake is a large earthquake with a magnitude of 8.8 and a maximum intensity of IX. The Chilean apartment structure has a structure very similar to the domestic bearing wall system in the apartment. Therefore, analyzing the 2010 Chile earthquake shows the following cases of damage to the vertical irregular structures.

Figure 1-3 Earthquake damage for geometric wall discontinuity

As shown in Figure 1-3, damage cases were mainly confirmed in the bearing wall system or pier-spandrel structure system with openings in the middle and high-rise buildings. This damage can be attributed to vertical irregularity due to changes in cross-sectional area and reinforcement.

Despite the risks caused by earthquakes of vertical irregularity, it is necessary to require openness and common space on the lower floors in the building plan. Therefore, transfer structures with large sections(thick slabs or transfer girder with large cross-sections, etc.) were generally used in high-rise RC structures that require vertical irregularity in Korea, as shown in Fig. 1-4.

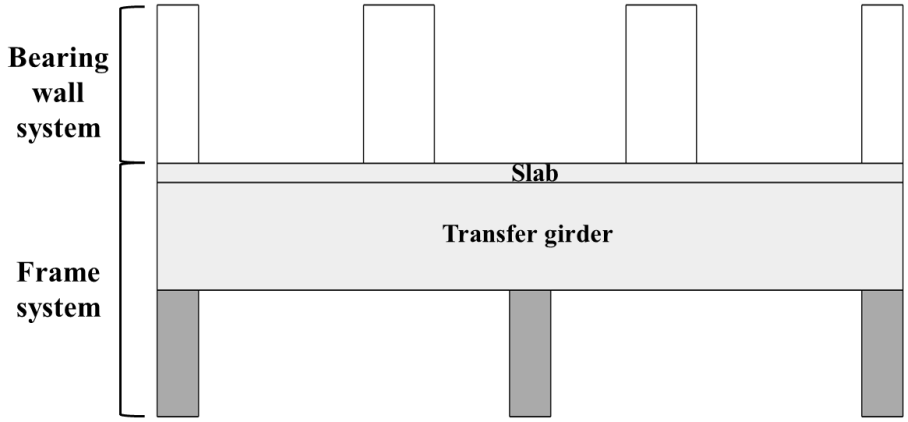

Figure 1-4 Transfer girder system

On the other hand, a method to simplify the transfer structure considering constructability and economic feasibility is being developed due to the inefficiency of the existing transfer structure. As an efficient transfer structure, a design method has been developed in which a spandrel beam with a relatively small width acts as a transfer zone while securing openness through a column with a reduced cross-section at the bottom of the wall through which the load is transferred. When such a wall-column transfer structure is used, the height of the transfer floor can be reduced, so economic efficiency and constructability can be significantly improved.

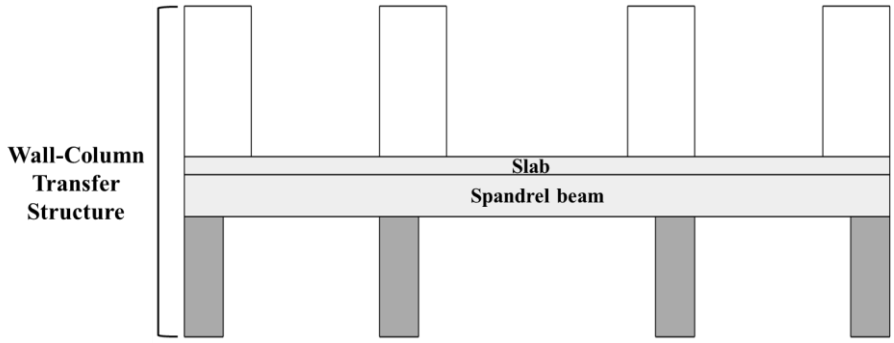

Figure 1-5 Wall-column tranfer structure

However, stress concentration and irregular load flow occur in the member of the transfer floor due to the reduction of the section in the wall-column transfer structure. As a result, local damage occurred in the previous earthquakes. Also, the increased demand for the dynamic amplification of the building in an earthquake is particularly severe in the transifer floor. If the wall-column transfer structure, as shown in Figure 1-5, is used in the RC buildings with many openings, the brittle failure of the system due to an earthquake may cause significant damages (torsional behavior, weak story, etc.) to the entire structure. Therefore, as a wall-column transfer structure, it is necessary to verify its seismic performance in the single-frame system.

According to the Seismic Building Design Code (Korean Building Code), special seismic loads are applied to vulnerable earthquake-resistant members such as transfer structures. Therefore, a bearing wall structure system such as an apartment has an overstrength factor of 2.5 applied under a special earthquake load, so the member must be designed with a very high earthquake demand and used as columns and beams with large sections. On the other hand, there is a provision that it is unnecessary to exceed the maximum load-carrying

capacity of the other seismic-force-resisting elements on which the load acts. In other words, capacity design can be applied. It is considered that economic efficiency and usability can be secured when this capacity design is used. So, this study proposes a design method for the wall-column transfer structure as a capacity design and conducts test verification. Through this study, the wall-column transfer structure serves as a transfer zone through the spandrel beam instead of the transfer girder with a large cross-section.

1.2 Scope and Objectives

This study aims to develop an economical seismic design method for wall-column transfer structures used in the transfer floor of high-rise RC structures with many openings. In the current design standards, special seismic loads are to be applied to such vulnerable earthquake-resistant members, but this requires columns and beams with large cross-sections. However, it is not necessary to exceed the maximum load capacity of the other seismic-force-resisting elements so that the capacity design can be applied. In addition, many previous tests conducted a transfer structure in which columns exist symmetrically. Therefore, the wall-column transfer structure of this study aims to verify the seismic performance of a single-frame system in transfer structure in consideration of an asymmetrical transfer structure. The purpose of this study is to propose a seismic design method for securing the economic feasibility and constructability of a wall-column transfer structure of single-frame system and to verify it.

Capacity design induces ductile behavior while preventing the collapse of building under seismic loads. Therefore, the ductile flexural behavior of the wall is induced in the wall-column transfer structure. And the members in the transfer floor, which are relatively at risk of brittle fracture, have sufficient strength by applying the overstrength factor. This study aims to develop a design method based on the strut-tie model in consideration of the significant cross-sectional change characteristics of the transfer structure.

To verify the seismic performance, a cyclic loading test is performed. The

test considers the plan and specimen size in consideration of the actual high-rise RC building. The test parameters are set according to boundary conditions, reduction in width, and whether lateral displacement is allowed. In addition, the effect of applying the overstrength factor of each member is considered based on the capacity design. Also, various re-bar (reinforcing bar) details are applied to the specimen to lower stress concentration due to cross-sectional changes in the wall-column transfer structure. Based on these Tests, the seismic design method of the wall-column transfer structure is proposed.

1.3 Outline of the Master's Thesis

The thesis is mainly comprised of three parts, establishment of design concept, verification of test, and proposal of design method, respectively.

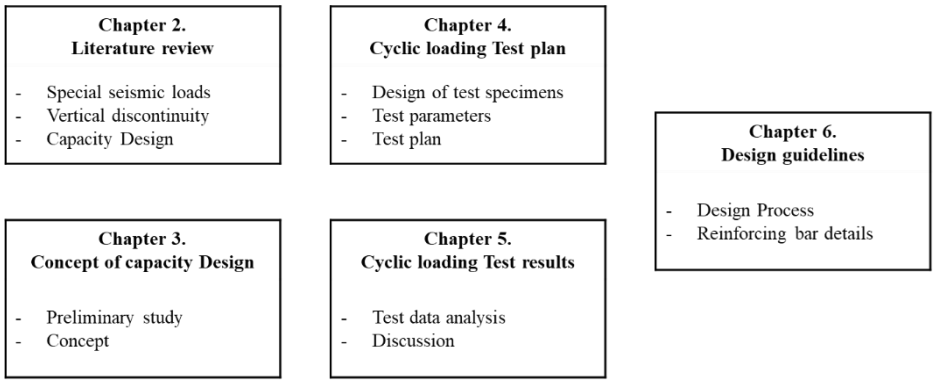

Figure 1-6 Outline of the master's thesis

Chapter 2 reviews the existing design methods and previous studies to develop the seismic design method of the transfer structure. Through this, Chapter 3 establishes the concept of the capacity design of the wall-column transfer structure based on the high-rise RC building.

The cyclic loading test is planned in Chapter 4. Based on the previous design concept, the specimen was designed by including the test parameters (failure mode, reduction in width, effect of overstrength factor, etc.). In addition, cyclic loading was planned at a constant compression force for actual seismic verification. In Chapter 5, the tests are analyzed to perform seismic performance verification. Based on the results of the specimen for each parameter, it is reviewed which method is appropriate to apply to the seismic design.

Based on the test, Chapter 6 presents a seismic design method that can be applied to the actual RC building. Considering the design process of the actual RC building, the seismic design process is shown for the wall-column transfer structure. It also presents details of the re-bars that have been effectively verified in the test.

Chapter 2. Literature Review

2.1 Review of Current Design Codes

2.1.1 KDS 41 17 00

According to KDS 41 17 00 9.8.4 of consideration for the piloti, when a piloti is used at the lower floor and a bearing wall structure is used at the upper floor, a transfer member (transfer slab, transfer girder, etc.) should be installed.

In addition, the members of the transfer floor are designed for the amplified seismic load by applying the special seismic load. Special seismic load is a load combination that should be applied to vulnerable earthquake-resistant members and the equation is as follows.

$$E_m = \Omega_0 E \pm 0.2 S_{DS} D \tag{2-1}$$

Where, Ω_0 = system Over strength factor, S_{DS} = Design spectral acceleration at short period, D = Dead load

The member appliying to this special seismic load shall be designed with a very high required strength compared to the seismic load. On the other hand, as an additional provision, it is not necessary to exceed the maximum load carrying capacity of the other seismic-force-resisting elements on which the load is applied.

Table 2-1 shows design factors of bearing wall systems commonly used in high-rise RC building.

Table 2-1 Design factor for Bearing wall systems (KDS 41 17 00, Table 6.2.1)

Seismic-force-resisiting system	Design factor			Limitations of system and height(m)		
	Response modification factor R	Ststem Over strength factor Ω_0	Displacement amplification factor C_d	Seismic Design Category A or B	Seismic Design Category C	Seismic Design Category D
Special reinforced concrete shear walls	5	2.5	5	-	-	-
ordinary reinforced concrete shear walls	4	2.5	4	-	-	60
Reinforced masonry shear walls	2.2	2.5	1.5	-	60	NP
Unreinforced masonry shear walls	1.5	2.5	1.5	-	NP	NP
Light-frame(wood) walls sheathed with wood structural panels	6	3	4	-	20	20
Light-frame (cold-formed steel) walls sheathed with wood structural panels or steel sheets	6	3	4	-	20	20

In addition, there are detailed regulations for each member(piloti, joint, etc.), which it is intended to prevent brittle failure of the transfer structure.

2.1.2 ACI 318-19 (Building Code Requirements for Structural Concrete)

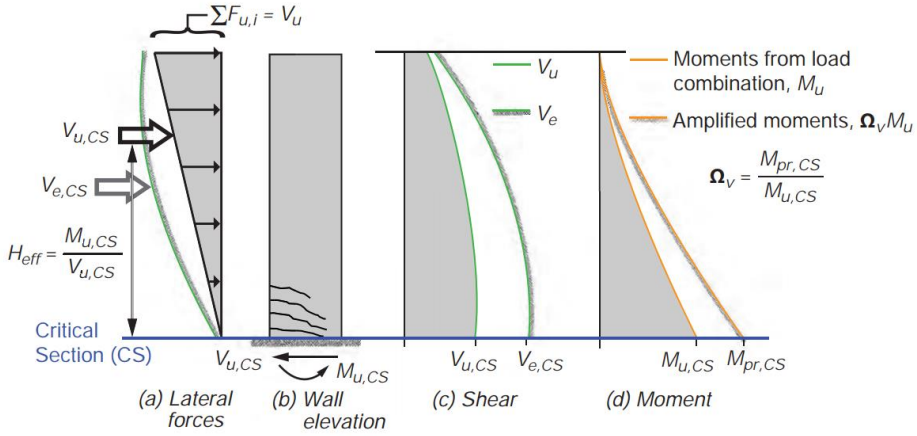

Figure 2-1 Demand with dynamic effect for slender wall

According to Design forces for special structural walls of ACI 318-19 18.10.3, h_{wcs}/l_w (the slenderness of the wall) and the material overstrength of the re-bars define Ω_v (Overstrengh factor). Based on this factor, the shear demand is calculated. This reflects the dynamic effect of an earthquake, which is the effect of amplification due to the higher-order mode of the building. In other words, this design procedure prevents shear failure of walls and induces flexural behavior in earthquakes.

Even in KDS 41 17 00 9.6, the design of the shear wall considers the shear amplification effect, but there is no detailed regulation to accurately calculate the demand force as the ACI 318-19 standard.

According to earthquake-resistant design of 23.11, it is possible to design based on the strut tie method for seismic-force-resisisting system. And,

Ω_0(overstrength factor, not less than 2.5) is applied to each member of the strut-tie model. This is to reflect the strength reduction caused by the earthquake. But, when the detailed analysis is applied, Ω_0 can be separately specified.

According to Special structural walls of ACI 318-19 18.10.1, design requirements are divided according to aspect ratio of the wall segment in the plane of the wall(h_w/l_w), aspect ratio of the horizontal cross section. These standards induce the flexural yielding of wall-pier for ductile design against earthquakes, and the strength required for the wall-pier should be limited.

Table 2-2 Governing design provisions for vertical wall segments (ACI 318-19,R18.10.1)

Clear height of vertical wall segment/length of vertical wall segment, (h_w/l_w)	Length of vertical wall segment/wall thickness (l_w/b_w)		
	(l_w/b_w) $\leq$ 2.5	2.5 $\leq$ (l_w/b_w) $\leq$ 6.0	(l_w/b_w)> 6.0
h_w/l_w < 2.0	Wall	Wall	Wall
$h_w/l_w \geq$ 2.0	Wall pier required to satisfy specified column design requirements; refer to 18.10.8.1	Wall pier required to satisfy specified column design requirements; refer to 18.10.8.1	Wall

* h_w: clear height / l_w: horizontal length / b_w: the width of the web of the wall segment

2.1.3 Eurocode 8 : Design of Structures for Earthquake Resistance

In 5.2.2.2 of Eurocode 8, vertical irregularity(setback) allowed to reduce q_0 (behaviour factor) by 20%. This reflects the decrease in ductility of the entire structure system for vertical irregularity.

This provision has a limitation in that it only specifically suggests the vertical irregularity of the overall shape of the building. So, it doesn't clearly present the local vertical discontinuity.

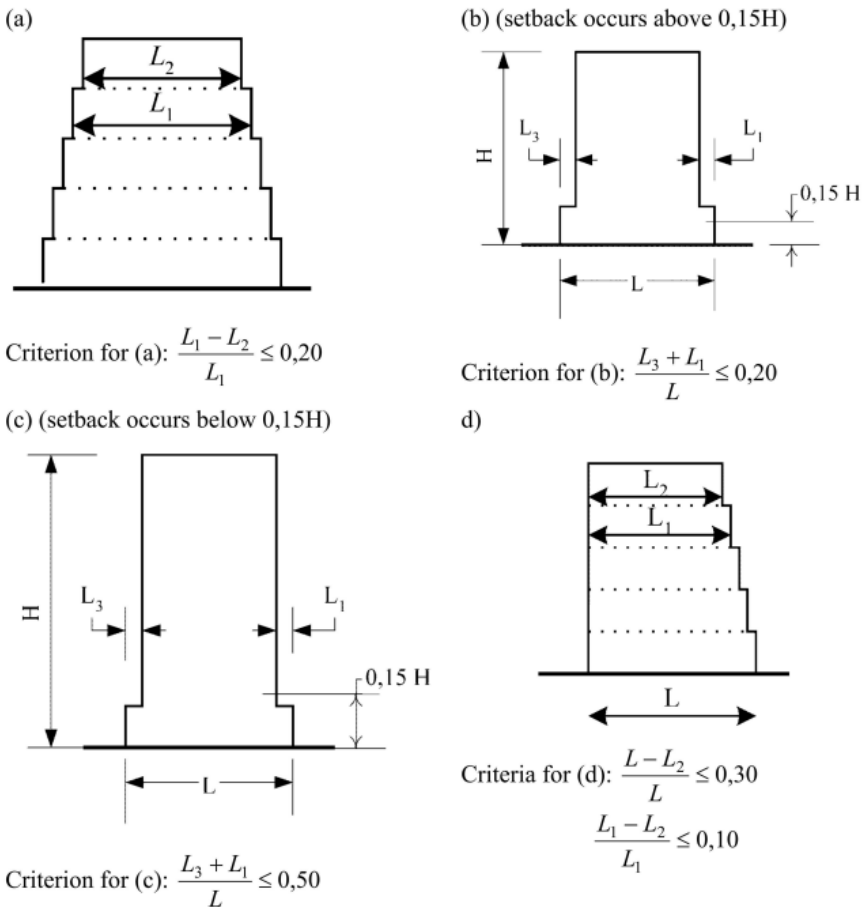

Figure 2-2 Criteria for regularity of building with setbacks

2.2 Review of research

2.2.1 NIST (National Institute of Standards and Technology) at etl (2014)

This report analyzes the damage in high-rise RC buildings with a bearing wall system in the 2019 Maule earthquake in Chile and proposes recommendations for each case. Many structural damages were found to be related to vertical discontinuity in strength and stiffness and changes in wall configuration. Significant damage was also observed at joints such as slab, spandrel beam, and stair.

According to the report, conventional elastic analysis, which evaluates the stiffness and strength of each story, is not adequate to detect the vulnerability of vertical discontinuity. Nonlinear analysis should be used to accurately evaluate damage such as brittle failures. As a recommendation, the report suggests limiting local changes in cross-section to less than 30% in order to minimize changes in the center line length and the location of the centroid relative to the wall length.

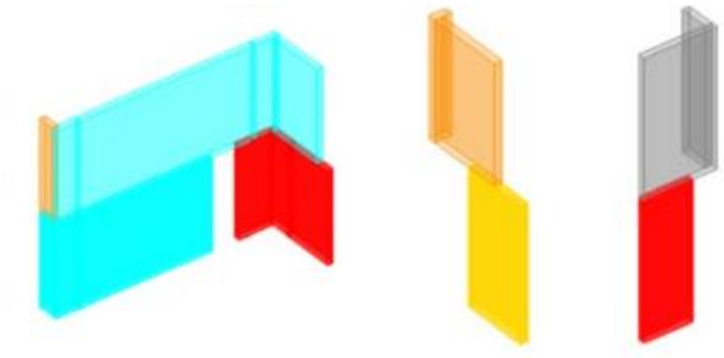

Figure 2-3 Examples of local wall discontinuities

2.2.2 AIK (Architecture Institute of Korea) et al (2018)

This report includes the earthquake damage, structure analysis, and guidelines for piloti structures by the Pohang earthquake. In particular, the damage was severe in the low-rise piloti structure as shown in Figure 2-4.

Figure 2-4 Damage in low-rise piloti structure

In the low-rise piloti structure, there is a risk of torsional behavior and eccentric effect amplification. Also, the need to apply special seismic loads was revealed. In particular, the risk of shear failure in the vertical discontinuity was revealed. It was confirmed that it was consistent with the actual earthquake damage case, as shown in Figure 2-5.

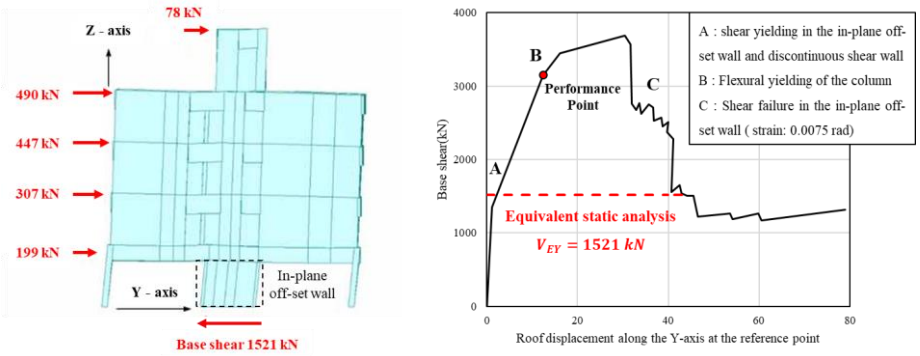

(a) Modeling (b) Push-over analysis result

Figure 2-5 Nonlinear static analysis to compare actual damage

In addition, it is analyzed the earthquake vulnerability of vertical irregular structures with ten stories RC building. The target building was designed in consideration of the special seismic load according to the KBC standard, and it showed an elastic response to the Pohang earthquake by securing sufficient system overstrength.

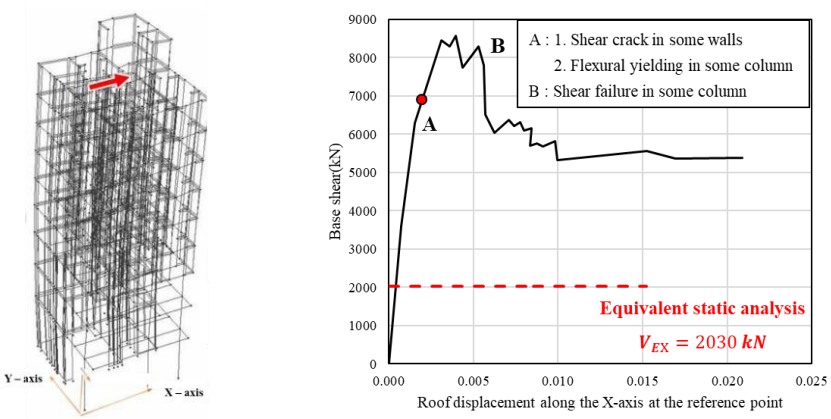

(a) Modeling (b) Push-over analysis result

Figure 2-6 Pushover analysis to analyze the behavior

2.2.3 Leonardo M. Massone et al (2019)

Leonardo M. Massone et al. analyzed discontinuous slender walls subjected to lateral loads with nominal constant axial load. It mainly studied the "flag wall" where the length of walls is reduced at the lower floors creating a setback at the edges in the residential buildings. According to the test results, flag walls behave similarly to rectangular walls when the zone of discontinuity is in compression. On the other hand, the deformation concentration occurred at the discontinuity when the zone of discontinuity was in tension. The test results were compared and analyzed through F.E. (Finite Element) analysis, numerical analysis, and Strut - Tie model. Through this, the local load flow of the flag wall could be identified and can help design the elements.

In particular, the strut-tie model was proposed for each direction of the lateral load to analyze test results. The angle of the strut was determined based on the observed crack at the ultimate displacement ratio (approximately 3%). And the tie was determined according to the arrangement of the re-bars.

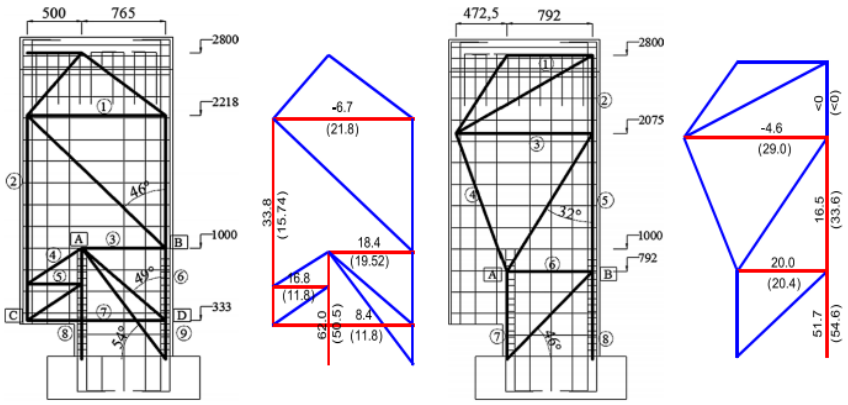

Figure 2-7 Strut-and-tie model for specimen of flag walls

Figure 2-7 reviews the correlation between the tension force through the strut-tie model and the measured test data. The strut-tie model and the test data showed similar tendencies except for ties at the top, and the proposed simple strut-tie model was valid.

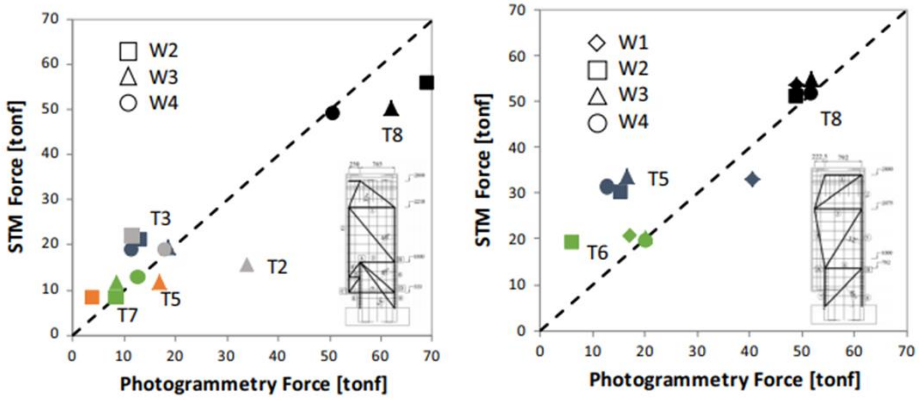

(a) Discontinuos side under tension (b) Continuos side under tension

Figure 2-8 Tie comparison between measured data and Strut-and-tie model

Therefore, the tension force of the flag walls where the lower plastic hinge occurs can be analyzed through the proposed strut tie model under the lateral load with the nominal constant axial load.

2.2.4 Kim et al (2020)

Kim at el. presented a capacity design method using a transfer wall based on the strut - tie model to prevent the brittle failure of the wall-piloti structure. Through the strut - tie model, re-bars and details according to the load-transfer mechanisms of gravity and lateral loads on the piloti structure were presented. This capacity design method induced flexural failure in the wall over the

transfer wall, and the test verified the design method.

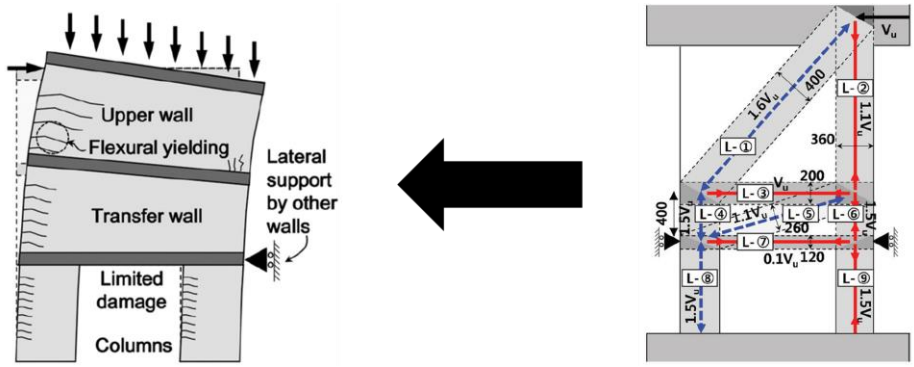

Figure 2-9 Capacity Design for piloti system

In addition, the wall-piloti structure of an actual RC apartment was compared directly with the previous design code (KBC 2016) and the capacity design through nonlinear F.E analysis. The comparison showed that the existing structure was a brittle failure due to concrete crushing at the piloti. In contrast, the capacity design secured higher ductility due to flexural behavior at the wall.

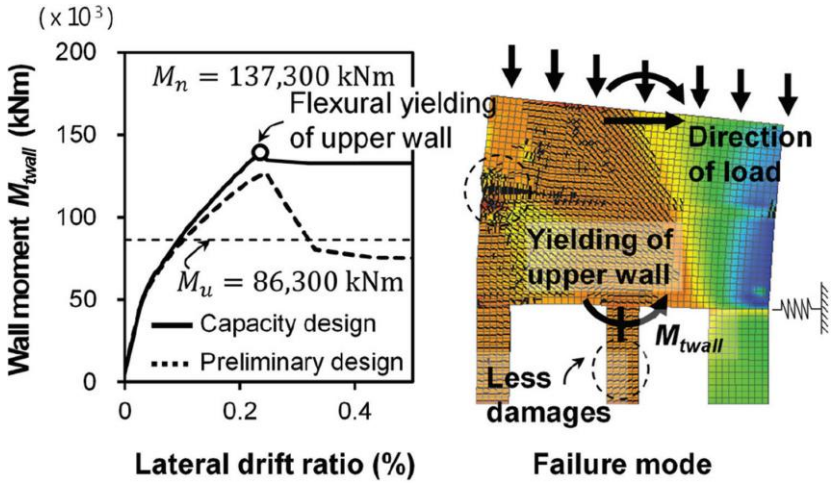

Figure 2-10 Comparison of Nonlinear FE analysis result of prototype wall

2.2.5 Han et al (2022)

Han at el. evaluated the compression performance of the wall-column transfer structure. Test parameters include ratio of lower wall length to the upper one, lower wall thickness, distance between stirrups, cross-tie and re-bar ratio. As a result of the test, concrete crushing and rebar buckling occurred on the upper inner side of the column within 15% of the target load.

Through the pure compression test, it was confirmed that the load transfers smoothly from the wall to the column despite section change. When the strain gauge at the measurement position is analyzed, it can be confirmed that the stress is concentrated around the critical section.

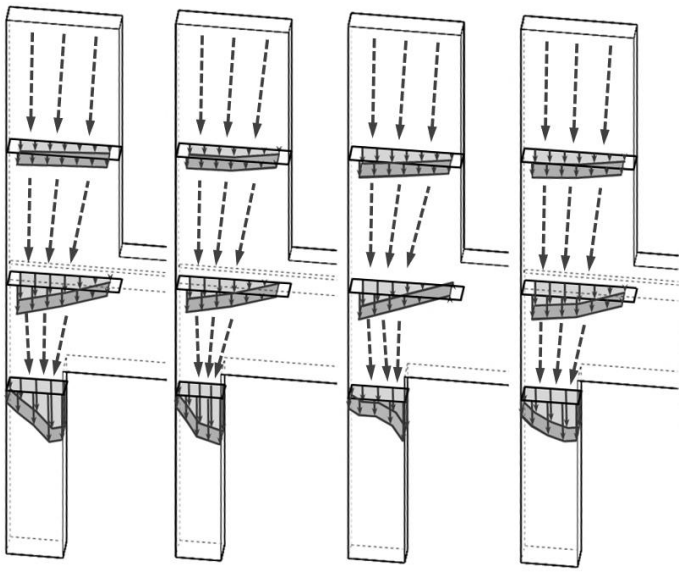

Figure 2-11 Strain distributions and load paths

Chapter 3. Capacity Design Concept for Wall-Column Transfer Structure

3.1 Preliminary study on prototype structure

3.1.1 Prototype apartment

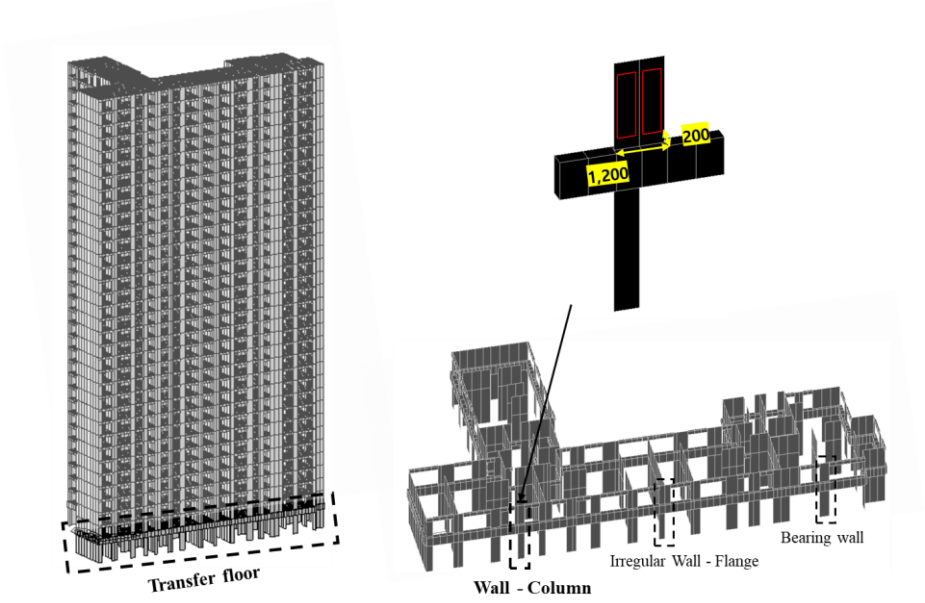

Figure 3-1 Prototype high-rise RC building

The prototype structure is an 'L'-shaped apartment with many openings in the front. This requires the frame system in front to resist the lateral load.

A wall-pier and a flange wall are placed in the front part of the transfer floor, and the wall-column transfer structures are partially used. A relatively large girder width is used in consideration of load transfer.

As shown in Figure 3-1, there are two types of wall-columns. One is perpendicular to the wall, the other exists alone. In the flange wall-column, relatively safety is secured due to the web wall. Therefore, a study was conducted on the transfer structure for the wall-column that behaves alone against the lateral load.

3.1.2 Wall-column of transfer structure

The properties of the upper wall in the transfer structure were analyzed for the prototype structure. The capacity design of the proposed wall-column transfer structure uses a concept that prevents damage by applying the overstrength factor to the members in the transfer floor based on the flexural yielding of the wall. Therefore, the loading condition for the capacity design is the nominal strength of the wall. (Refer to 3.2 concept of capacity design)

To accurately estimate the demand force, the structural analysis was used based on the current design load combination by performing the conventional elastic analysis (Midas Gen). This program utilizes a macro plane stress element and a line element for members. Thus, the local behavior, such as vertical discontinuity, cannot be accurately captured. Based on this analysis, the main parameters of nominal strength (axial force and re-bar ratio) were investigated on the wall with the largest sectional reduction ratio in the wall-column transfer structure.

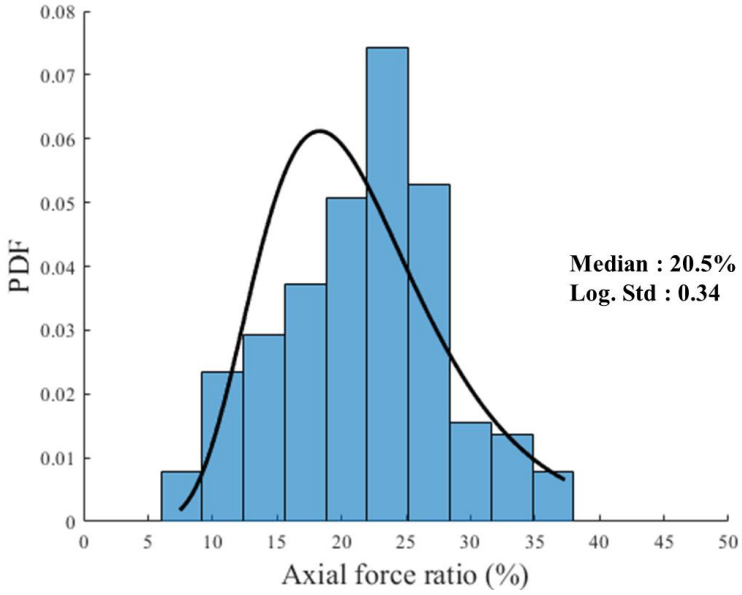

Figure 3-2 Log-normal distribution of axial force ratio

In the upper wall, the axial compression is applied by the seismic load and the gravity load. The transfer floor is the lowest floor of the apartment, and has a relatively high axial compression. The compression in the elastic analysis result includes uncertainty. Since the elastic analysis is the result of the load combination, it is assumed to follow the lognormal distribution. The axial force ratio was calculated as follows based on the required strength by the design load combination.

$$\text{Axial compression ratio} = \frac{P_u \text{ (Required strength)}}{P_n \text{ (Nomianl strength)}} \tag{3-1}$$

$$P_n = f_{ck} \times l \times h \tag{3-2}$$

Where, $f_{ck} = 30\text{MPa}$, $l(\text{length}) = 1{,}200\text{mm}$, $h(\text{thickness}) = 200\text{mm}$

Based on this calculation, the axial compression ratio distribution was made

into a lognormal distribution as shown in Fig. 3-2. Since the compression applied to the wall column transfer structure is highly random, the median value (20%) of the lognormal distribution was determined as the axial compression ratio of the seismic test.

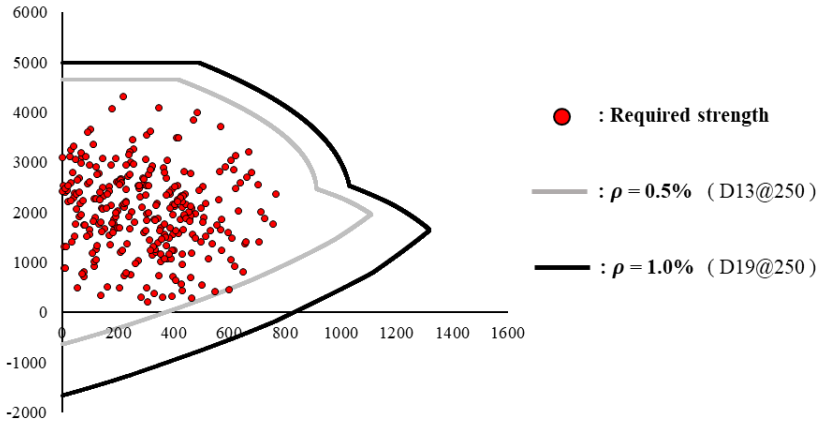

Figure 3-3 P-M interaction diagram of the wall in the prototype

For the prototype apartment, the required strength by the design load combination was confirmed through structural analysis. The distribution of the required strength applied on the wall with the largest sectional reduction rate in the wall-column transfer structure is plotted in the P-M curve, as shown in Figure 3-3. Based on this distribution, the vertical rebar ratio of the wall that allows the required strength to be distributed within the P-M curve where the strength reduction factor is applied was investigated in the same way as in the actual design. According to the capacity design concept, the P-M curve should not be excessively formed for the required strength. The rebar ratio of 0.5% was insufficient for the required strength, whereas the rebar ratio of 1.0% was satisfactory.

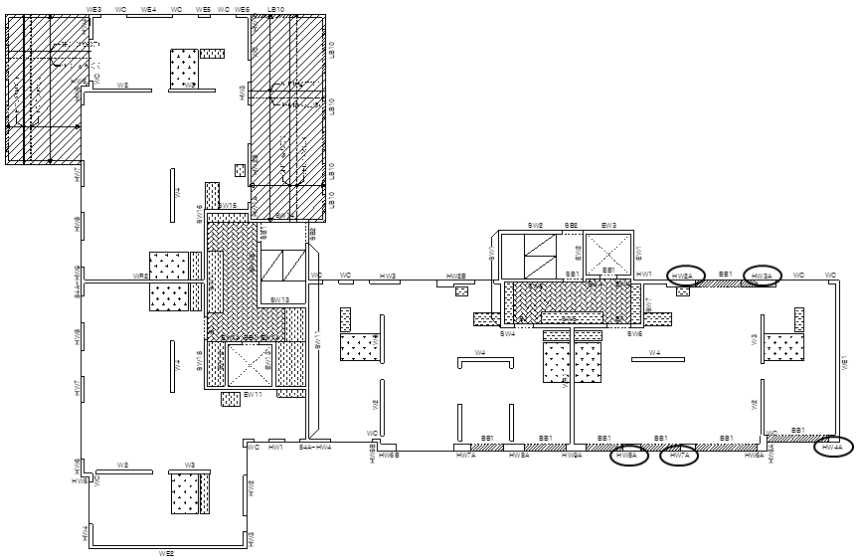

Figure 3-4 Walls of transfer structure in the other apartment

Table 3-1 Reinforcement ratio of wall with tranfer structure

Wall	Demension (Length X depth)	Vertical Reinforcement	Steel ratio (ρ)
HW2A	2500 X 200	D 10 @ 280	0.26%
HW3A	2000 X 200	D 10 @ 450	0.18%
HW4A	1440 X 200	D 10 @ 450	0.2%
HW7A	1400 X 200	D10 - 10	0.25%
HW8A	1600 X 200	D13@180	0.73%

In addition, the vertical rebar ratio of the wall using the transfer structure in the other apartment is 0.75% at the maximum as shown in Table 3-1. Based on this actual design, the vertical rebar ratio of the specimen was determined to be 0.91% (D10@120mm) considering the wall size of the specimen (600 × 130 mm^2).

3.2 Concept of capacity design

Capacity design is known as the basic philosophy of seismic design, and was proposed by New Zealand's Bob Park and Tom Paulay in the mid-late 1960s. A schematic diagram of this concept is presented in Figure 3-5. This leads to the ductile behavior of the chain by causing the preceding yield of the ductile link where both brittle links and ductile links exist.

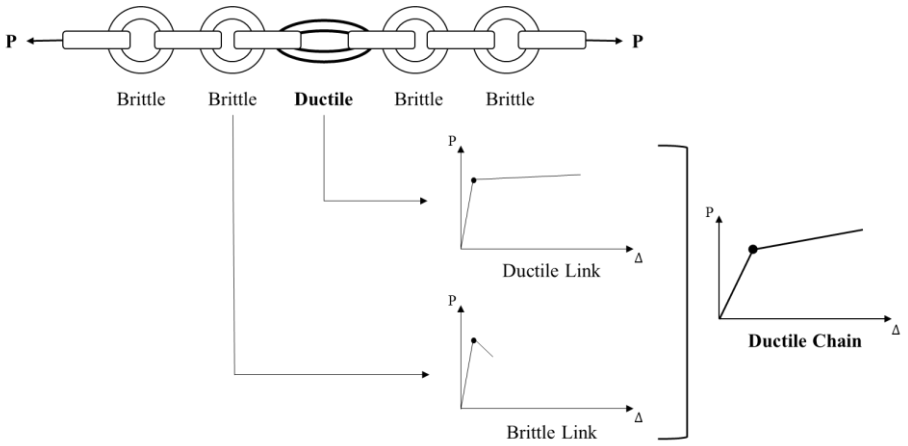

Figure 3-5 Basic concept of capacity design

Applying this concept to seismic design, the purpose is to prevent the collapse of the building under seismic load and to generate ductile behavior. Therefore, it is a design method that causes ductile behavior in the predictable failure mode of the specific element and provides sufficient ductility to the entire building system.

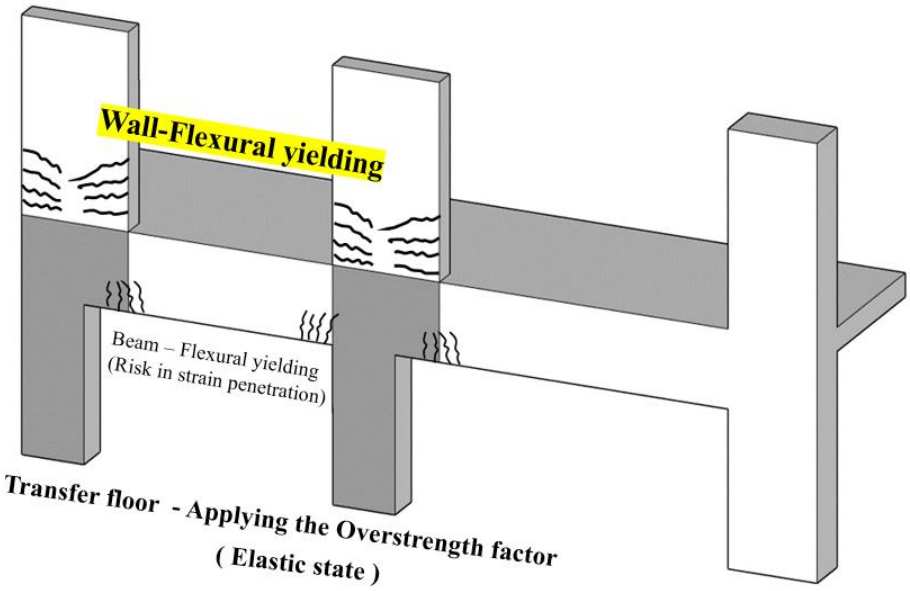

Figure 3-6 Capacity design concept for wall-column transfer structure

Based on this capacity design concpet, it is intended to be applied to a wall-column transfer structure. The wall-column transfer structure serves as a load transfer through the spandrel beam instead of the existing large cross-sectional transfer beams. Excessive stress concentration and irregular load flow occur due to relatively rapid cross-sectional changes. Therefore, failure of members (column, joint, etc.) in transfer floor at risk of brittle failure can cause significant damage (torsional behavior, weak-story, etc.) to the entire structure, so it should be designed to prevent significant damage to the transfer structure before the flexural behavior of the wall. That is, the increase in the lateral load is suppressed through the plastic hinge of the upper wall, and damage to the transfer member is not generated.

Therefore, it is necessary to calculate the target lateral load (V_n) based on the flexural yield strength of the upper wall. Also, tranfer members should be designed as a design load applying the overstrength factor (1.25) to the required strength by the target lateral load (V_n). Through this capacity design, no significant damage occurs before the ultimate behavior state. That is, the purpose is to cause limited damage to the transfer members according to the occurrence of the plastic hinge on a flexural member in the system. Accordingly, the target lateral load for flexural yield of the upper wall is calculated. Each transfer member is designed using the overstrength factor by the required strength for the target lateral load.

3.3 Summary

In this chapter, the prototype RC building using the wall-column transfer structure was analyzied and design concept based on the capacity design was considered. The major findings are summarized as follows.

There are many openings in the prototype RC structure, and the front elevation has not many structure walls. So, the wall-column transfer structure considers to resist the lateral load. In particular, a wall-column transfer structure that exists alone is considered to be more dangerous than the irregular wall.

The capacity of the wall-column transfer structure was determined by considering the axial force and rebar ratio of the upper wall. Therefore, the median value of the lognormal distribution for the axial force was determined considering the uncertainty and randomness of the load combination based on the result of the performing the conventional elastic analysis of the prototype RC building. And the re-bar ratio was determined by the P-M interaction diagram with the strength reduction factor and the actual re-bar ratio in the wall-column transfer structure.

The capacity design aims to induce ductile behavior in the system, inducing the predictable failure of ductile elements. The design conept focuses on preventing brittle failure of transfer members by inducing flexural failure of the upper wall. Therefore, the transfer members should be designed with an overstength factor (1.25) of flexural overstrength based on the target later load that causes the flexural yielding of the upper wall.

Chapter 4. Cyclic Loading Test Plan

4.1 Introduction

The purpose is to cause little damage to the members in the transfer floor by occurring the plastic hinge of the flexural member in a system according to the previously proposed capacity design concept. Therefore, the member that can cause ductile behavior is the upper wall. Also, the spandrel beam outside the transfer zone can be considered. However, unlike the ordinary beam-column, the lower column is discontinuous with the upper wall. Therefore, damage to the joint where the load is transferred is dangerous. The yielding of the beam causes damage to the joint. So, to induce flexural yielding of the upper wall for the ductile behavior of the system, the lateral target load for the flexural yield of the wall is calculated. Moreover, the column and spandrel beam are designed considering the overstrength factor (1.25) for the required strength for the target lateral load.

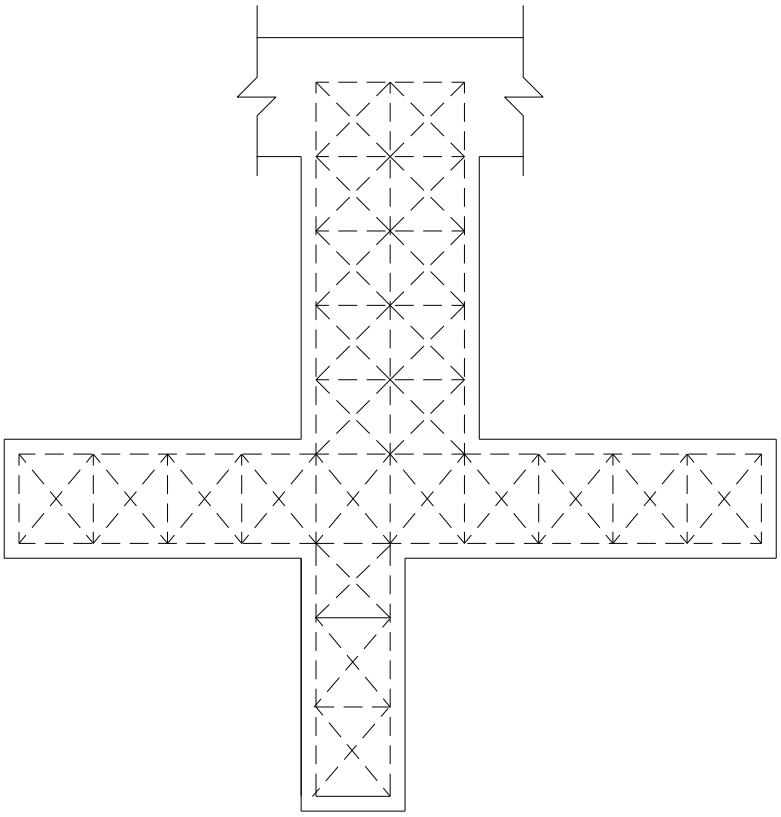

Figure 4-1 Strut-Tie model of specimen

For the purpose of the capacity design, the wall-column transfer structure is designed as a Strut-Tie-Model. The transfer structure is known as the ‘D region’ because stress concentration occurs. In these regions, the assumption of bending behavior generally used is not established. Therefore, after cracking in concrete, it is necessary to design based on the strut-tie model composed of a truss model under the assumption that concrete and rebar support flexural compression and flexural tensile stress, respectively.

4.2 Design of test specimen

4.2.1 Boundary conditions of specimen

The conditions assumed for the test are as follows. When the wall of the transfer structure reaches the yield moment, it has a dominant influence on the whole system. In fact, the behavior of the transfer floor is composed of both the moment-resisting frame including the beam and the lateral support condition according to the diaphragm effect. However, the mechanism of the ultimate behavior according to extreme boundary condition is identified by considering two boundary conditions that may occur in the transfrer floor.

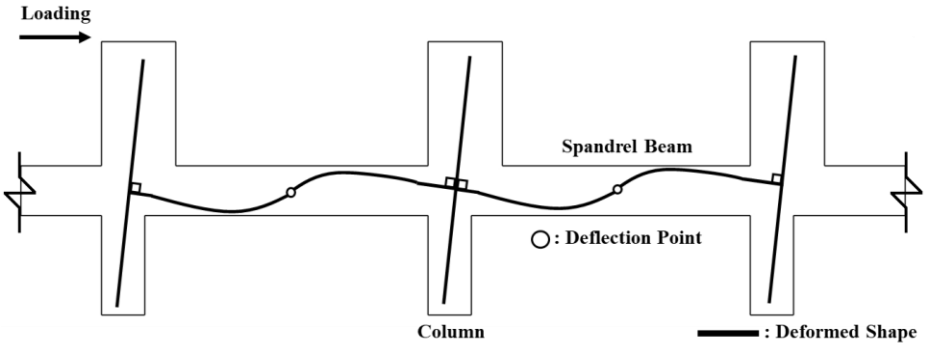

Figure 4-2 Moment-resisting frame behavior on the transfer floor

The first boundary condition is as follows. A moment-resisting frame of the same rigidity is continuous next to the wall-column transfer system used in the transfer floor as shown in Figure 4-2. In this case, bending moment resistance is generated against the lateral load in the beam of the continuous frame. In other words, it becomes a lateral support by the moment frame action of the continuous wall-column transfer structure against the lateral load.

In this case, the specimen idealizes the end of the beam as an inflection point (bending moment = 0), and provides a boundary condition that allows lateral displacement at the same time.

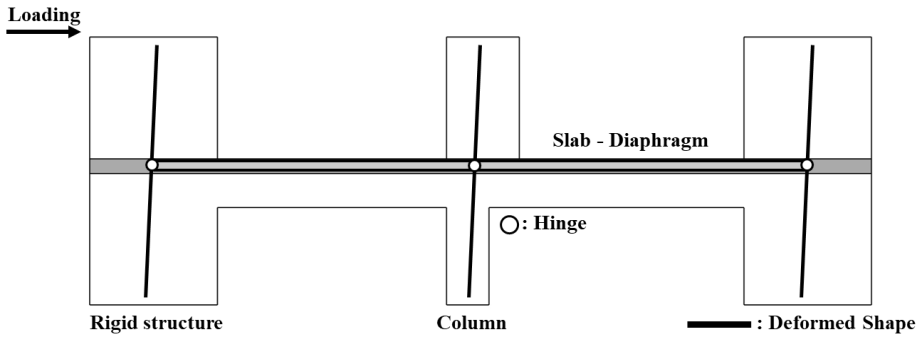

Figure 4-3 In-plane lateral support behavior on the transfer floor

The second boundary condition is as follows. There is a lateral resisting structure (shear wall, etc.) with higher rigidity next to the wall-column transfer structure, as shown in Figure 4-3. In this case, the wall-column transfer structure was laterally supported by the rigid structure. Lateral displacement may occur depending on the rigidity of the rigid structure, which may affect the wall-column transfer structure. Therefore, the behavior according to the allowable lateral displacement is analyzed while providing lateral support.

4.2.2 Dimension and Target strength

Considering the test setup, the size of the specimen was decided as reduced size of 1/2 the width, thickness, and 1/3 the height of the prototype structure. The size of the specimen's wall is 600 × 130 mm^2(length × thickness), the beam is 400 × 250 mm^2(width × depth), and the size of the column is 450 × 200 mm^2 only with a reduced rate of 25%, and other specimens are 350 × 200 mm^2 with a reduced rate of 40%. In addition, the specimen consisted of a 120 mm thick slab in the out-of-plane direction considering the actual apartment. The height of the specimen is 3,400 mm, the foundation is 800 mm, and the loading slab is 400 mm, which was planned for the out-of-plane direction support of the specimen, as shown in Figure 4-4.

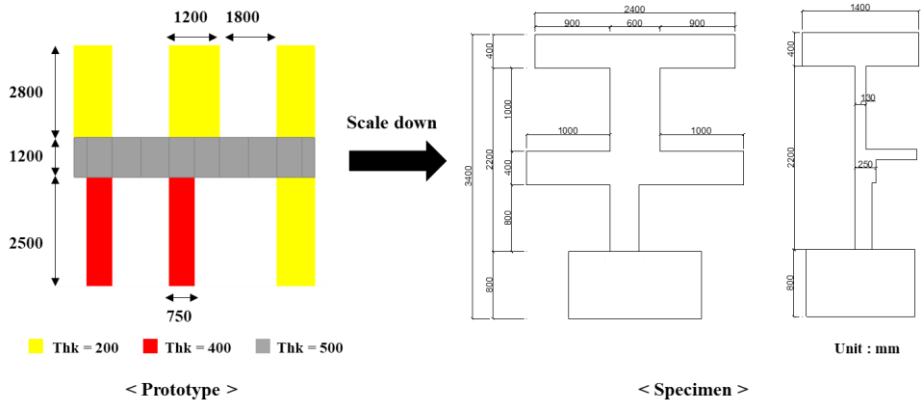

Figure 4-4 Scaled-down specimen

The design process of the specimen is as follows.

1. Determine the nominal strength (axial loading, lateral loading) that causes flexural yielding according to the bottom of the wall.

2. Construct a strut-tie model that reflects this nominal strength and each

boundary condition, and confirm the required strength for each member.

3. Capacity design is performed based on failure mode and the dimension in each specimen.

The nominal strength of the specimen calculates the target lateral load that induces flexural yielding in the wall. According to the the prototype apartment analysis, the target nominal strength to induce flexural yielding of the wall was determined as the axial load with 20% of the wall and the vertical re-bar ratio (0.91%, D10@120mm). The target nominal strength is calculated by dividing the nominal bending moment of the wall, M_n(174kN·m) by net height(h), which indicates the difference between the loading slab and the bottom of the wall.

$$\begin{aligned} P_g &= 0.2 f_{ck} bh \\ &= 0.2 \times (30 \times 600 \times 130) \times 10^{-3} = 468kN \end{aligned} \tag{4-1}$$

$$V_n = 174(M_n) / 1.2(h) = 145kN \tag{4-2}$$

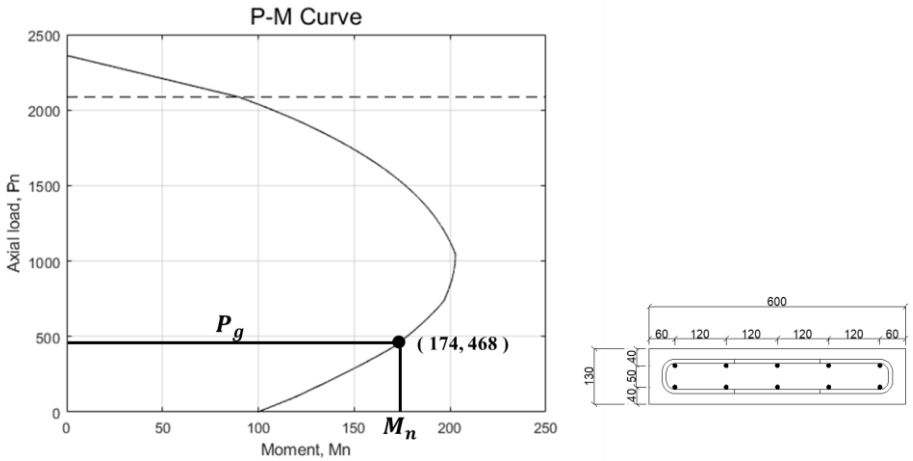

Figure 4-5 P-M interaction diagram of the wall in the specimen

4.2.3 Strut-and-tie model analysis

The strut-tie model consists of struts, nodal zones of the compression element, and a tie of the tensile element. The ties are configured in the same direction as the arrangement of each re-bar, and struts are placed in vertical, horizontal, and diagonal directions. However, it is difficult to construct a diagonal member by accurately predicting the direction of the load flow. Therefore, a diagonal member was constructed using a compression-only element built into a structural analysis program. After recognizing the force flow of the compression, only the main strut element should be left. The application factor (β_s, β_n) for each strut and nodal area was determined according to the design standard for concrete structures (KDS 14 20 24). Also, the width of the node was applied by referring to the hydrostatic nodal zone and the effective width of the design standard. As a result, the load flow of the strut-tie model is shown in Figures 4-6 ~ 4-8.

In this study, tests were conducted on three boundary conditions. In the case of the Moment-resisting frame specimen, the roller support was modeled at the end of the beam. And the specimen with in-plane lateral support that limits the lateral displacement was modeled at the end of the beam. In the case of specimen with in-plane lateral support that allows lateral displacement, a spring boundary conditon was modeled at the end of the beam.

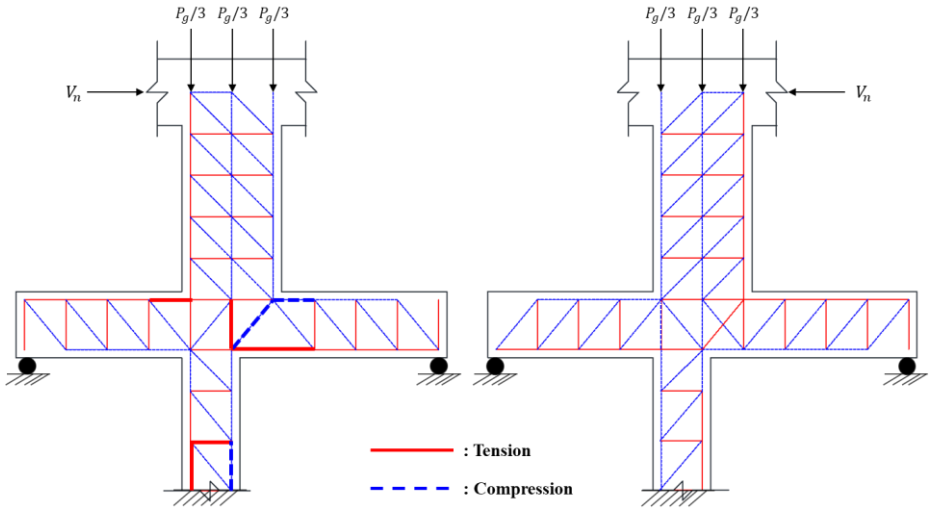

Figure 4-6 Strut-Tie Model for Moment-resisting frame specimen

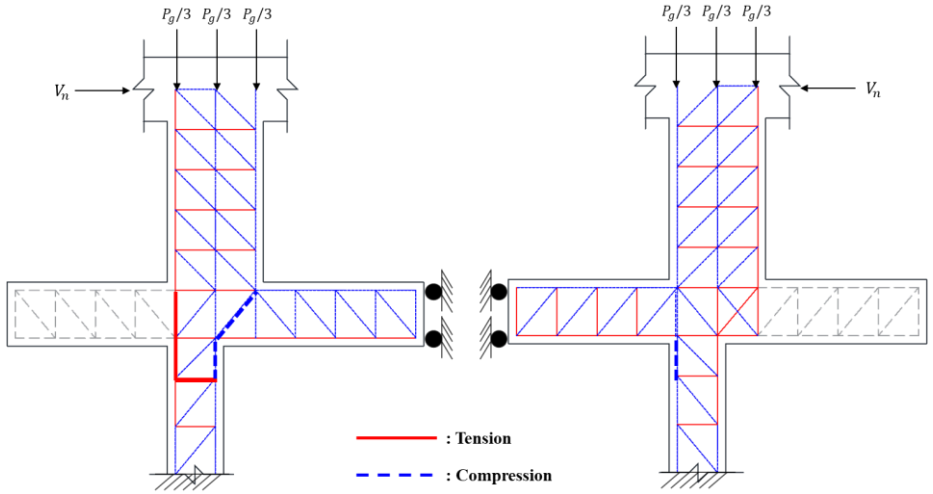

Figure 4-7 Strut-Tie Model for specimen with in-plane lateral support

(limit the lateral displacement)

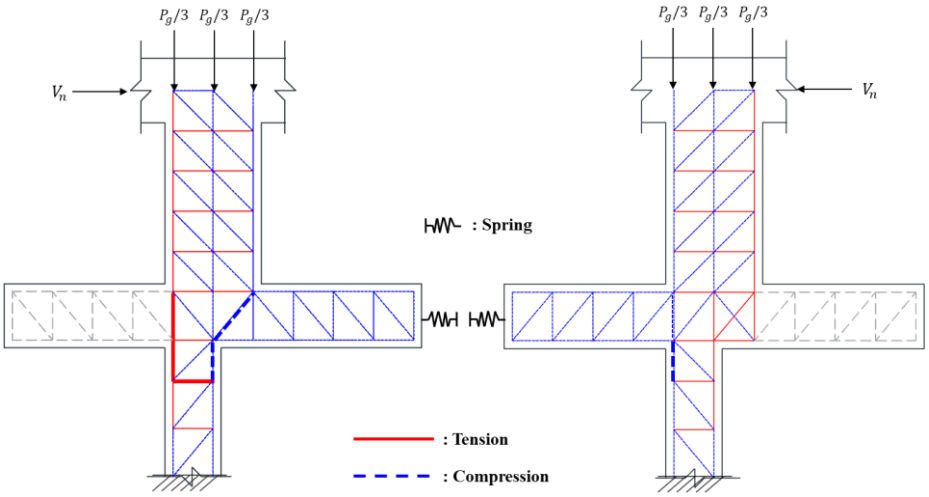

Figure 4-8 Strut-Tie Model for specimen with in-plane lateral support (allow the lateral displacement)

4.2.4 Design of Moment-resisting frame specimen

In the moment-resisting frame specimen, two failure modes were considered. In other words, it is planned that one specimen yields a wall, and the other specimen yields a wall and beam. A roller supported specimens at the end of the beam so that the lateral force is resisted by the flexure of the specimen. As shown in Figure 4-6, the target strength for flexural yielding of the wall is given as a loading condition to the strut-tie model. The required forces acting on the members in transfer floor are confirmed. For the required compression strength, general concrete strength (30 MPa) used in the RC buildings is reviewed according to the conditions of the design standard. In the case of rebars, the overstrength factor (1.25) is applied to the column and the beam according to the capacity design.

The W-R40-BR specimen is designed as follows. As a specimen that induces only yielding of a wall, it is designed by applying an overstrength factor to prevent significant damage to the beam and column, which are moment-resisting members.

$$\text{Reinforcement for Beam and Column} = 1.25 \times \text{Required } A_s$$

The WB-R40-BR specimen is designed as follows. For ductile behavior, flexural yielding of the wall is induced, and an overstrength factor is applied to the members in the transfer zone. However, this specimen is to study whether there will be any problem in the ductile behavior of the system when the wall and beam yield at the same time. So, the column is only applied to overstrength factor.

$$\text{Reinforcement for Beam} = 1.25 \times \text{Required } A_s$$

$$\text{Reinforcement for Column} = 1.0 \times \text{Required } A_s$$

In addition, considering that the use of this specimen is an RC apartment, the design standards for the transverse reinforcement of the intermediate moment-resisting frame (KDS 2016, Requirement for intermediate moment-resisting frame) and piloti (KDS 41 17 00, Consideration for the piloti structure) were applied to the design.

Table 4-1 Summary of design for moment-resisting frame specimen(BR) through Strut-Tie Model

Specimen	Member (Overstrength factor) & Location		Demand		Design	
			Required strength (kN)	Rebar (mm^2) Or Concrete (MPa)	Reinforcement	Rebar (mm^2) Or Concrete (MPa)
W-R40-BR	Spandrel beam (1.25)	Logitudinal Tension (Top)	248.4	621.0	5-D13	633.5
		Logitudinal Tension (Bottom)	415.8	866.3	5-D16	993.0
		Transverse Tensile	126.7	36.2	D13@80mm	126.7
		Nodal zone	-277.2	18.5	-	30
		Strut	-478.5	30.7	-	30
	Column (1.25)	Vertical Tension	310.5	1293.8	9-D16	1787.4
		Horizontal Tension	145.0	42.3	D10@70mm	71.3
		Nodal zone	-582.5	29.1	-	30
WB-R40-BR	Spandrel beam (1.0)	Logitudinal Tension (Top)	248.4	496.8	3-D13 2-D10	522.8
		Logitudinal Tension (Bottom)	415.8	693.0	3-D16 2-D10	738.5
		Transverse Tensile	126.7	29.0	D13@80mm	126.7
		Nodal zone	-277.2	18.5	-	30
		Strut	-478.5	30.7	-	30
	Column (1.25)	Vertical Tension	310.5	1293.8	9-D16	1787.4
		Horizontal Tension	145.0	42.3	D10@70mm	71.3
		Nodal zone	-582.5	29.1	-	30

※ For the critical elements, mark the S-T Model with a bold line

4.2.5 Design of specimen with in-plane lateral support (According to the lateral displacement)

In the specimen with in-plane lateral support, whether lateral displacement is allowed or not was considered as main parameter. The specimen that limits the lateral displacement was implemented as a boundary condition that is a complete constraint condition at the end of the beam, as shown in Figure 4-7. Whereas the specimen that allows lateral displacement was implemented as a boundary condition (only compression spring) that allowed lateral displacement (0.35 mm) from the transfer floor in the preliminary structural analysis of the prototype building, as shown in Figure 4-8. Based on this boundary conditions, the required strength is checked by applying the loading condition in the same way as previously introduced. The specimen with in-plane lateral support does not apply a large required strength to the beam due to the lateral support. On the other hand, if lateral displacement is allowed, the required tie force of the column increases. Reflecting this, the specimen was designed.

The W-R25-BL specimen was designed as follows. The beam did not apply the overstrength factor because the beam does not pass large forces due to the in-plane lateral support. Whereas, the column applies the overstrength factor. There is a risk of failure due to the concrete crushing with a strut at the joint. So, the reduction in width was reduced for the study to lower the strut action.

$$\text{Reinforcement for Beam} = 1.0 \times \text{Required } A_s$$

$$\text{Reinforcement for Column} = 1.25 \times \text{Required } A_s$$

The W-R40-BL specimen was designed as follows. In the in-plane lateral

support that allows lateral displacement, the cantilever behavior acts on the column due to lateral displacement. So, required strength for the column is relatively large. In capacity design concept, the overstrength factor should be considered in the design of the transfer column. However, in order to study the effect of the overstrength factor in the design, the factor is not applied.

$$\text{Reinforcement for Beam and Column} = 1.25 \times \text{Required } A_s$$

In addition, considering that the use of this specimen is an RC apartment, the design standards for the transverse reinforcement of the intermediate moment-resisting frame (KDS 2016, Requirement for intermediate moment-resisting frame) and piloti (KDS 41 17 00, Consideration for the piloti structure) were applied to the design.

Table 4-2 Summary of design for specimen with in-plane lateral support(BL) through Strut-Tie Model

Specimen	Member (Overstrength factor) & Location		Demand		Design	
			Required strength (kN)	Rebar (mm2) Or Concrete (MPa)	Reinforcement	Rebar (mm2) Or Concrete (MPa)
W-R25-BL (Limit the displacement)	Spandrel beam (1.25)	Logitudinal Tension (Top)	193.3	386.6	3-D13 2-D10	522.8
		Logitudinal Tension (Bottom)	91.2	182.4	3-D13 2-D10	522.8
		Transverse Tensile	50.9	14.5	D13@80mm	126.7
		Nodal zone	-236.6	15.8	-	30
		Strut	-449.2	29.7	-	30
	Column (1.25)	Vertical Tension	130.6	544.2	9-D16	1787.4
		Horizontal Tension	118.0	34.4	D10@70mm	71.3
		Nodal zone	-500.8	25	-	30
W-R40-BL (Allow the displacement)	Spandrel beam (1.0)	Logitudinal Tension (Top)	248.2	496.4	5-D13	633.5
		Logitudinal Tension (Bottom)	150.2	300.4	5-D13	633.5
		Transverse Tensile	50.7	14.4	D13@80mm	126.7
		Nodal zone	-301.4	20.1	-	30
		Strut	-501.7	32.1	-	30
	Column (1.0)	Vertical Tension	417.1	1390	9-D16	1787.4
		Horizontal Tension	179.4	41.9	D10@70mm	71.3
		Nodal zone	-677	33.9	-	30

※ For the critical elements, mark the S-T Model with a bold line

4.3 Test parameters

For each specimen, a strut-tie model is analyzed according to the reduction in width ratio, boundary condition, and failure mode. When designing according to analysis, the test parameters are shown in Table 4-3. The compression force acting on the specimen was planned to be 20%(468kN) of the wall. Considering the design concept of this test, the dimension and material characteristics of the wall are the same for all specimens.

Moment-resisting frame specimens have different types of failure mode induced by test parameters. The W-R40-BR specimen induces only flexural yielding of a wall. On the other hand, the WB-R40-BR specimen induces flexural yielding of a wall and beam. Therefore, the difference in the re-bar ratio of the beam occurs due to the difference in the application of the overstrength factor in the capacity design.

The specimen with in-plane lateral support is the main test parameter determining whether the lateral displacement is allowed. The W-R25-BL specimen has a lower reduction in width to decrease higher diagonal strut strength at the joint due to in-plane lateral support. The W-R40-BL specimen with in-plane lateral support allows lateral displacement. In addition, it was planned whether damage to the column caused by lateral displacement would affect the safety of the transfer structure.

Table 4-3 Test parameters of the specimens

Specimen	Failure mode	Vertical reduction in width, (mm)	Boundary condition (Ends of beam)	Reinforcing bar ratio (%)					
				Wall		Column		Beam	
				Vertical	Horizontal	Vertical	Horizontal	Longitudinal	Transverse
W-R40-BR	Wall	250	Roller	0.91	0.98	2.56	1.01	1.5	1.29
WB-R40-BR	Wall, Beam	250	Roller			2.56	1.01	1.27	1.29
W-R25-BL	Wall	150	Lateral support (Limit the displacement)			1.99	1.01	1.29	1.29
W-R40-BL	Wall	250	Lateral support (Allow the displacement)			2.56	1.01	1.29	1.29

4.4 Test specimens

4.4.1 Details of specimens

There is no difference in the dimension and re-bar of the wall in all specimens. Moment-resisting frame specimens are shown in Figure 4-9 and 4-10, and specimens with in-plane lateral support are shown in Figure 4-11 and 4-12. The main difference is the length of the beam. The length of the beam was extended by 600mm because it was required to connect pin support to the end of the beam in the moment-resisting frame specimen. Except for this, the length of the beam is the same at 2,600mm.

Since the Moment-resisting frame specimens have different application of the overstrength factor, the longitudinal re-bar of the beam is different. Therefore, the WB-R40-BR specimen, which induces flexural yielding of a wall and beam, has a lower rebar ratio than the W-R40-BR specimen, which induces only flexural yielding of a wall. The re-bar ratio and width of the column are the same for both specimens. The purpose of this study was to investigate the effect of flexural yielding of beam on the ductile behavior of the system.

The specimens with in-plane lateral support differ in whether the lateral displacement is allowed. Since the beam has in-plane lateral support, it does not flow much force. So, the re-bar ratio is lower than moment-resisting frame specimens. W-R25-BL, which has limited lateral displacement, lowers the reduction in width due to a higher strut at the joint. As a result, the column width becomes 450mm, unlike other specimens. So, the rebar ratio is lower than

other specimens with the same amount of rebar. On the other hand, the W-R40-BL, which allows lateral displacement, requires a high strength for the column. Nevertheless, it does not apply an overstrength factor, so it was designed with the same re-bars as other specimens.

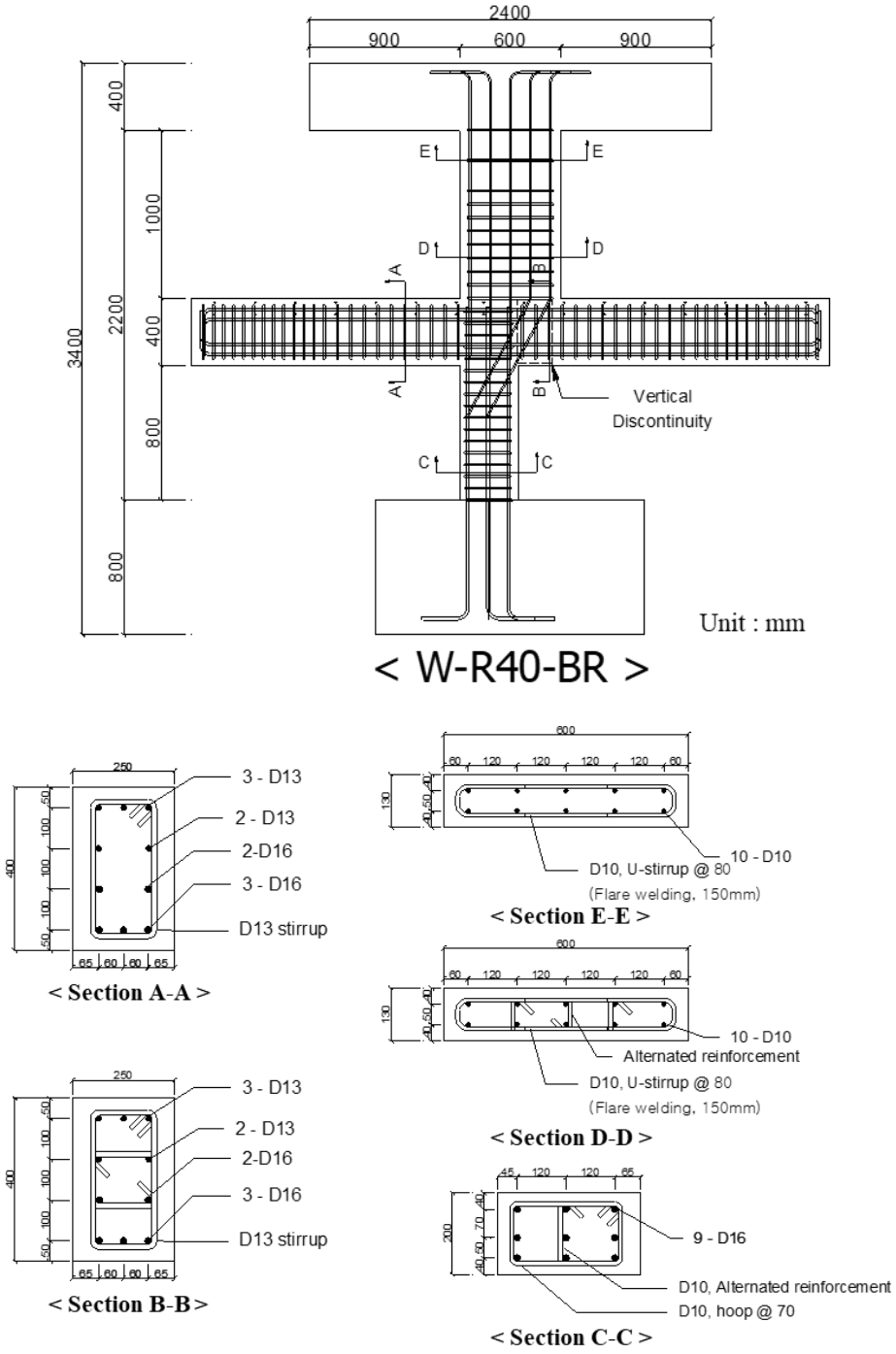

Figure 4-9 Detail of W-R40-BR

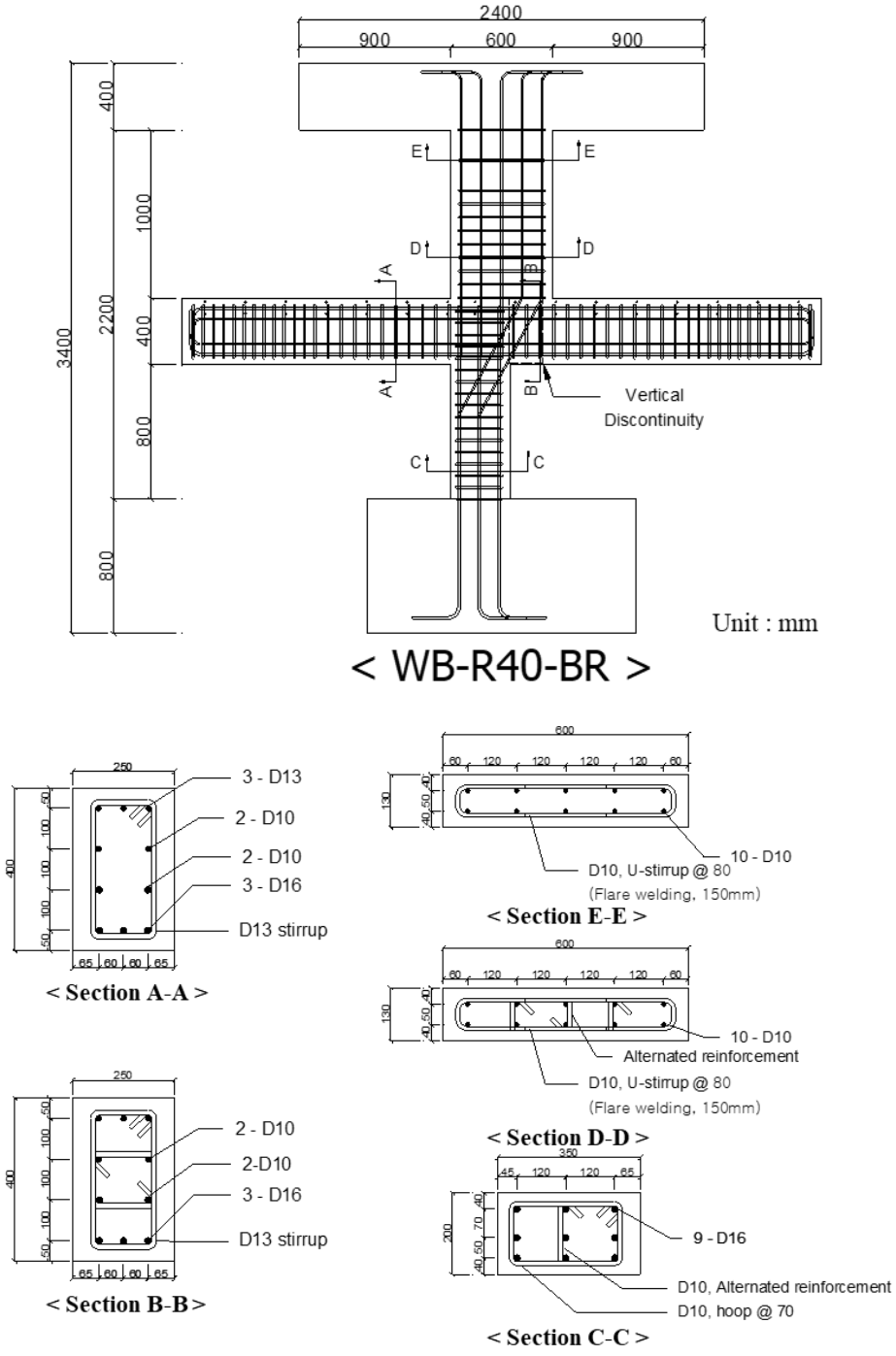

Figure 4-10 Detail of W-R40-BR

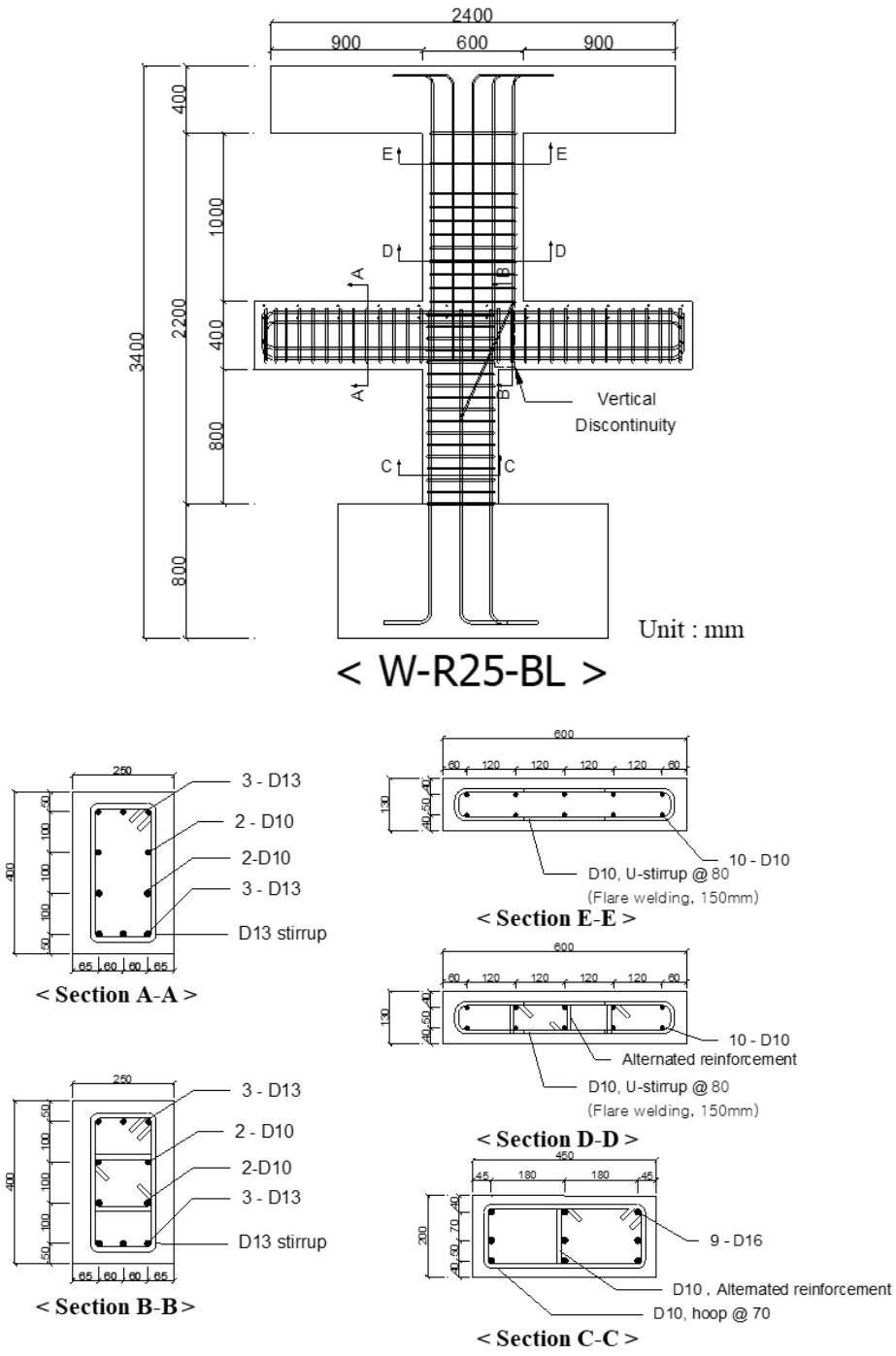

Figure 4-11 Detail of W-R40-BR

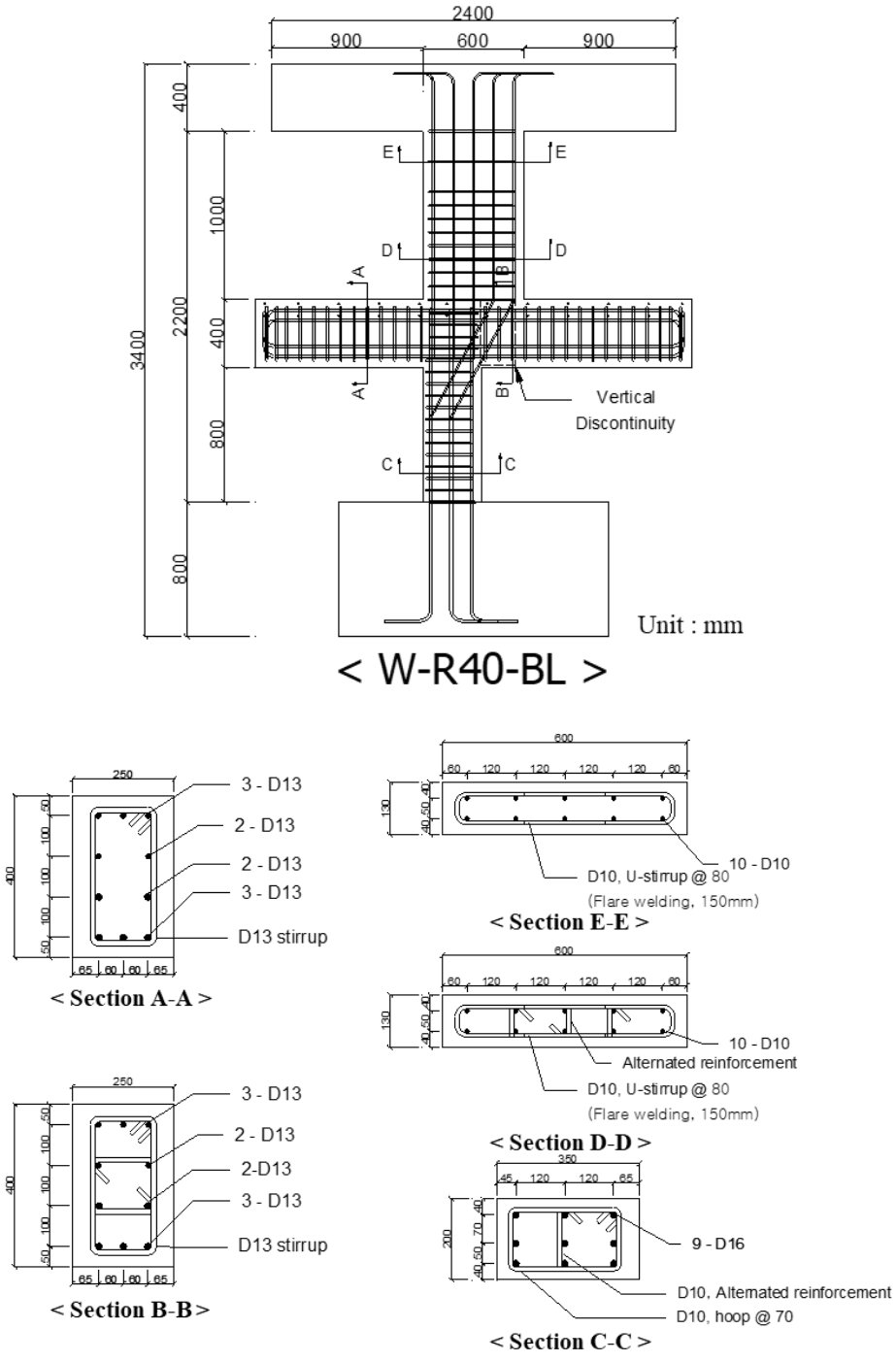

Figure 4-12 Detail of W-R40-BR

4.4.2 Rebar details for test specimens

The slab of the specimens was designed with a minimum re-bar ratio of 0.2% and a minimum cover thickness of 20mm or more by considering the current design standards (KDS 14 20 50). Also, in the case of development, the development method used in general RC apartments was designed to be 150mm, which meets the standard (KDS 14 20 70), as shown in Figure 4-13.

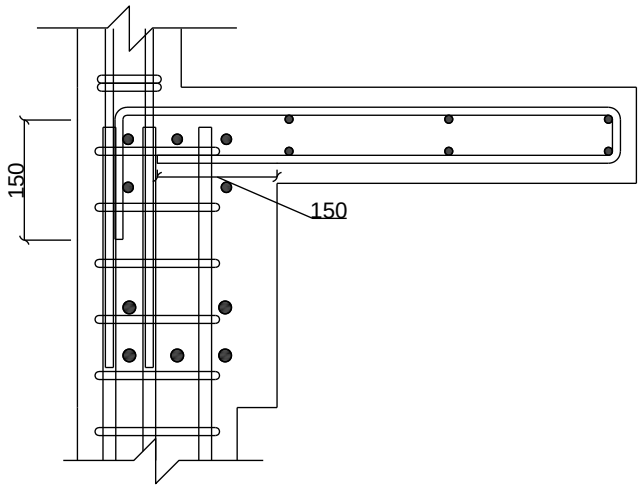

Figure 4-13 Development of slab reinforcement (unit:mm)

The transfer spandrel beam has a small width in the wall-column transfer structure. Therefore, unlike the transfer girder system, the problem is the higher diagonal strut in the discontinuous section and the development length of the wall vertical re-bars. Therefore, the following details were applied.

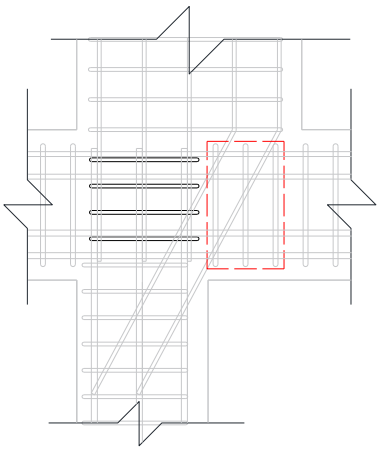

Joint

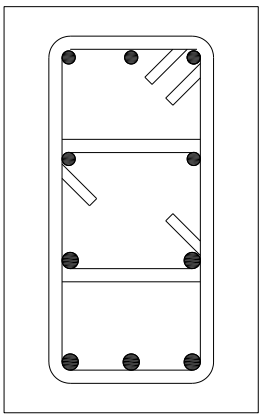

Vertical discontinuity – detail of shear reinforcement

Figure 4-14 Details of joint in specimens

Joints in the piloti structures generally defines a wide width. However, the diagonal strut of the discontinuous section is further increased according to the plastic hinge on the bottom of the wall. There is a risk of brittle failure under lateral loading by such higher diagonal struts.

Therefore, the joint details are applied up to the continuous section of a wall-column structure, and the shear reinforcement details (transverse reinforcement) of the beam are applied to the discontinuous section. It is intended to prevent the concrete crushing caused by the higher diagonal strut and to confine the concrete.

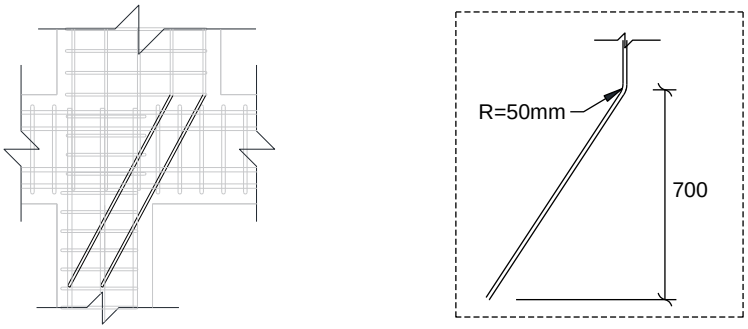

Figure 4-15 Detail of Diagonal re-bar (unit:mm)

Due to the small width of the discontinuous section, it is not easy to develop vertical re-bars for the wall. Therefore, the detail of the diagonal re-bar in the discontinuous section is used and extended to the column. Also, this diagonal re-bar performs not only as a compression reinforcement, but also as a role of connecting the tension force of the wall to the column in cyclic loading. This is because the re-bars of the spandrel beam have a role in the distributed reinforcement for the strut in the discontinuous section.

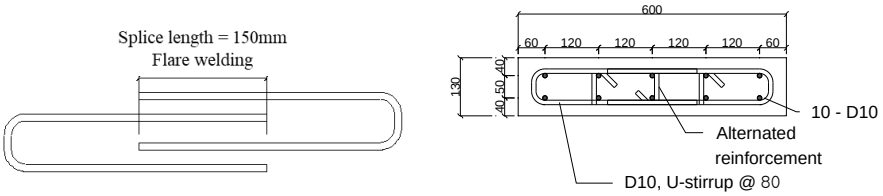

Figure 4-16 Details of wall boundary in the test specimens (unit:mm)

In the scaled-down specimens, securing the development length of the U-stirrups is difficult because the wall length is short. However, the wall of the specimens requires horizontal confinement details. Therefore, U- stirrups were inserted on both sides, and the center was welded to make a closed hoop. In addition, D10 hooks were placed alternately to prevent the buckling of the vertical reinforcement and confine the concrete.

4.4.3 Construction of specimens

Figure 4-18 shows the construction process of the specimens. The production and concrete pouring was planned by dividing the member the same way as in the RC apartment. The first pouring was the foundation, the second was columns, beams, and slabs, and the third was walls and loading slab. All specimens were poured with the same concrete strength of 30 MPa.

For the test setup, the thin steel plate for preventing concrete crushing is placed in in-plane and out-of-plane support. The bolts for pin support, actuator, and LVDT (Linear Variable Differential Transformer) were embedded in the specimens. Additionally, a strain gauge was attached to measure the re-bar strain of each member.

As designed, only details of joint used in the continuous section, and details of shear reinforcement in beam are placed in the the discontinuous section. Also, after inserting horizontal U-stirrups on both sides of the wall, the center was welded to idealize a closed-hoop. The actual appearance of details can be shown in Figure 4-17.

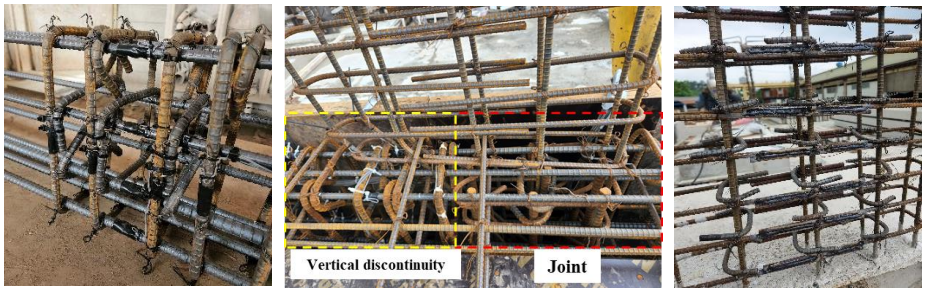

(a) Shear reinforcement (b) Joint (c) U-stirrup

Figure 4-17 Actual re-bar details

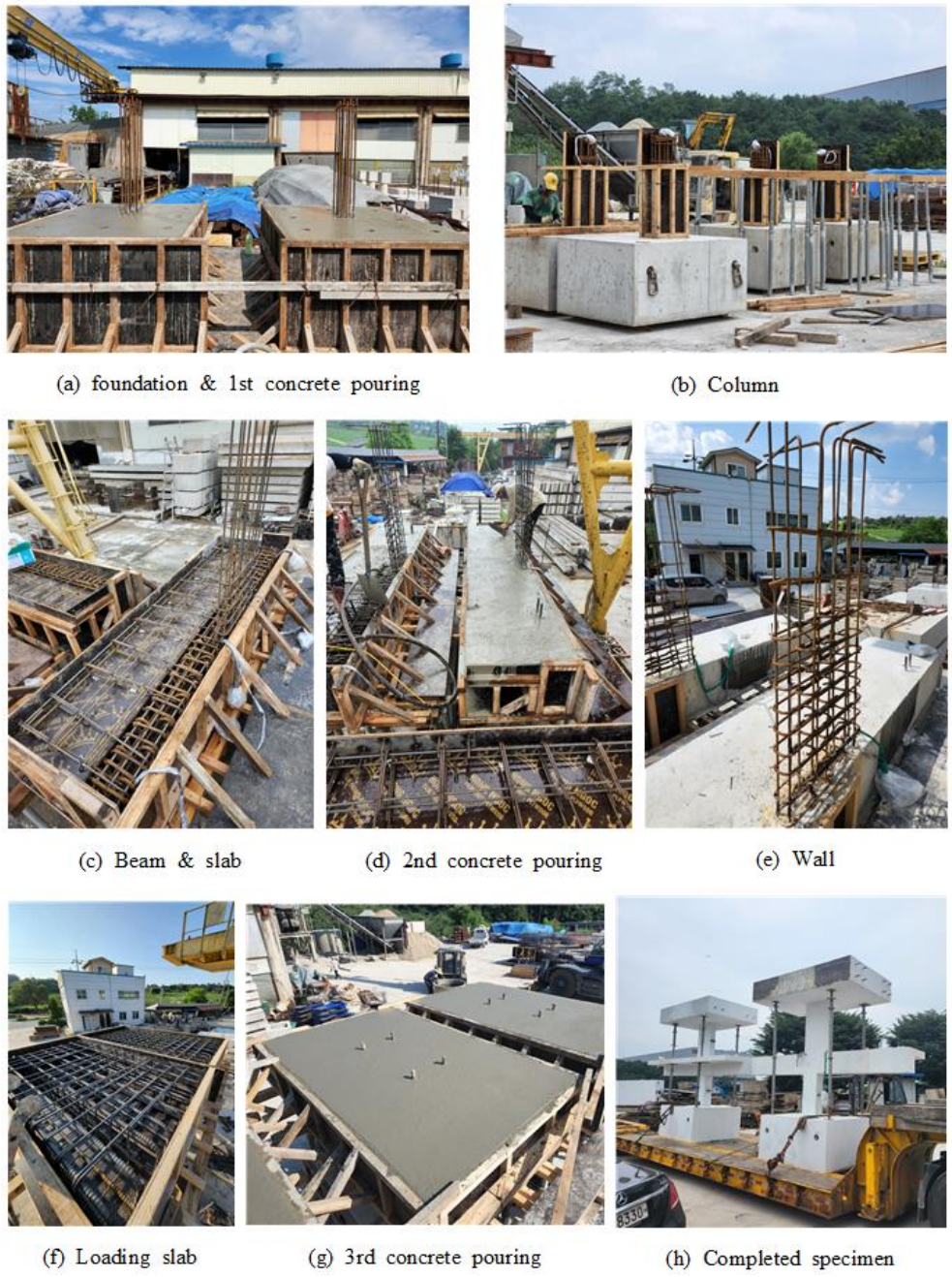

Figure 4-18 Construction procedures of the specimens

4.5 Test setup and measurement

4.5.1 Out-of-plane

The test setup was designed for cyclic loading under the constant compression force (468kN, 20% axial force of the wall) applied to all the specimens. It was planned to compression force with a 150ton actuator and apply the cyclic loading with a 50ton actuator simultaneously. During the test, the magnitude of compression force was maintained uniformly by controlling the vertical actuator. A plate was placed at each specimens' loading point to prevent Saint Venant’s principle.

The specimens are a scaled-down model of an RC apartment. So, the out-of-plane direction of the specimens is supported by other structures in the RC apartment. So, out-of-plane supports were installed on both sides of the test. In addition, a teflon sheet was attached to the end of the out-of-plane support to minimize the friction and allow the specimens to move in the in-plane direction for the cyclic loading.

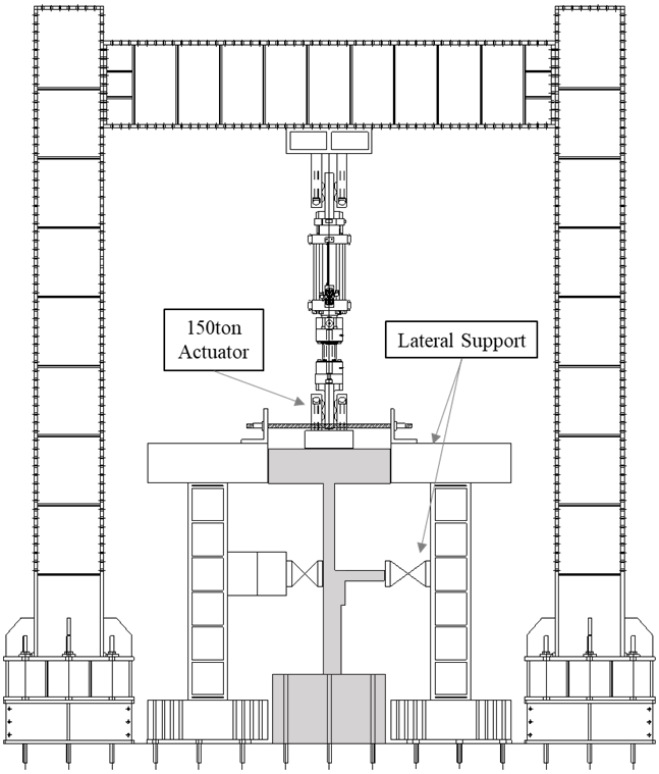

Figure 4-19 Test setup in Out-of-plane

4.5.2 Moment-resisting frame specimens

Figure 4-20 shows the setup of the moment-resisting frame specimen. Since the beam was resisted by bending moment in lateral loading, pin supports are placed at the top and bottom of the end of the beam. In roller supports, load cells can receive tension and compression force. The roller support was installed at 600mm at the end of the beam on the specimens so that the beam with the same length as specimens with in-plane lateral support was planned to resist the lateral loading.

During the constant compression load, the roller support and the specimen were not completely attached, so that the axial force was not applied to the roller support. That is, the compression force was only applied to the specimen. After compression force, the roller support was completely attached to the specimen before cyclic loading, so that the roller support was made by the bending moment of the beam as planned.

The measurement plan of the moment-resisting frame specimen is shown in Figure 4-21 and Figure 4-22. The LVDT was planned for the purpose of examining the lateral displacement, flexural deformation, shear deformation, and slip. To confirm the yielding of each member, a strain gauge was attached to the column, beam, etc. Due to the WB-R40-BR specimen induced flexural yielding of a wall and beam, it was planned to confirm the yielding of the beam by attaching more strain gauges to it.

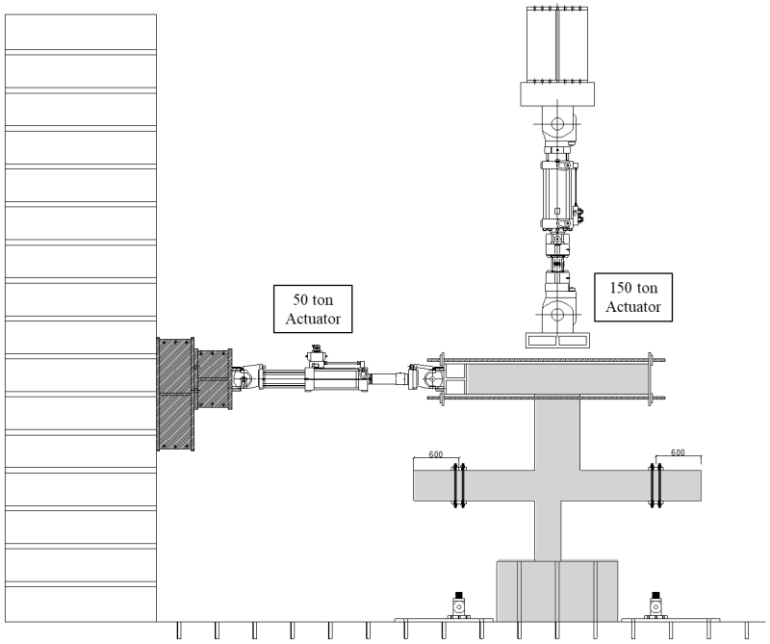

(a) Test setup in compression loading

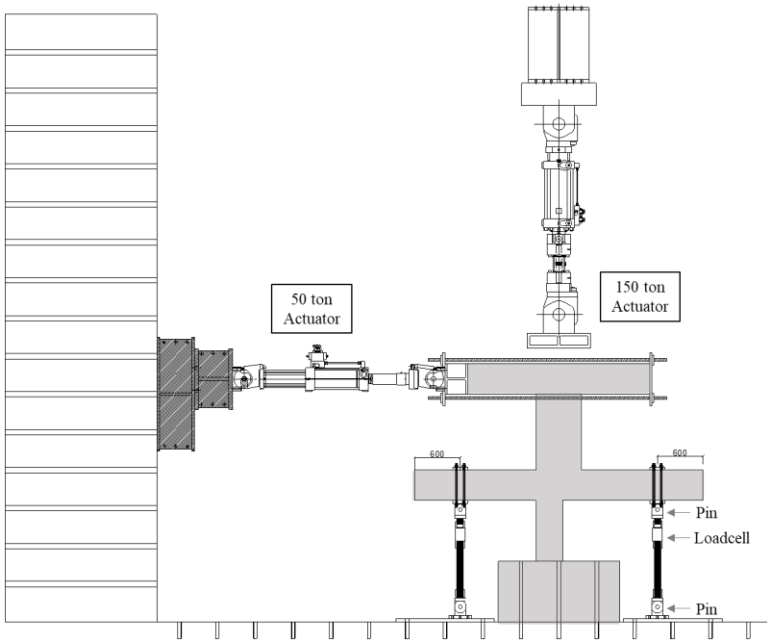

(b) Test setup in Cyclic loading

Figure 4-20 Test setup for moment-resisting frame specimen

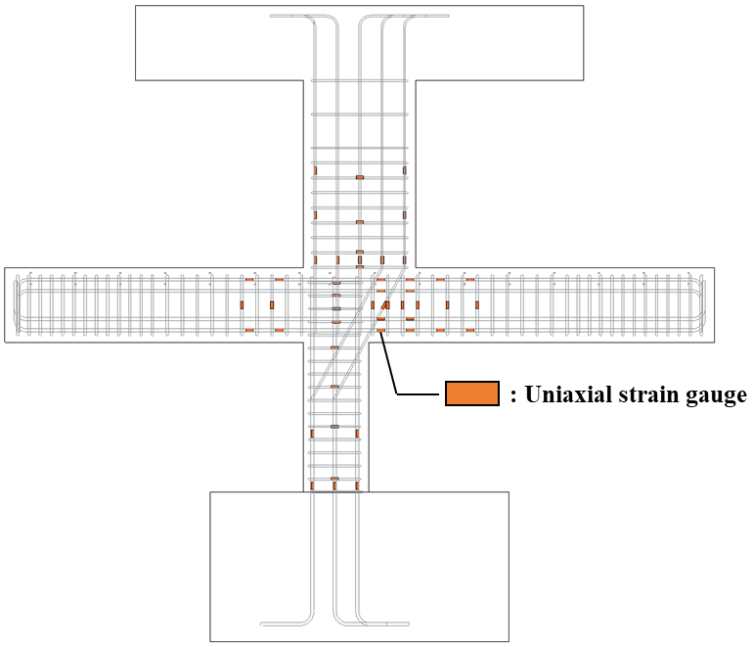

(a) W-R40-BR

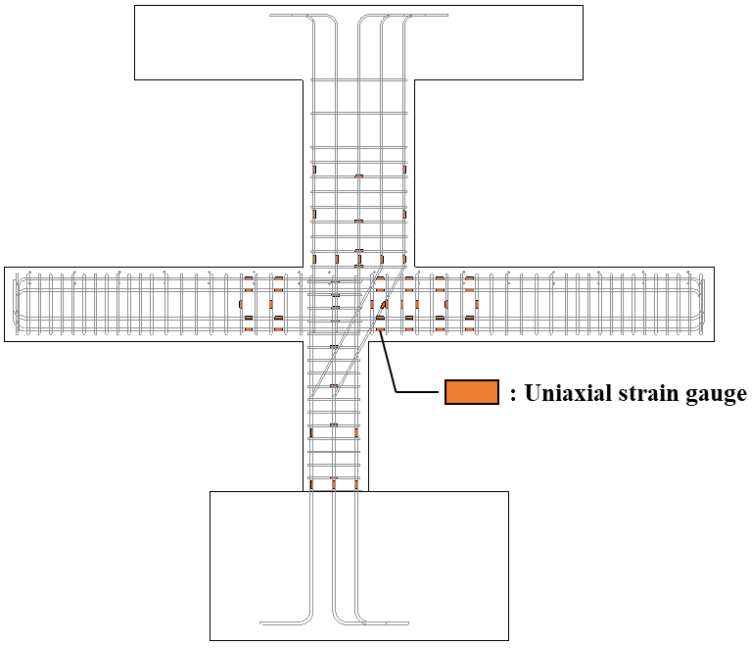

(a) WB-R40-BR

Figure 4-21 Strain gauge plan for moment-resisting frame specimen

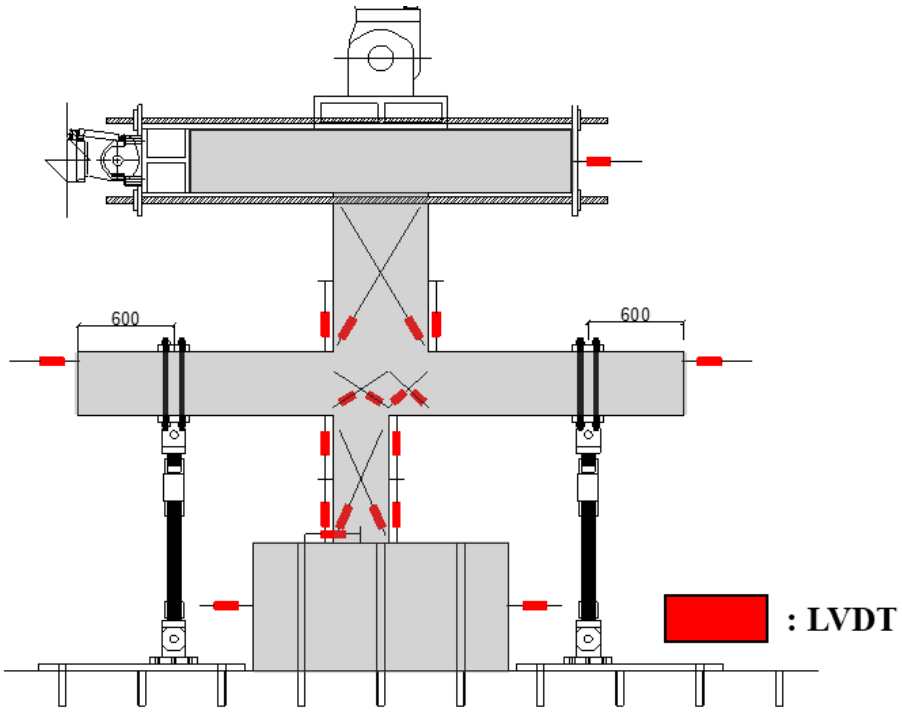

Figure 4-22 LVDT plan for moment-resisting frame specimen

4.5.3 Specimens with in-plane lateral support

Figure 4-23 shows the setup of the specimens with in-plane lateral support. The load cell received compression force was placed at the end of the beam so that the specimen was supported in the in-plane direction. A roller was installed at the bottom of the load cell for lateral displacement that could occur during cyclic loading.

During the constant compression force through the actuator, the in-plane lateral supports and the specimen were not thoroughly attached. So, only the specimen received the compression force. Before starting the cyclic loading, the in-plane lateral supports were completely attached to the specimen. So, a specimen was partially supported in the in-plane direction.

In the W-R25-BL specimen that does not allow lateral displacement, there is a distance between the in-plane lateral support and a specimen during cyclic loading. So, it was planned to periodically remove the gab through the screw jack in the cyclic loading. On the other hand, in the W-R40-BL specimen, it was planned to allow the lateral displacement that occurs during cyclic loading.

The measurement plan of the specimens with in-plane lateral support is shown in Figure 4-21 and Figure 4-22. The LVDT and strain gauge was planned for the same purpose as the moment-resisting frame specimens. However, the moment-resisting frame specimens and specimens with in-plane lateral support have different gauge measurement plan on the column. This plan reflects the strut-tie model analysis with a different maximum strength between the two boundary conditions.

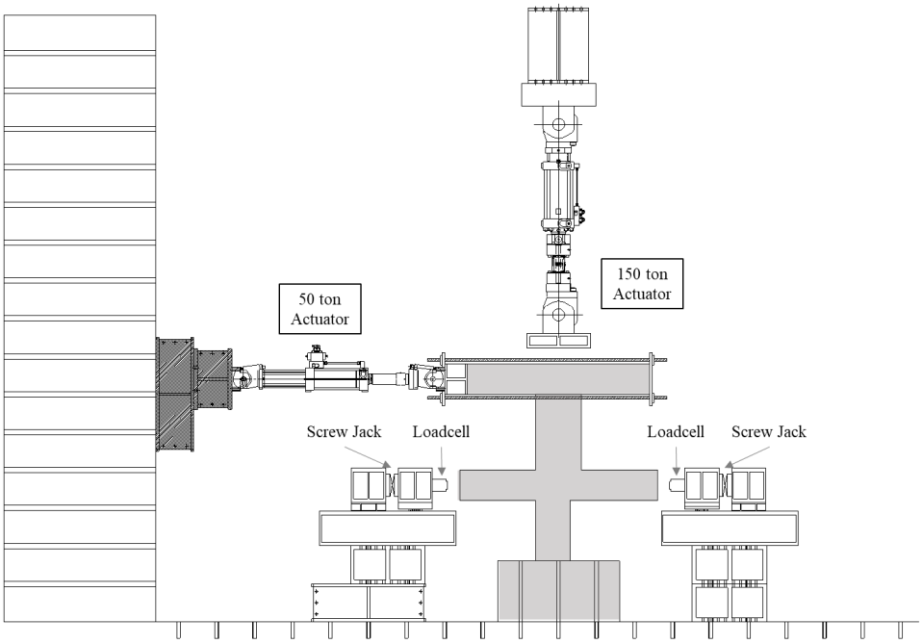

(a) Test setup in compression loading

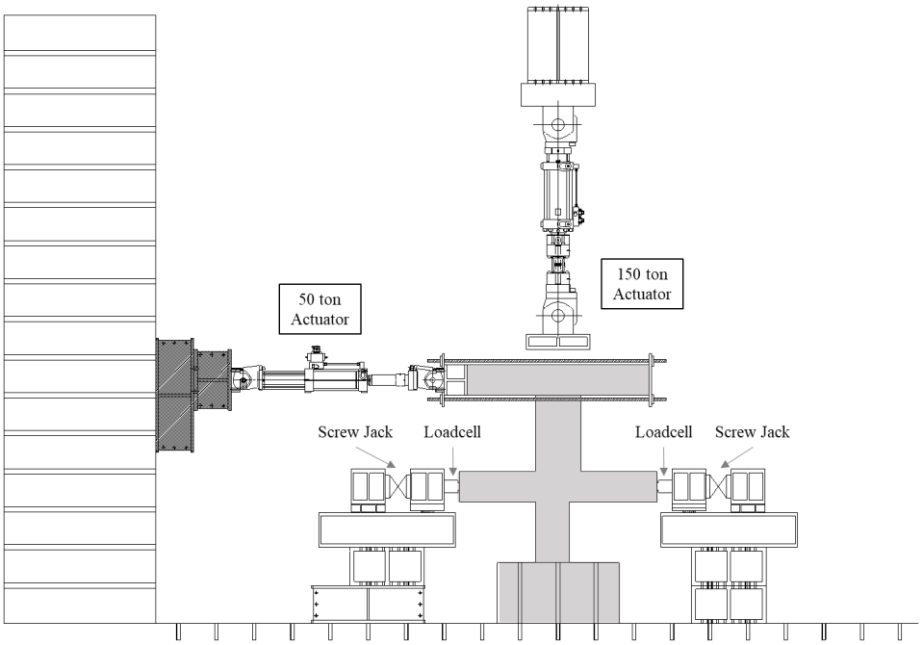

(b) Test setup in Cyclic loading

Figure 4-23 Test setup for specimen with in-plane lateral support

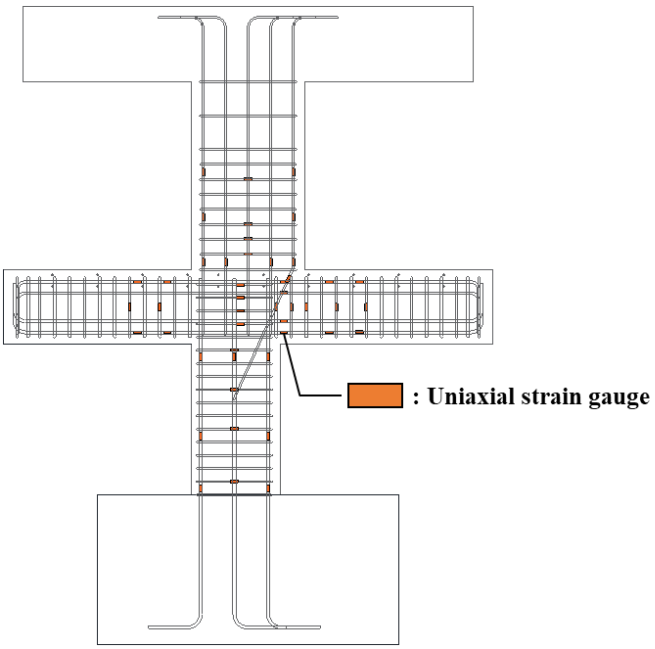

(a) W-R25-BL

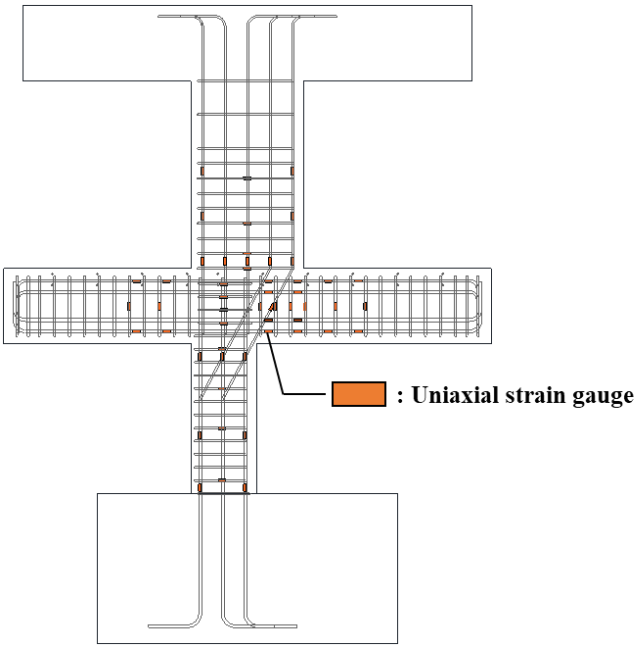

(b) W-R40-BL

Figure 4-24 Strain gauge plan for specimen with in-plane lateral support

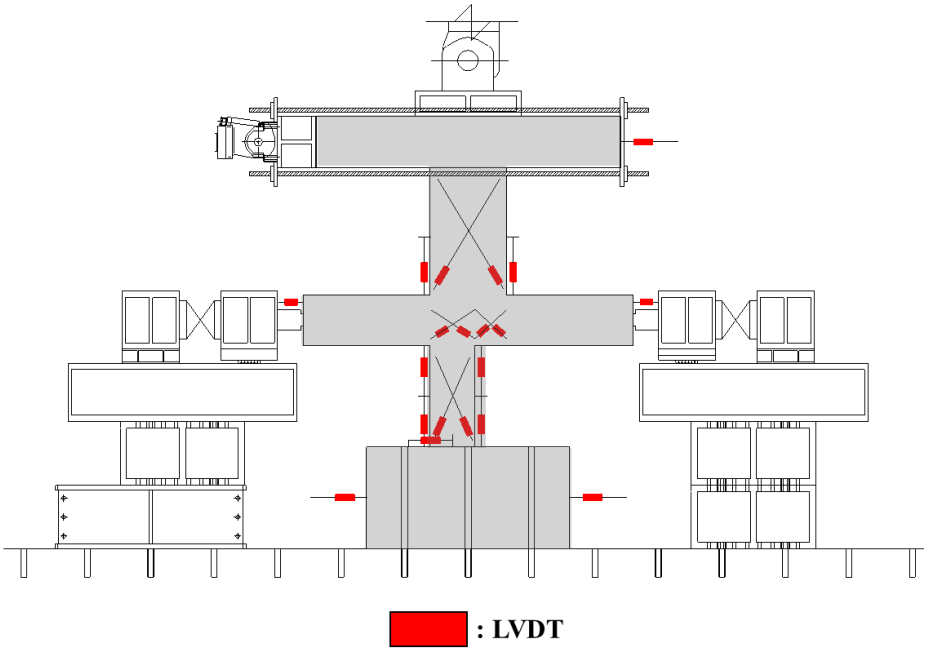

Figure 4-25 LVDT plan for specimen with in-plane lateral support

4.5.4 Loading plan

The test assumes an earthquake load under the gravity load. Therefore, cyclic loading was performed with a constant compression force(468kN) in the setup.

Figure 4-26 and Table 4-4 show the loading plan. The cyclic loading was applied in the method proposed in ACI 374, and the following criteria were satisfied.

- The initial larteral drift ratio must be within the elastic range.
- The increase rate of the lateral drift ratio should be not less than 1.25 times and not more than 1.5 times.
- At each loading step, the lateral drift ratio should be applied three times.

The lateral drift ratio presented in the loading protocol is the height of 2400mm from the loading slab to the column excluding the foundation.

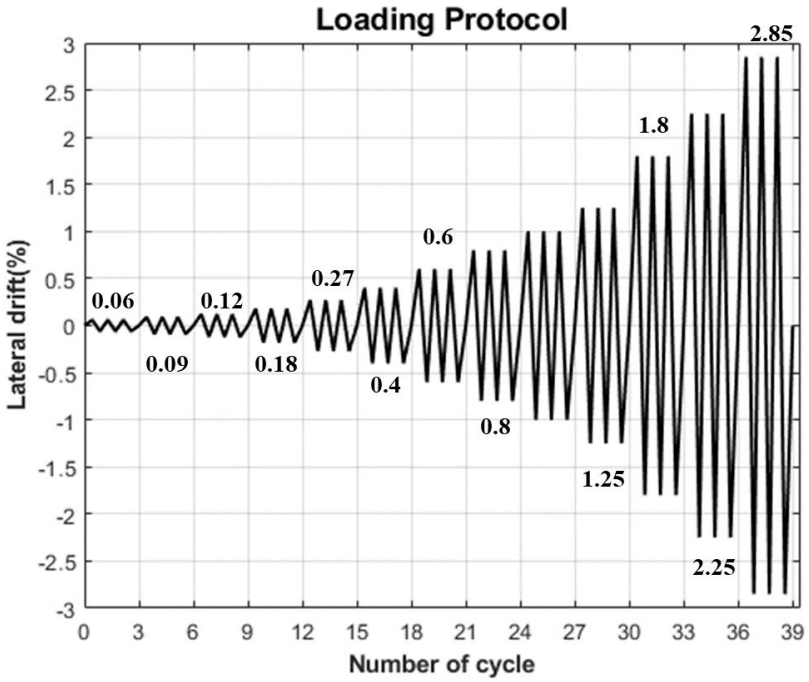

Figure 4-26 Loading protocol

Table 4-4 Value of loading protocol by step

Step	Lateral Drift (%)	Lateral displacement (mm)
1	0.06	1.44
2	0.09	2.16
3	0.12	2.88
4	0.18	4.32
5	0.27	6.48
6	0.4	9.60
7	0.6	14.40
8	0.8	19.20
9	1	24.00
10	1.25	30.00
11	1.8	43.20
12	2.25	54.00
13	2.85	68.40

4.6 Summary

In this chapter, the design and plan of the specimen based on the capacity design concept of the wall-column transfer structure were described. The summary of the design method, test parameters, and test plans is as follows.

A change in the geometry for the wall-column transfer structure is a D-region where can be not applied assumptions of flexural theory. Therefore, the capacity design of the specimen was conducted through the strut-and-tie model. The boundary condition of specimen considers two extreme support conditions. One is assumed that the moment-resisting frame with a similar stiffness is continuous to support lateral force. It is supported by flexural moment resistance on the beam. The other is assumed that it was laterally supported due to the rigid structure.

The specimen has reduced dimensions (1/2 width, 1/3 height, and 1/2 thickness) of the prototype structure. The test parameters include boundary conditions, re-bar ratio, reduction in width, allowable lateral displacement according to lateral support, and use of an overstrength factor.

The test setup was planned to a cyclic loading test with a nominal constant compression load of 0.2 $f_c^{'}A_g$. After the compression force was applied, the lateral boundary condition for each specimen was planned to be set. Considering the actual RC building, the out-of-plane direction of the specimens is supported in the test setup.

Chapter 5. Test Results

5.1 Material test

5.1.1 Concrete

For the concrete compressive strength test, three or more concrete specimens ($\emptyset 100 \times 200 mm^2$) were manufactured on the date of concrete pouring. The concrete strength was tested using a U.T.M (Universal Testing Machine) according to the KS standard on the day of the test. Each test result is shown in Table 5-1.

Table 5-1 Concrete Strength by specimen

	W-R40-BR		WB-R40-BR		W-R25-BL		W-R40-BL	
	f_{ck} (MPa)	$f_{ck,avg}$ (MPa)	f_{ck} (MPa)	$f_{ck,avg}$ (MPa)	f_{ck} (MPa)	$f_{ck,avg}$ (MPa)	f_{ck} (MPa)	$f_{ck,avg}$ (MPa)
Foundation	32.1	33.3	32.1	33.3	37.2	36.1	37.2	36.1
	33.4		33.4		35.3		35.3	
	34.5		34.5		35.9		35.9	
1st floor	36.4	36.7	32.8	32.6	31.7	32.5	35.0	40.3
	36.8		31.6		32.0		38.6	
	36.9		33.5		33.8		41.7	
2nd floor	36.2	36.6	40.0	37.0	35.5	34.9	30.8	34.1
	38.1		36.9		32.8		34.0	
	35.6		34.2		36.3		37.6	

※ 1st floor : column, beam, slab

※ 2nd floor : wall, loading slab

5.1.2 Steel

The specimens used SD500 rebar for under the D13 and SD600 rebar for over the D16 as in the RC apartment. Although re-bar of various diameters was used in the specimen, tensile tests were performed on D10 and D16 as representatives of SD 500 and SD600. A 600mm specimen was prepared for the tensile test of the re-bar used in the specimen, and the tensile test was performed using a U.T.M. The results of the tensile test are shown in Table 5-2, and the stress-strain curve is shown in Figure 5-1.

Table 5-2 Tensile test results of re-bar

Grade / Diameter	f_y (MPa)	$f_{y,avg}$ (MPa)	$\varepsilon_{y,avg}$ (mm/mm)	f_u (MPa)	$f_{u,avg}$ (MPa)
SD 500 / D10	572	574	0.0029	675	672
	566			668	
	585			675	
SD 600 / D16	649	657	0.0033	796	804
	662			811	
	659			806	

※ f_y : Yield strength

※ f_u : Tensile strength

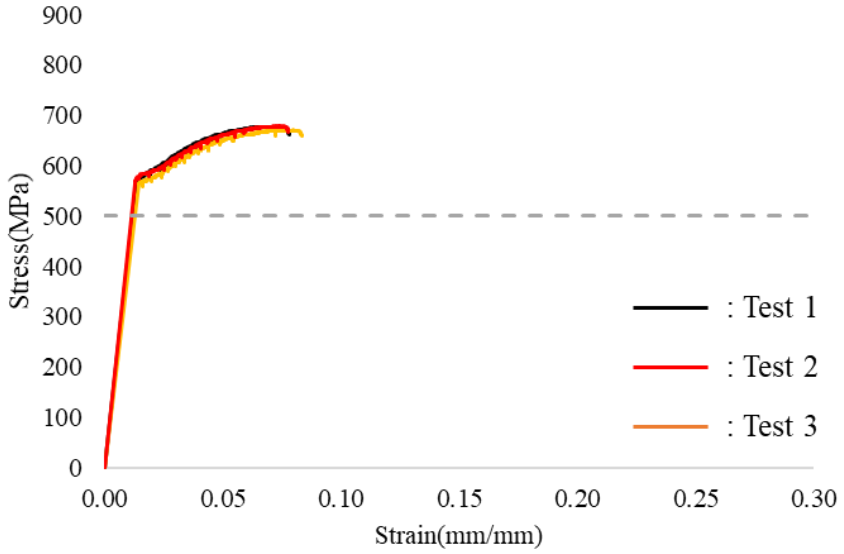

(a) SD500 re-bar (D10)

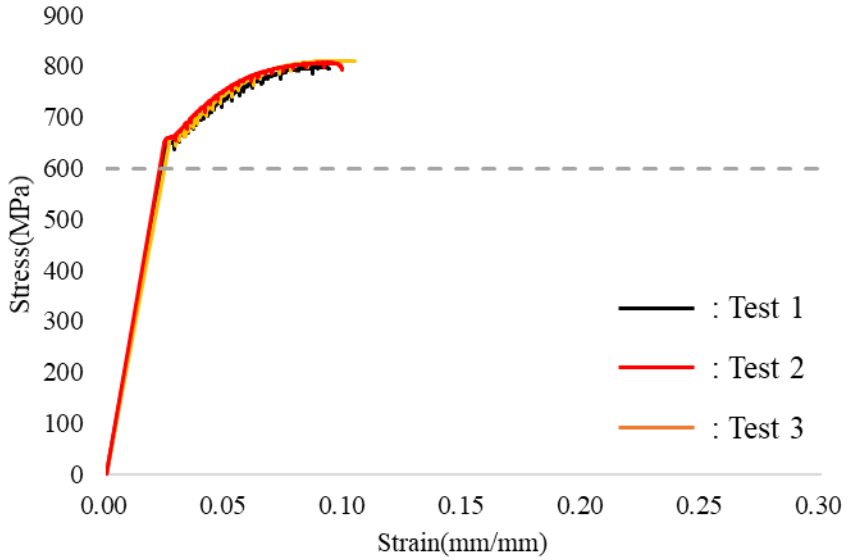

(b) SD 600 re-bar (D16)

Figure 5-1 Stress-strain relationship of re-bar

5.2 Load-displacement relationships

Figures 5-2 to 5-4 show the lateral load - lateral drift ratio curve for each specimen. The lateral drift ratio (δ) indicates the net lateral displacement divided by the net height. The net lateral displacement indicates the difference between the lateral displacements measured at the loading slab and the slab of beam. The net hight (1,260mm) is the distance between the measurement points. That is, the behavior of wall was analyzed with the concept of story drift. Because the upper wall is the main purpose of capacity design.

$$\delta = \frac{\Delta_{net}}{h} \tag{5-1}$$

Where, δ = Lateral drift ratio, Δ_{net} = Net lateral displacement (Δ-Δ_{1st}), h = Net height (1,260mm)

V_n in Figures 5-2 to 5-3 and $V_{n,wall}$ in Figure 5-4 are the target strength that induce flexural yielding of the wall, which was determined as the design lateral load of the specimens.

$$V_n(V_{n,wall}) = 174(M_n)/1.2(h) = 145kN \tag{5-2}$$

Where, $M_n =$ Nominal strength of wall, $h =$ Net wall height

Except for the W-R40-BL specimen, the ultimate strength exceeded the target strength in the positive direction. Flexural compression failure (progressive concrete crushing) occurred at the top of the column as shown in Figure 5-12. Therefore, $V_{n,col}$ was calculated to determine whether the reason of the strength smaller than the target strength V_n was due to the flexural

failure of the column.

$$V_{n,col} = 160(M_n) / 1.6(h) = 100kN \quad (5\text{-}3)$$

Where, $M_n =$ Nominal strength of column, $h =$ Distance from loading to crushing

There was a difference of 30% between the calculated nominal strength of column, $V_{n,col}$ and the ultimate strength in the positive direction (130kN). On the other hand, there was a difference of about 5% from the ultimate strength(-106.1kN) in the negative direction. In Figure 5-21 (Strain distribution of vertical rebar in W-R40-BR), the net tensile strain of the wall also reached the yield strain. So, the strength increased relatively in the positive direction. As a result, W-R40-BL specimen did not reach the target strength due to the flexural compression failure of column. Contrary to the intention of making the flexural yielding of the wall in the system, the flexural compression failure of the column was formed as the dominant behavior. Therefore, it is necessary to apply overstrength factor to the column so that the failure of the column is not concentrated.

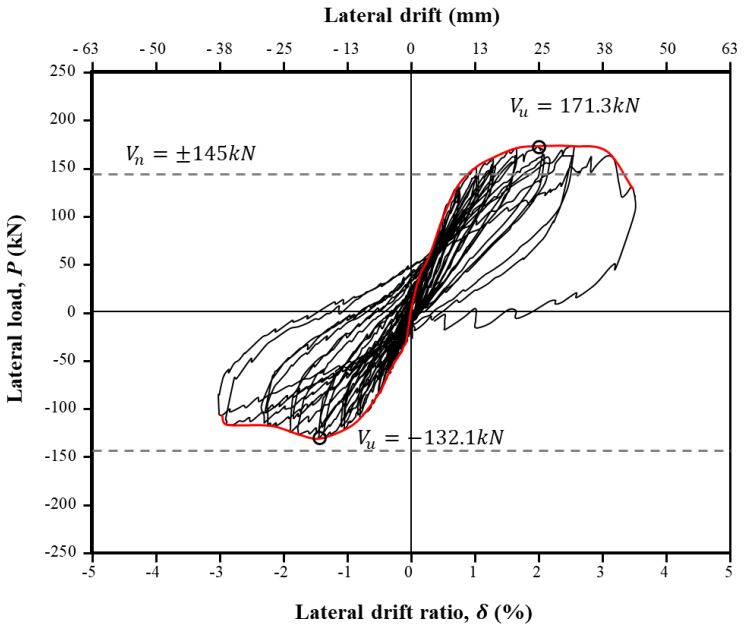

Figure 5-2 Lateral load - lateral drift relationship of W-R40-BR

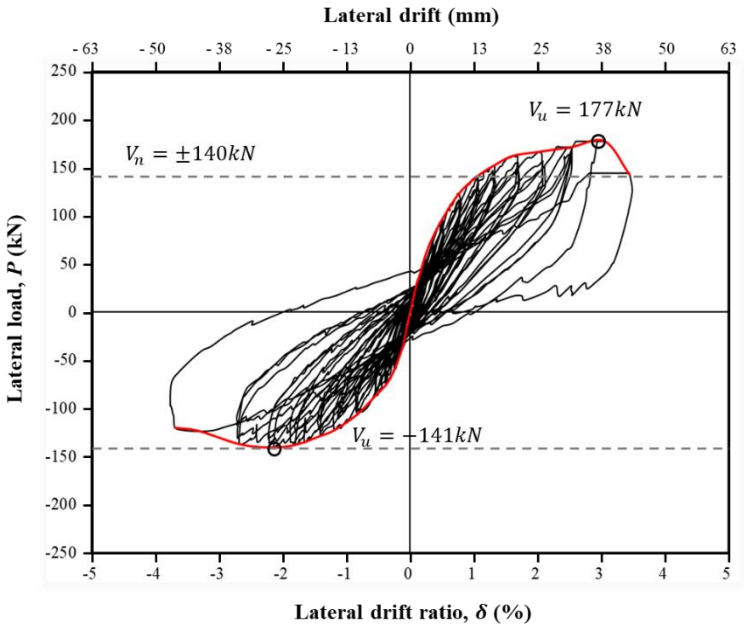

Figure 5-3 Lateral load - lateral drift relationship of WB-R40-BR

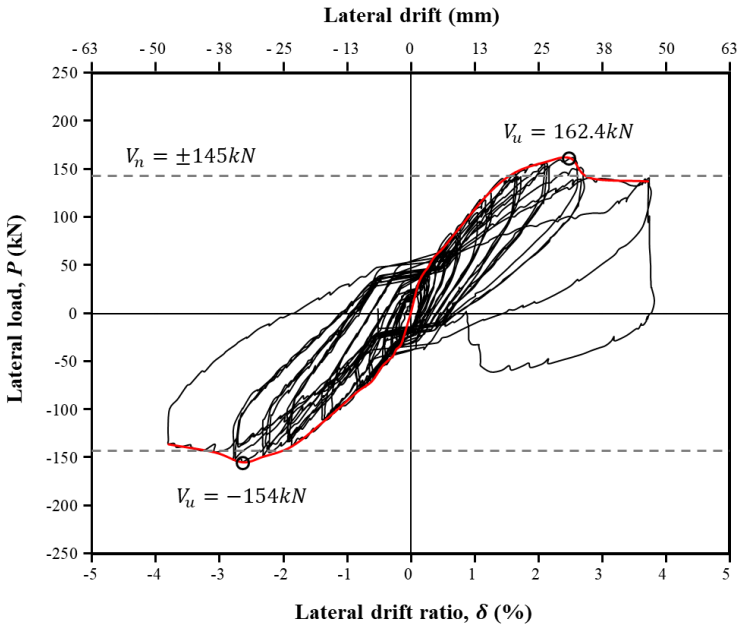

Figure 5-4 Lateral load - lateral drift relationship of W-R25-BL

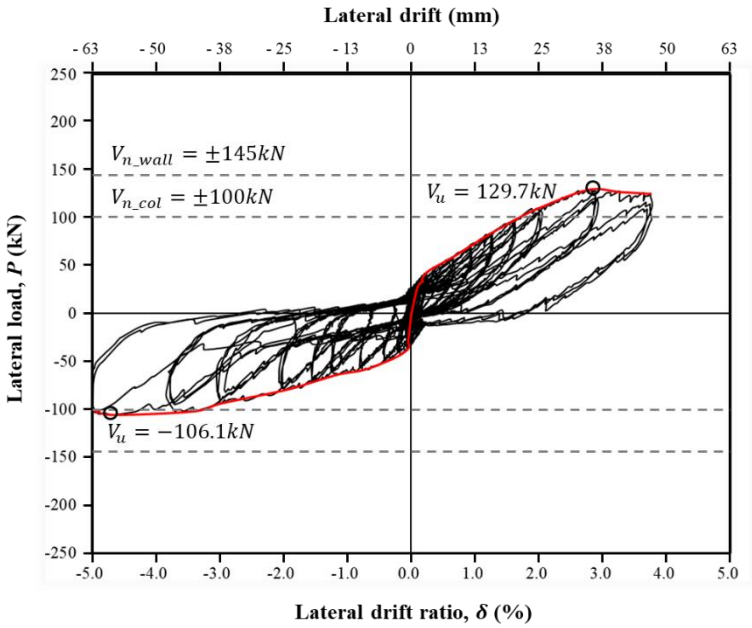

Figure 5-5 Lateral load - lateral drift relationship of W-R40-BL

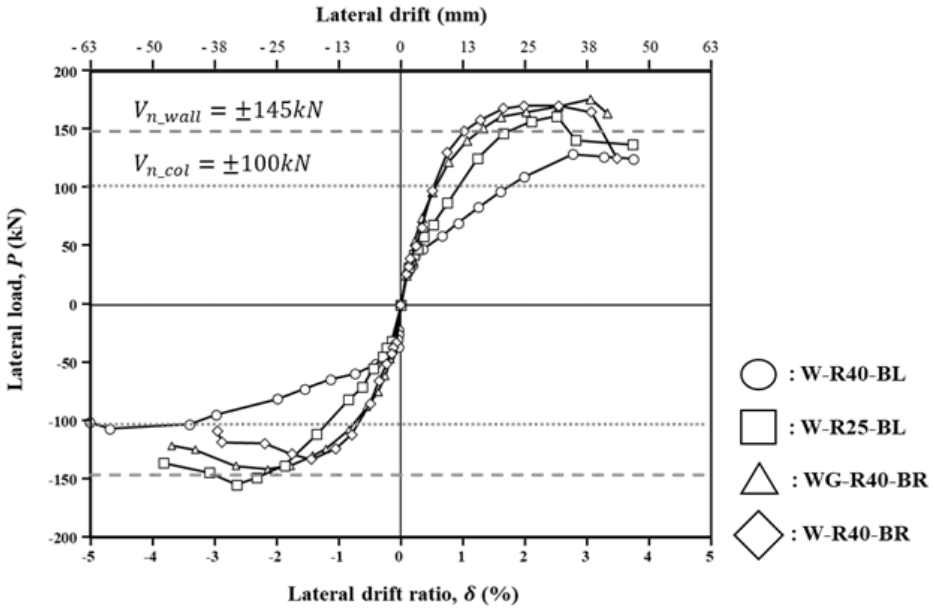

Figure 5-6 Envelope curve of specimens

Figure 5-6 is the envelope curve of each specimen. The graph shows the maximum lateral drift ratio and load of each step in the load-displacement relationship. The load-displacement relationship showed that ductile behavior occurred without premature brittle failure in all specimens. The structural performance diffed in the ultimate strength in terms of the reduction in width and loading direction. On the other hand, the same performance was shown in the displacement.

In most of the specimens, the ultimate strength in the negative direction was smaller than in the positive direction. Even the W-R40-BR and WB-R40-BR specimens with a high reduction in width did not reach the target strength within 10%. The tensile rebar of the wall in the negative direction did not reach the

inelastic deformation compared to the tensile rebar in the positive direction. (Refer to Ch5.6 Strain of Re-bar) Therefore, the ultimate strength in the negative direction did not result in the the target strength and over-strength. Therefore, the target strength (design strength) of the wall is not reached in the positive direction should be reflected in the design guidelines.

5.3 Ductility

The specimens were evaluated for ductility through the yield strength, yield displacement, and ultimate displacement as shown in Figure 5-7. Yield displacement and ultimate displacement can be defined in various methods. Considering that the prototype of this test is an RC structure, the yield displacement was defined as the lateral displacement in which the secant stiffness, which exceeds 75% of the maximum strength, reaches the ultimate strength. The ultimate displacement was defined as the later displacement in which a constant compression force is no longer applied due to the concrete crushing of the specimens.

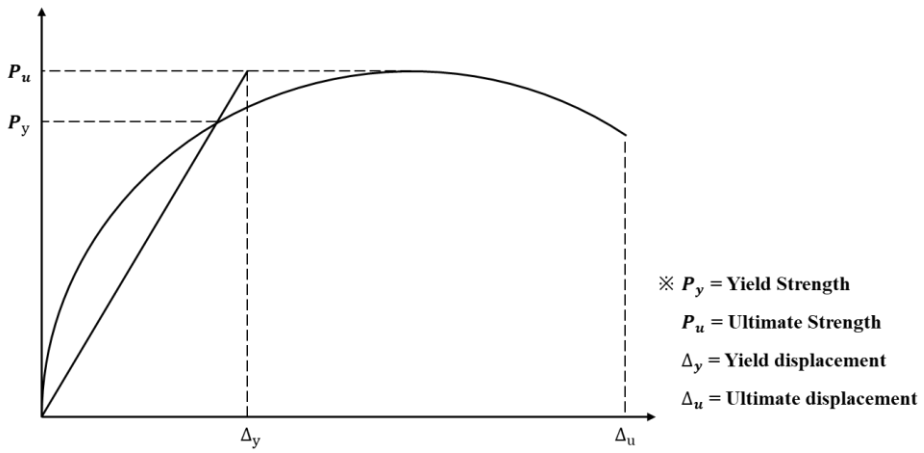

Figure 5-7 Definition of yield and ultimate displacement

Based on the definitions, the yield and ultimate strength, yield and ultimate displacement, and ductility for each specimen are summarized as shown in Table 5-3. The ductility is the ultimate lateral displacement divided by the yield displacement, and the yield stiffness is the ultimate strength divided by the yield displacement.

Table 5-3 Summary of ductility by the specimens

	P_y (kN)		P_u (kN)		K_{sec} (kN/mm)		Δ_y (mm)		Δ_u (mm)		μ	
	Pos (+)	Neg (-)	Pos (+)	Neg (-)	Pos (+)	Neg (-)	Pos (+)	Neg (-)	Pos (+)	Neg (-)	Pos (+)	Neg (-)
W-R40-BR	128	-99	171	-132	9.1	6.4	18.9	-20.8	46.9	-46.1	2.5	2.2
WB-R40-BR	125	-106	177	-141	8.4	7.0	21.0	-20.0	54.4	-56.7	2.6	2.8
W-R25-BL	122	-115	162	-154	8.2	8.9	19.7	-17.4	43.1	-44.3	2.2	2.5
W-R40-BL	97	-80	130	-106	4.1	2.5	31.4	-41.8	53.4	-69.3	1.7	1.7

The ductility ranged from 2.2 to 2.8 in the test where the flexural failure of the wall occurred. On the other hand, the ductility of the W-R40-BL specimen where flexural compression failure of the column takes place is 1.7. The lateral load - drift relationship showed the same ductile behavior, but the ductility evaluation confirms that flexural yielding of wall has better performance.

In the moment-resisting frame specimen, WB-R40-BR specimen has higher ductility than W-R40-BR specimen. This is because the concrete crushing of the wall occurred relatively late. So, the ultimate displacement was higher.

5.4 Energy dissipation

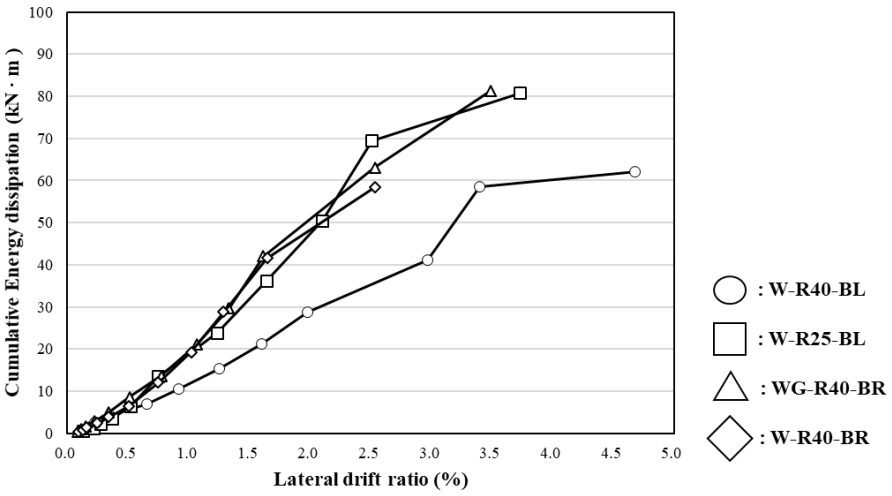

Figure 5-8 Energy dissipation by the specimens

Table 5-4 Energy dissipation by loading step

Step	Cumulative energy dissipation (kN·m)			
	W-R40-BR	WB-R40-BR	W-R25-BL	W-R40-BL
1	0	0	1	0
2	1	1	1	1
3	1	2	2	2
4	2	3	4	3
5	4	5	6	4
6	6	9	13	7
7	12	14	24	11
8	19	21	36	15
9	29	30	51	21
10	42	42	69	29
11	58	63	81	41
12	-	81	-	58
13	-	-	-	62

Figure 5-8 and Table 5-4 show the cumulative energy dissipation according to the displacement ratio of each specimen. Energy dissipation capacity is defined as the area of the closed curve at each cycle in the load-displacement relationship.

Moment-resisting frame specimens (WB-R40-BR, W-R40-BR) show almost similar energy dissipation capacity up to 2.0 lateral drift ratio. But there is a difference in energy dissipation as the lateral drift ratio increases in the inelastic region. In particular, as the WB-R40-BR specimen behaved up to a higher ultimate displacement, the difference in the final cumulative energy dissipation was large.

Since specimens with in-plane lateral support (W-R25-BL, W-R40-BL) have different failure mode, there is a large difference in cumulative energy dissipation from a low later drift ratio. The ultimate displacement is larger for the W-R40-BL specimen whose failure mode is a flexural compression failure of the column, but the W-R25-BL specimen with flexural failure of the wall has high strength capacity.

5.5 Failure mode

Figures 5-9 to 5-12 show the crack pattern and failure mode of each specimen due to cyclic loading with constant compression loading.

Flexural cracks of the wall induced in all the specimens were found. Except for the W-R40-BL specimen, flexural failure dominated in the wall. The tests were terminated due to the concrete crushing due to compression and lateral loading at high lateral drift ratio.

The W-R40-BL specimen allowed lateral displacement in the in-plane lateral support, so the crack pattern and failure mode differed. When the lateral displacement was small, the behavior was similar to that of other specimens. But as the lateral displacement increased, cracks were concentrated on the upper column. It is analyzed that the compressive stress is relatively concentrated on the discontinuous section, as the cantilever behavior is added to the column by allowing lateral displacement. Accordingly, flexural compression failure occurred at the upper of the column at a high lateral drift ratio. Cracks of a column around the diagonal re-bar are caused by not acquiring a concrete cover due to construction problems.

In specimens except for W-R40-BL, shear cracks in the joint and flexural cracks in the column occurred when cyclic loading at a high lateral drift ratio. However, as the crack width was generally small compared to the wall, it was not dominant.

In the specimen with a 40% reduction ratio in width, diagonal strut cracks

were seen in the discontinuous section between the wall and the column. The crack width gradually increased as the lateral drift ratio increased. This strut crack extends from the negative direction to a nearby tensile crack. In addition, the compression force from the wall is transferred to the lower column through the 1:2 inclined strut axis in the transfer zone. In general, it is known that the compression force spreads with the above slope. So, it is analyzed that the axis comes out in the transfer zone as the compression force was transferred from the wall to the column. On the other hand, such cracks occurred in the specimen with a relatively small reduction in width were relatively small.

The moment-resisting frame specimen was laterally supported by the flexural moment of the beam, and flexural cracks occurred at the bottom of the beam. As the minimum reinforcement of the slab was added in addition to the strut-tie model design, flexural cracking hardly happened due to the relatively high flexural stiffness on top of the beam. The flexural crack pattern of the beam was clear in WB-R40-BR induced yielding of the wall and beam. (Refer to Ch5.6 Strain of Re-bar) In fact, the tensile rebar of beam reached the yield strain in the discontinuous section. Even the flexural crack by the beam led to the column as the lateral drift ratio increased. On the other hand, the cracks were not severe and didn’t lead to the column in the W-R40-BR specimen induced yielding of the wall.

In the specimens with in-plane lateral support (W-R25-BL, W-R40-BL), there was almost no cracks in the beam due to the in-plane lateral support.

(a) Crack of vertical member

(b) Flexural failure of wall

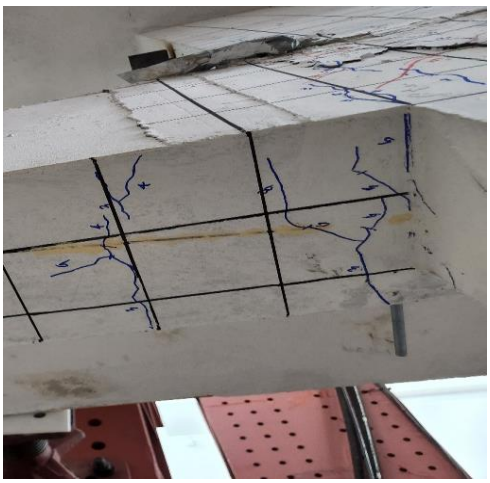

(c) Flexural crack on left side of beam

(d) Flexural crack on right side of beam

Figure 5-9 Failure mode of W-R40-BR

(a) Crack of vertical member

(b) Flexural failure of wall

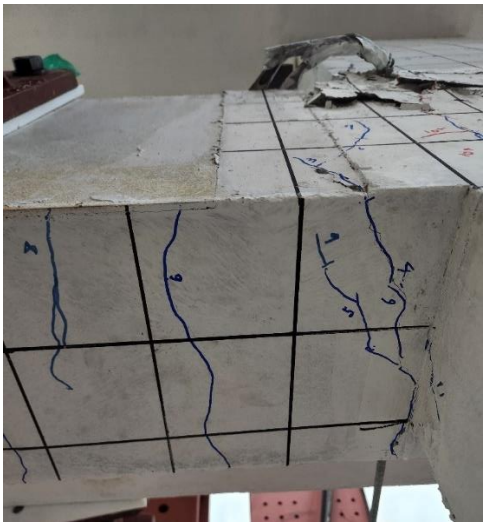

(c) Flexural crack on left side of beam

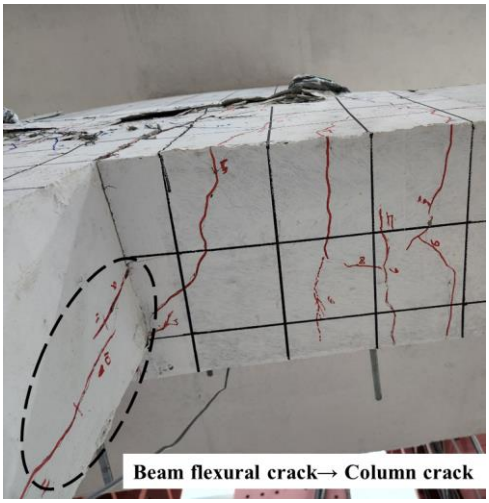

(d) Flexural crack on right side of beam

Figure 5-10 Failure mode of WB-R40-BR

(a) Crack of vertical member

(b) Flexural failure of wall

Figure 5-11 Failure mode of W-R25-BL

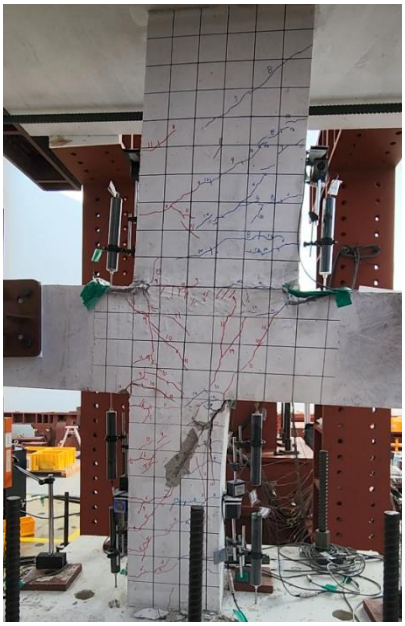

(c) Crack of vertical member

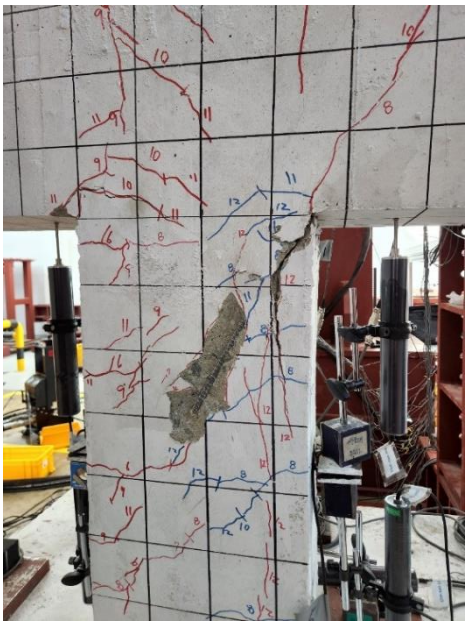

(d) Flexural compression failure of wall

Figure 5-12 Failure mode of W-R40-BL

5.6 Strain of rebar

5.6.1 Yielding state of member

In order to examine whether the member designed by capacity design yields or not, the rebar strain gauge attached to each member of the specimens was conformed. Figures 5-13 ~ 5-16 show the location of the strain gauge in the re-bars.

The dotted line in the graph represents the yield strain of the re-bar. The yield strain varies depending on the diameter of the rebar used for each member. The yield strain of re-bars below D13 is $\varepsilon_y = 0.0029$ and the rebars above D16 is $\varepsilon_y = 0.0033$.

Figures 5-17 to 5-18 and Table 5-5 show the strain of members in the W-R40-BR specimen. As a capacity design intended, the tensile re-bars of the wall reach or exceed the yield strain, and the tensile re-bars and transverse reinforcement of other members do not reach the yield strain and maintain an elastic state.

Figures 5-19 to 5-20 and Table 5-6 show the strain of members in the WB-R40-BR specimen. As a capacity design intended, the tensile re-bars in the wall and beam of the discontinuous section yield at the ultimate strength. However, the tensile re-bars of the column also yield in the positive direction in the last loading step. It is analyzed that the moment redistribution to the column occurred as the wall behaved inelastic stage due to flexural bending.

Figures 5-21 to 5-22 and Table 5-7 show the strain of members in the W-

R25-BL specimen. The tensile re-bars of the wall reach or exceed the yield strain. The other rebars do not reach the yield strain and maintain an elastic state.

Figures 5-23 to 5-24 and Table 5-8 show the strain of members in the W-R40-BL specimen. At the ultimate strength in the positive direction, the tensile re-bar in the wall and the column reaches the yield strain. Therefore, it is analyzed that the strength is the middle according to the nominal flexural strength ($V_{n,wall}$ and $V_{n,col}$) of the wall and the column. In the negative direction, flexural compression failure took place at the top of the column, so the strain of the tensile re-bar at the top of the column did not increase. (Refer to Ch5.5 Failure mode) In addition, other re-bars maintain the elastic state as other specimens.

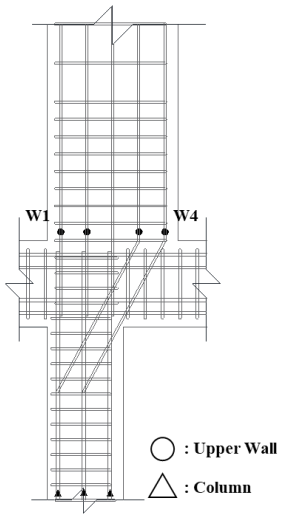

(a) Moment-resisting frame specimen

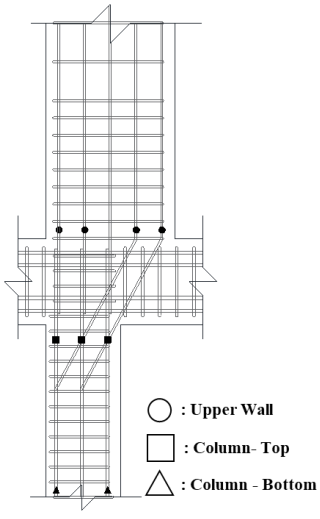

(b) Specimen with in-plane lateral support

Figure 5-14 Gauge location of vertical member

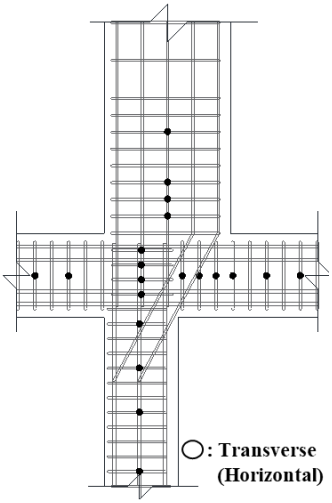

Figure 5-13 Gauge location of Transverse reinforcement

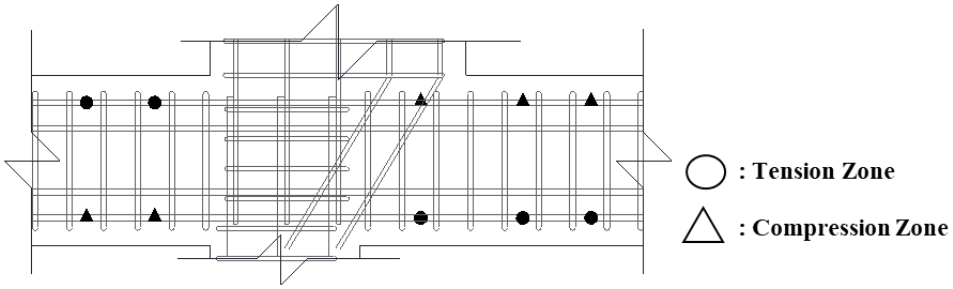

Figure 5-15 Gauge location of horizontal member (Excluding WB-R40-BR)

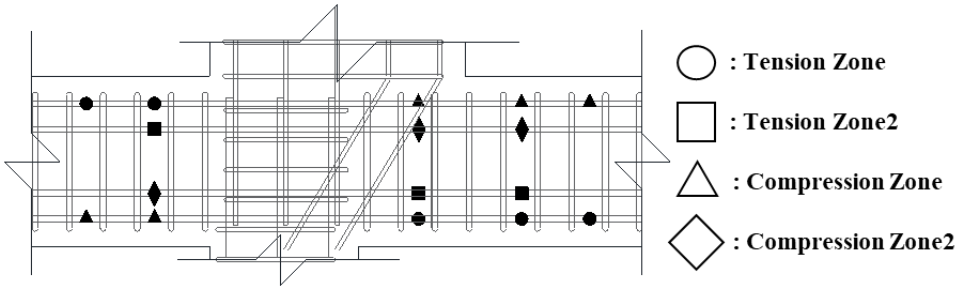

Figure 5-16 Gauge location of horizontal member (Only WB-R40-BR)

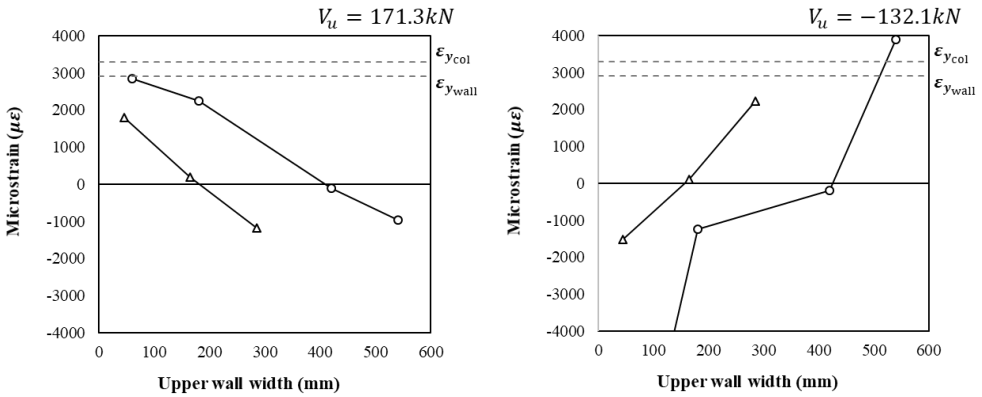

(a) Peak strength in the positive direction (b) Peak strength in the negative direction

Figure 5-17 Strain distribution of vertical rebar in W-R40-BR

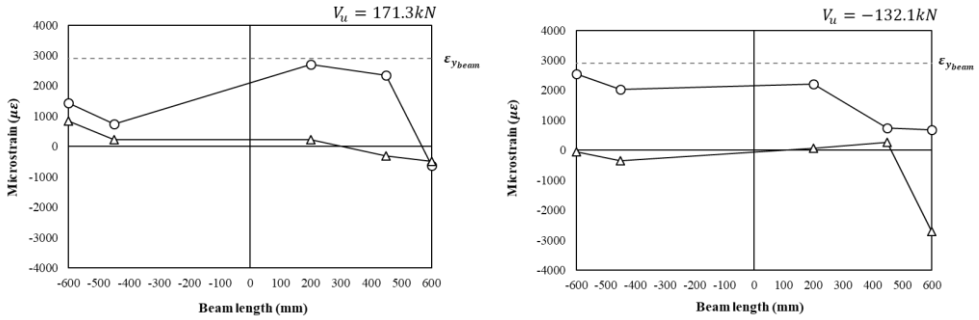

(a) Peak strength in the positive direction (b) Peak strength in the negative direction

Figure 5-18 Strain distribution of longitudinal rebar in W-R40-BR

Table 5-5 Maximum strain of horizontal (transverse) reinforcement

Location of horizontal (transverse) reinforcement	$\varepsilon_{max}\ (strain, mm/mm)$
Wall	0.0022
Column	0.0022
Beam	0.0006
Joint	0.0011
Yield strain	0.0029

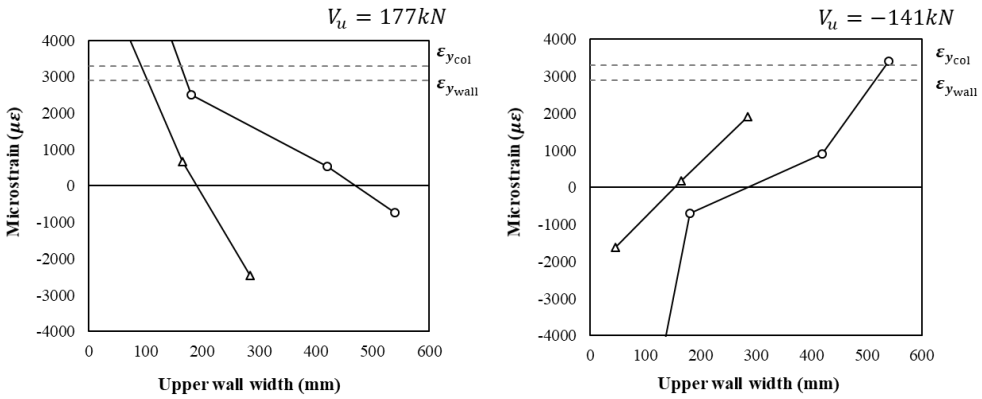

(a) Peak strength in the positive direction (b) Peak strength in the negative direction

Figure 5-19 Strain distribution of vertical rebar in WB-R40-BR

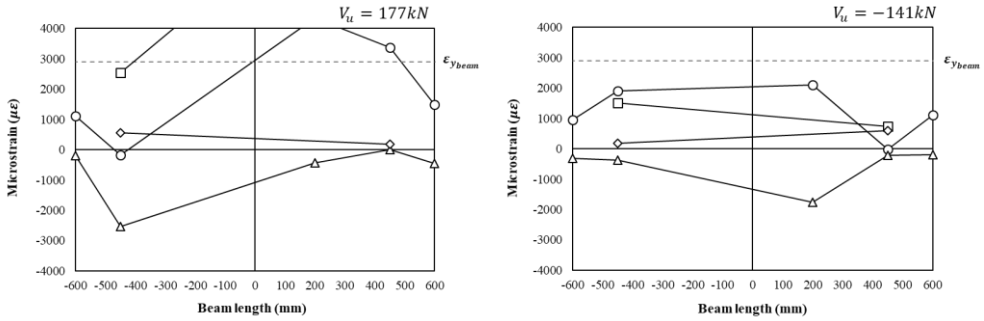

(a) Peak strength in the positive direction (b) Peak strength in the negative direction

Figure 5-20 Strain distribution of longitudinal rebar in WB-R40-BR

Table 5-6 Maximum strain of horizontal (transverse) reinforcement

Location of horizontal (transverse) reinforcement	$\varepsilon_{max}\ (strain, mm/mm)$
Wall	0.0009
Column	0.0012
Beam	0.0015
Joint	0.0003
Yield strain	0.0029

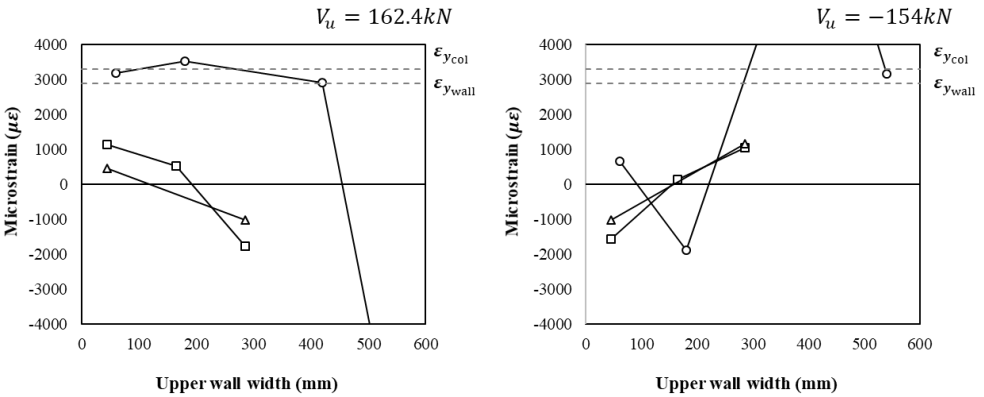

(a) Peak strength in the positive direction (b) Peak strength in the negative direction

Figure 5-21 Strain distribution of vertical rebar in W-R25-BL

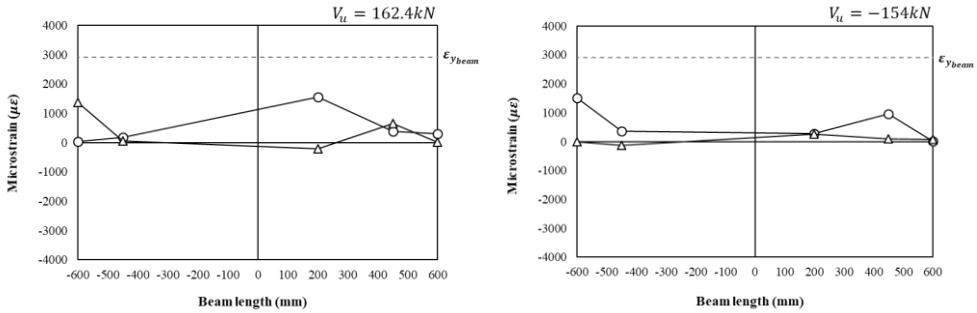

(a) Peak strength in the positive direction (b) Peak strength in the negative direction

Figure 5-22 Strain distribution of longitudinal rebar in W-R25-BL

Table 5-7 Maximum strain of horizontal (transverse) reinforcement

Location of horizontal (transverse) reinforcement	$\varepsilon_{max}\ (strain, mm/mm)$
Wall	0.0003
Column	0.0001
Beam	0.0005
Joint	0.0006
Yield strain	0.0029

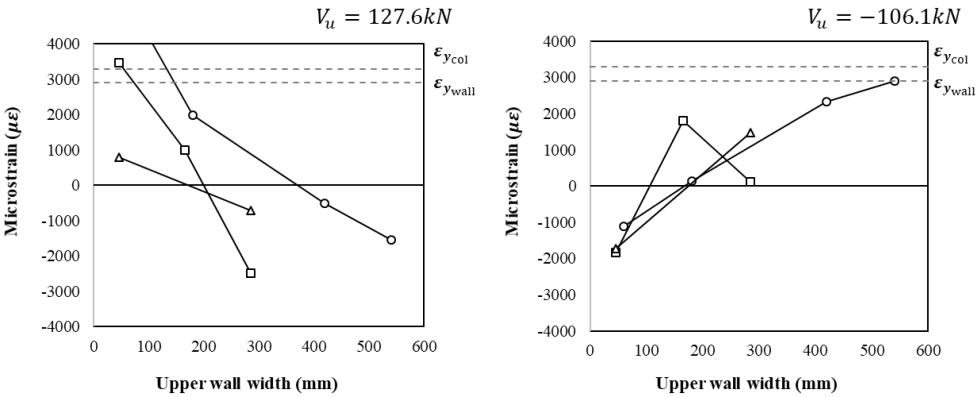

(a) Peak strength in the positive direction (b) Peak strength in the negative direction

Figure 5-23 Strain distribution of vertical rebar in W-R40-BL

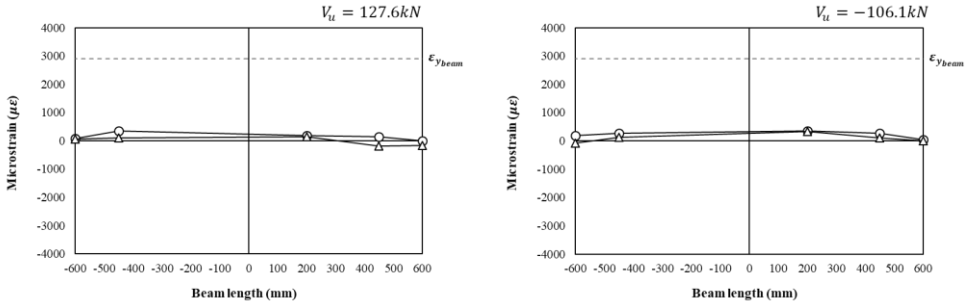

(a) Peak strength in the positive direction (b) Peak strength in the negative direction

Figure 5-24 Strain distribution of longitudinal rebar in W-R40- BL

Table 5-8 Maximum strain of horizontal (transverse) reinforcement

Location of horizontal (transverse) reinforcement	$\varepsilon_{max}\ (strain, mm/mm)$
Wall	0.0006
Column	0.0011
Beam	0.0003
Joint	0.0006
Yield strain	0.0029

5.6.2 Strength degradation in the negative direction

Compared to the positive direction, the decrease of strength in the negative direction happens in all specimens as shown in Figures 5-2 to 5-5. (Refer to Ch 5.2 load-displacement relationships) In order to analyze the cause of this, the strain of re-bars in the wall where the plastic hinge occurs was confirmed in detail. The location of rebars where plastic hinge occurs is shown in Figure 5-13.

Figure 5-25 to 5-26 shows the net tensile strain of the wall according to the strength of the specimen with high reduction in width. As the net tensile strain along each loading direction of the plastic hinge region, yielding and plastic deformation occurred in the tensile rebar in the positive direction. Therefore, it is analyzed that the strength in the positive direction is greater than the target strength. However, the tensile rebar in the negative direction did not yielding or plastic deformation. Therefore, the strength in the negative direction did not reach about 10% of the target strength. In Figure 5-27, the strain of the rebar in the W-R25-BL specimen with a small reduction in width, plastic deformation occurred in both directions. As a result, both directions exceeded the target strength.

The ultimate strength according to the loading direction differs as the reduction in width increases. Therefore, it is analyzed that the difference in strength is caused by the location of the plastic hinge depending on the discontinuous geometry.

In the W-R40-BL specimen, plastic hinges were generated on the column. So, plastic deformation was not confirmed in the tensile rebar. However, both

the tensile rebars of the column and the wall yielded in the positive direction. (Refer to Fig. 5-23) That is, both the wall and the column exhibited flexural behavior. On the other hand, the wall did not fully reach the yield strain under the negative direction. The rebar did not receive tensile force due to the concrete crushing at the top of the column. Therefore, it is analyzed that this result causes a strength imbalance.

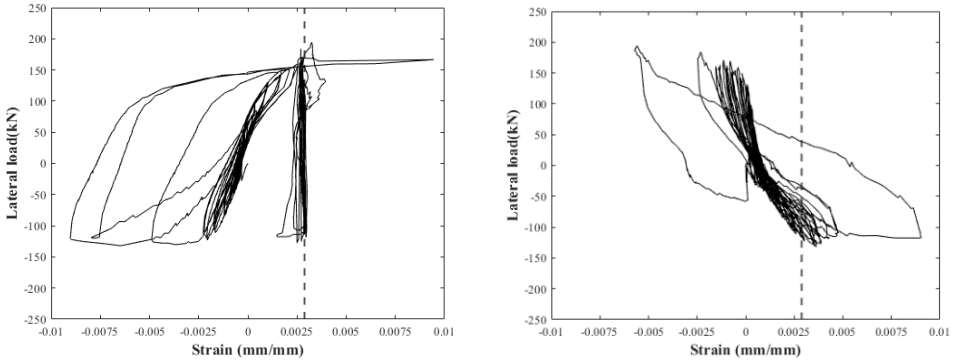

(a) Net tensile strain in positive direction (b) Net tensile strain in negative direction

Figure 5-25 Load – net tensile strain relationship of wall in the W-R40-BR

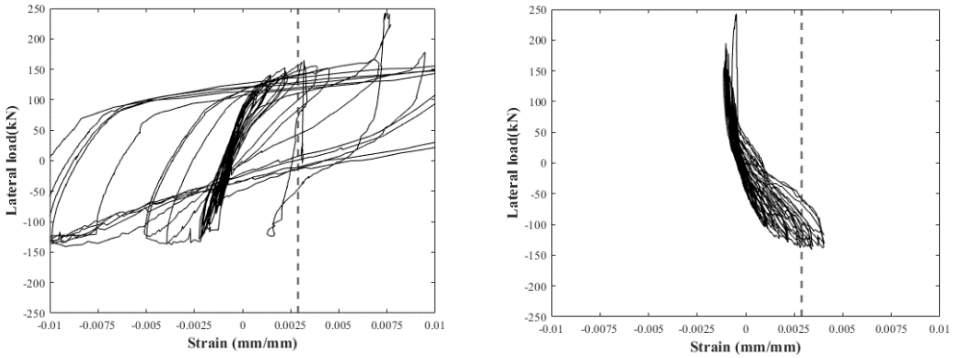

(a) Net tensile strain in positive direction (b) Net tensile strain in negative direction

Figure 5-26 Load – net tensile strain relationship of wall in the WB-R40-BR

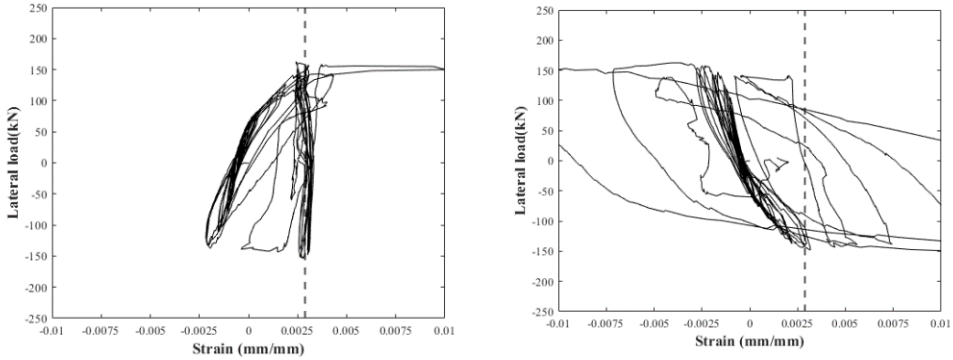

(a) Net tensile strain in positive direction (b) Net tensile strain in negative direction

Figure 5-27 Load – net tensile strain relationship of wall in the W-R40-BL

5.7 Lateral displacement participation

5.7.1 Specimen behavior

Unlike general beam-column joint tests, the boundary condition of the column for this test was defined as a fixed condition. Therefore, it behaves as an indeterminant structure for the lateral load. To confirm each deformation for the lateral displacement in the frame, it was idealized as a simple model based on the approximate analysis method, as shown in Figure 5-28.

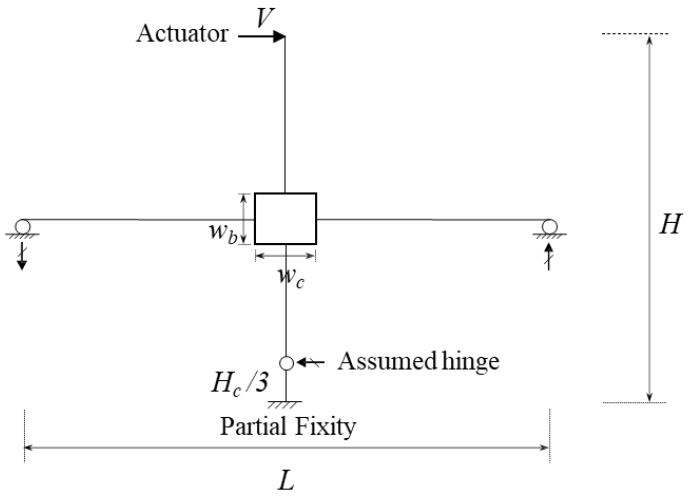

Figure 5-28 Method of approximate analysis for specimen

In an actual structure, it isn't easy to construct the foundation as a completely fixed condition, and the test results also did not show a completely fixed boundary condition. From these facts, a boundary condition is assumed as a partial fixity that a slight rotation occurs. The relatively small lateral displacement occurring under the assumed hinge condition is ignored. Also, the effect (P-Δ effect) of the compression force applied to the specimen was ignored.

Based on the idealized model, each behavior in frame system is identified as follows. The lateral displacement can be divided into the contribution of the vertical member (Δ_V), the horizontal member (Δ_H), and the panel zone (Δ_{pz}). In this displacement, the lateral displacement measured in the first-floor slab (Δ_{1st}) partially includes participation for behavior by column, beam, and panel zone. Considering the occurrence of plastic hinge for the wall and specimen with in-plane lateral support, the analysis was conducted from the perspective of the wall except for Δ_{1st}. Therefore, this study intends to confirm the contribution of deformation due to each behavior in the lateral displacement, except for the Δ_{1st}.

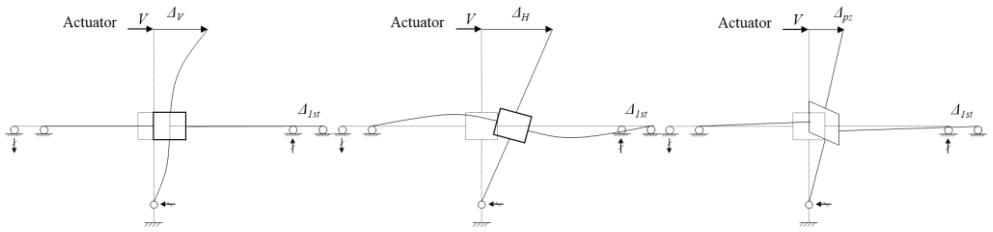

(a) Vertical member (Wall, Column)

(b) Horizontal member (Beam)

(b) Panel zone

Figure 5-29 Displacemet contribution by each behavior

5.7.2 Panel zone deformation

In the moment-resisting frame specimen, as the lateral displacement increases, the shear distortion (γ_{pz}) occurs due to the deformation of the panel zone. Thus, the panel zone deformation and lateral displacement contribution of panel zone (Δ_{pz}) were confirmed as follows.

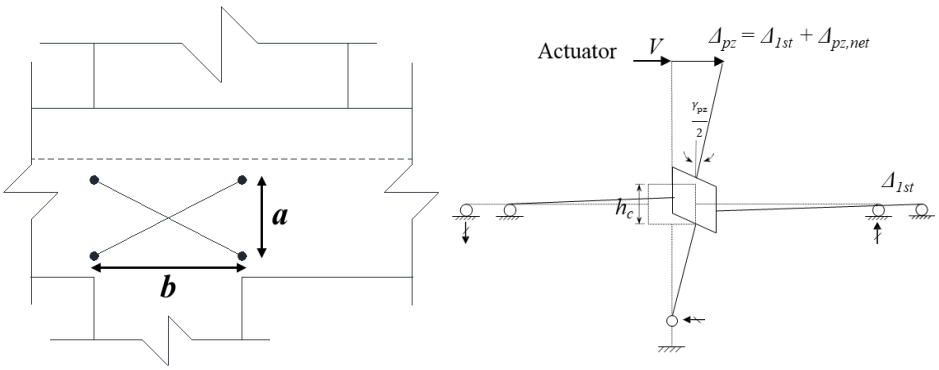

(a) LVDT (b) Deformed shape of panel zone

Figure 5-30 Measurement and contribution of the panel zone

The the shear distortion of the panel zone can be calcuated from the measurement of the diagonal LVDTs (as shown in Figure 5-30), as follows

$$r_{pz} = (\delta_j - \delta_j^{'}) \frac{\sqrt{a^2 + b^2}}{2ab} \tag{5-4}$$

Where, δ_j and δ_j' are the measured values of the diagonal LVDTs, and *a* and *b* are the vertical and horizontal length of the diagonal LVDTs, respectively.

The contribution of Δ_{pz} can be calculated through γ_{pz}. The Δ_{pz} is divided into the lateral displacement occurring on the first-floor ($\Delta_{pz,1st}$) and the net panel zone deformation ($\Delta_{pz,net}$) excluding it. Therefore, $\Delta_{pz,net}$ is as follows.

$$\Delta_{pz,net} = \frac{r_{pz}}{4}(h - h_c) \tag{5-5}$$

Where, h is the height from the loading slab to the column, and h_c is the panel zone height (beam width).

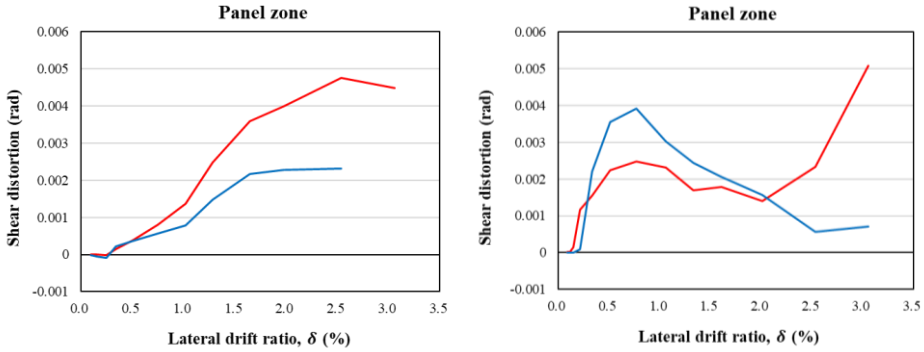

※ Positive direction : — Negative direction : —

(a) W-R40-BR (b) WB-R40-BR

Figure 5-31 Shear distorsion of panel zone

γ_{pz} in the moment-resisting frame specimens is shown in Figure 5-31. Considering a constant compression force of the specimens and the plastic hinge for the wall, the γ_{pz} should hardly occur. Also, γ_{pz} of the positive and negative direction occurs symmetrically in general. However, it is analyzed that the γ_{pz}, which happened relatively large in the positive direction, was affected in the negative direction due to the discontinuous section.

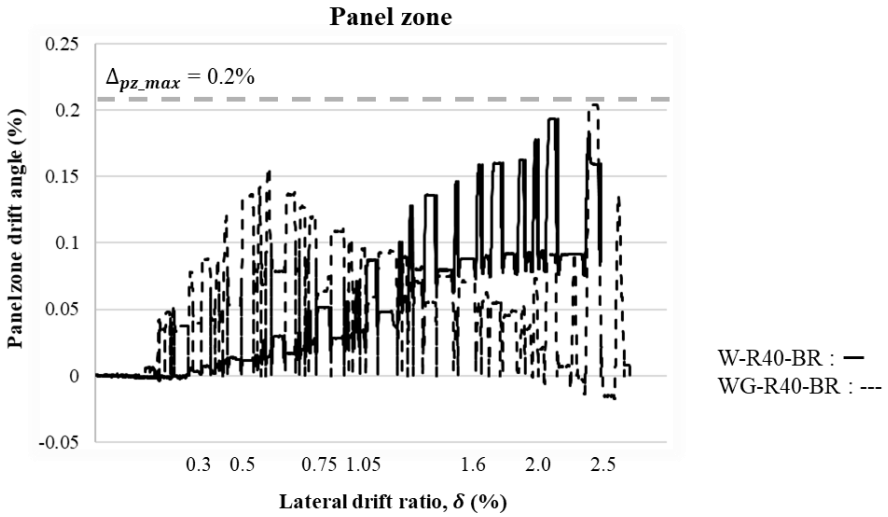

Figure 5-32 Participation of lateral drift ratio in the panel zone

Figure 5-32 shows the lateral drift ratio due to the panel zone deformation in the moment-resisting frame specimens. The contribution of the lateral drift ratio by the panel zone at 2.5% was 0.2%, and the effect was insignificant.

The specimens with in-plane lateral support are difficult to deform the panel zone by the lateral support. Therefore, in the W-R25-BL specimen that did not allow lateral displacement, γ_{pz} of the panel zone did not occur. So, the lateral displacement contribution by the panel zone did not happen. However, since the W-R40-BL specimen allowed lateral displacement, it occurred at a maximum of less than 0.002 rad over the 2.0% drift ratio. Therefore, the maximum contribution of the lateral drift was 0.08%, which was relatively low.

5.7.3 Beam deformation

Specimens with in-plane lateral support hardly generate beam deformation due to the in-plane lateral support. Therefore, lateral displacement according to the behavior of the beam does not occur. On the other hand, in the moment-resisting frame specimens, the beam resists flexural moment, so lateral displacement by the behavior of the beam occurs. It can be considered that the beam designed by the concept of flexural yielding of the wall is assumed to have an elastic behavior. Therefore, the lateral displacement generated by the beam with elastic behavior is shown in Figure 5-33.

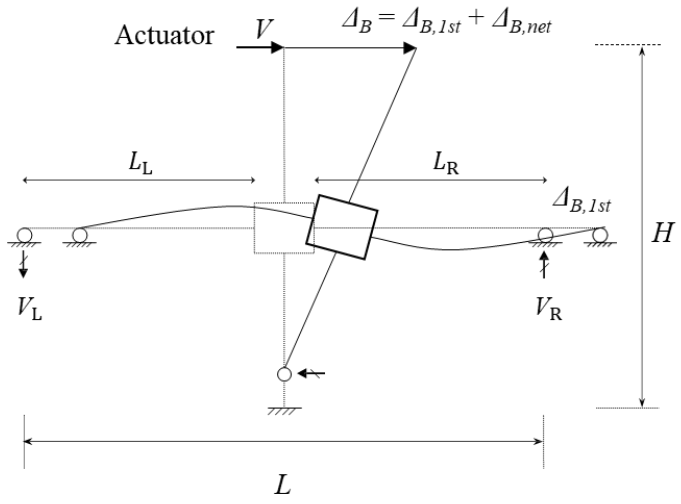

Figure 5-33 Deformed shape by elastic beam behavior

Based on the load cell (Refer to Appendix) measured at the end of beam and the elastic modulus of the concrete used in the material test, the elastic deformation of the beam (Δ_B) is as follows.

$$\Delta_B = (\frac{V_R L_R^3}{3EI} + \frac{V_L L_L^3}{3EI} + \frac{V_R L_R}{GA} + \frac{V_L L_L}{GA})(\frac{H}{L}) \quad (5\text{-}6)$$

Where, E is the elastic modulus of the beam, I is the moment of inertia of the beam, V_R and V_L are the reactions measured at the load cells, L_L(1,000mm) and L_R(1,250mm) are the net length of the beam, and H is the height of the specimen, A is the effective shear area of the beam, where L-shaped section including a slab is the beam width × (beam depth + slab thickness)/1.0, and G is the shear modulus of the beam. For E and I, the modulus of elasticity was calculated based on the concrete strength of each specimen, G was $E/2(1+\nu)$, and ν was 0.2 as the concrete Poisson's ratio.

Based on Δ_B, the first-floor displacement by the beam behavior ($\Delta_{B,1st}$) can be calculated. Also, the net lateral displacement ($\Delta_{B,net}$) excluding $\Delta_{B,1st}$ can be estimated. The results of deformation are shown in Table 5-9.

Table 5-9 Lateral displacement by elastic beam behavior

Specimen	Δ_B (Total)		$\Delta_{B,1st}$ (First floor displacement)		$\Delta_{B,net}$ (Net displacement)	
	Pos	Neg	Pos	Neg	Pos	Neg
W-R40-BR	4.32	-2.40	1.57	-0.87	2.75	-1.53
WB-R40-BR	4.46	-2.47	1.62	-0.9	2.83	-1.57

5.7.4 Shear deformation

Based on the average shear strain of the wall, the contribution of lateral displacement due to shear behavior was confirmed. The lateral displacement contribution can be calculated through the average shear strain and the height (h) to the loading slab. Therefore, the average shear strain was confirmed in the following calculation based on the measurement through the diagonal LVDTs.

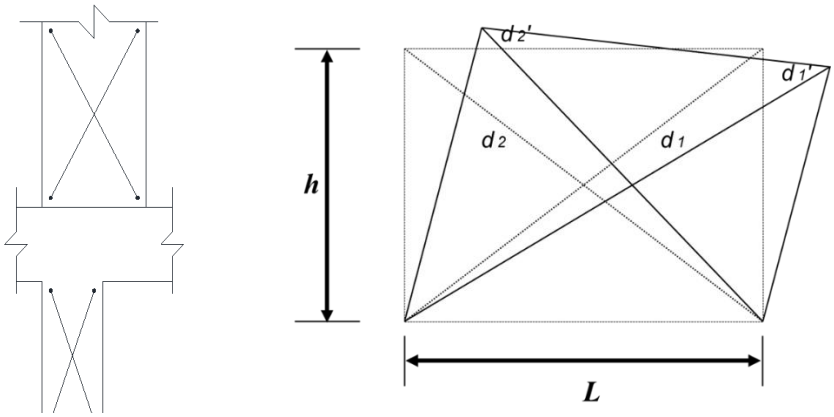

(a) LVDT (b) Deformed shape by shear deformation

Figure 5-34 Measurement of average shear strain

$$r_{avg} = \frac{(d_1 - d_1^{'})d_1 - (d_2 - d_2^{'})d_2}{2hL} \tag{5-7}$$

Where, d_1' and d_2' are the deformed values of the diagonal LVDTs, and L and h are the horizontal and vertical length of the diagonal LVDTs, respectively.

The equation of average shear strain has a risk of overestimating the value after the maximum strength of the specimen. Therefore, Figure 5-35 shows the average shear strain up to the maximum strength.

Based on the average shear strain, the contribution of lateral displacement due to shear behavior in the wall is shown in Table 5-10. In all specimens, it was

confirmed that the maximum average shear strain was less than 0.005 rad, and the lateral displacement participation was within 10% (Refer to Table 5-11).

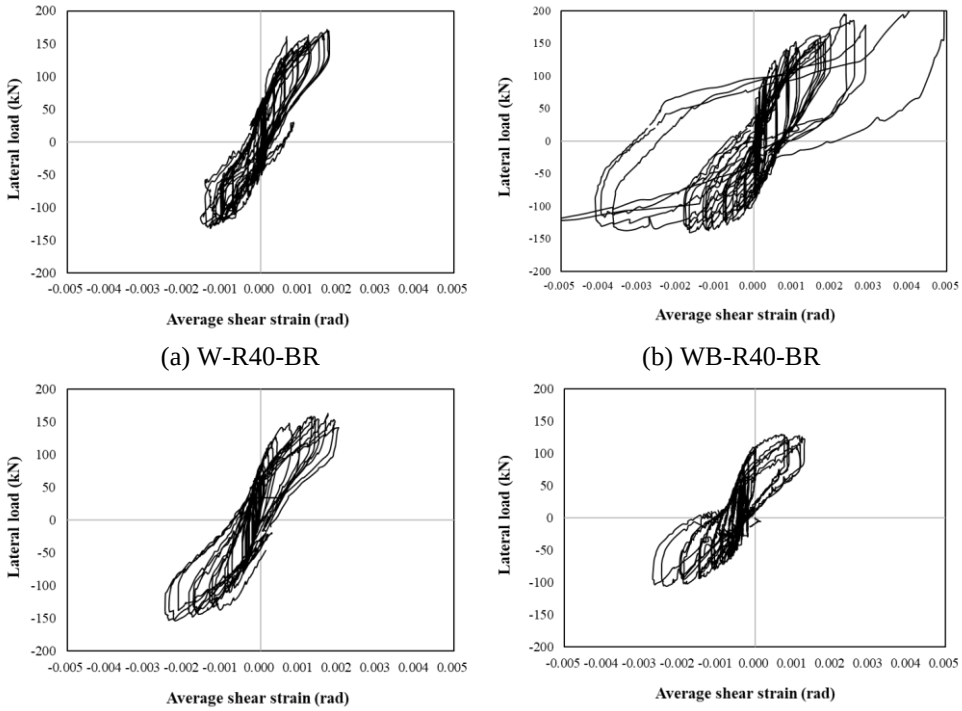

(a) W-R40-BR (b) WB-R40-BR

(c) W-R25-BL (d) W-R40-BL

Figure 5-35 Lateral load – shear strain relationship of wall

Table 5-10 Average shear strain at the ultimate strength

Specimen	Average shear strain		Shear deformation	
	Pos	Neg	Pos	Neg
W-R40-BR	0.0017	-0.0014	2.10	-1.71
WB-R40-BR	0.0049	-0.0018	5.90	-2.18
W-R25-BL	0.0020	-0.0025	2.42	-2.96
W-R40-BL	0.0009	-0.0027	1.07	-3.23

5.7.5 Displacement participation

The lateral displacement caused by the cyclic loading consists of the Δ_{1st} (lateral displacement on the first floor), $\Delta_{B,net}$ (the beam deformation excluding the Δ_{1st}), $\Delta_{pz,net}$ (the panel zone deformation excluding the Δ_{1st}), the $\Delta_{wall,shear}$ (shear deformation of the wall), and $\Delta_{wall,shear}$ (the flexure deformation of the wall). Δ (the total lateral displacement) and Δ_{1st} can be known through the measurement. $\Delta_{B,net}$, $\Delta_{pz,net}$, and $\Delta_{wall,shear}$ were obtained through the previous calculation. Furthermore, since the plastic hinge occurred in the bottom of the wall, both elastic and plastic deformation occurred in the flexural deformation of the wall. Therefore, it can be estimated that the flexural deformation in the wall was obtained by excluding the previous deformation from the total lateral displacement. Figure 5-36 and Table 5-11 show the displacement participation at the ultimate strength of each specimen.

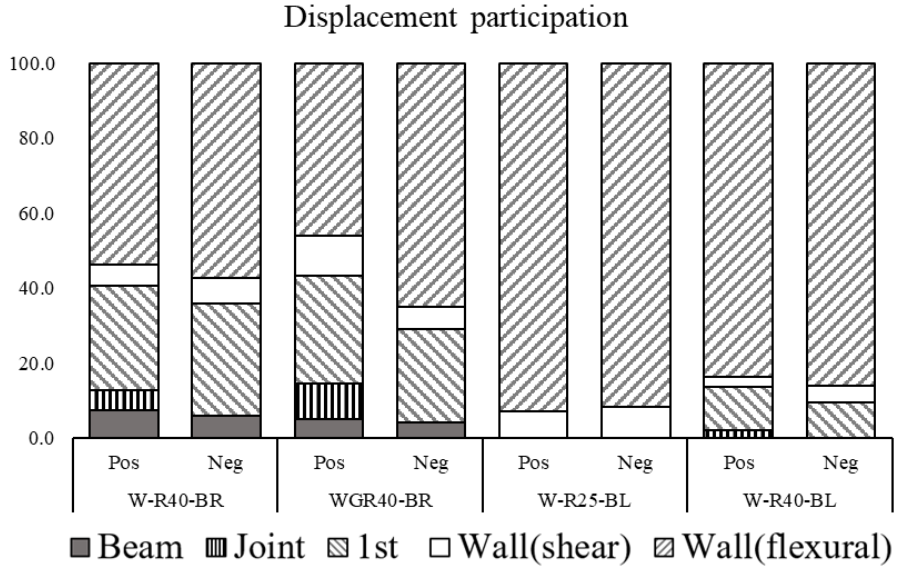

Figure 5-36 Displacement participation measured at the ultimate strength

Table 5-11 Parameter for the Lateral displacement participation

	W-R40-BR		WB-R40-BR		W-R25-BL		W-R40-BL	
	Pos	Neg	Pos	Neg	Pos	Neg	Pos	Neg
$\Delta_{wall,flexure}$	53.9 (20.2)	57.4 (-14.8)	46.0 (25.1)	65.2 (-24.3)	92.9 (31.9)	91.6 (-32.1)	83.8 (35.0)	86.0 (-59.6)
$\Delta_{wall,shear}$	5.6 (2.1)	6.6 (-1.7)	10.8 (5.9)	5.9 (-2.2)	7.1 (2.4)	8.4 (-3.0)	2.6 (1.1)	4.7 (-3.2)
Δ_{1st}	27.8 (10.5)	30.1 (-7.8)	28.7 (15.7)	24.8 (-9.2)	0.0 (0.0)	0.0 (0.0)	11.7 (4.9)	9.3 (-6.5)
$\Delta_{pz,net}$	5.4 (2.0)	0.0 (0.0)	9.4 (5.1)	0.0 (0.0)	0.0 (0.0)	0.0 (0.0)	2.0 (0.8)	0.0 (0.0)
$\Delta_{B,net}$	7.3 (2.7)	5.9 (-1.5)	5.2 (2.8)	4.2 (-1.6)	0.0 (0.0)	0.0 (0.0)	0.0 (0.0)	0.0 (0.0)
Total	100 (37.6)	100 (-25.8)	100 (54.7)	100.0 (-37.3)	100 (34.3)	100 (-35.0)	100 (41.8)	100 (-69.3)

※ Each value : Percentage,%(Displacement,mm)

Figure 5-36 and Table 5-11 show that the wall behavior (flexure + shear) accounts for about 60% or more in all specimens. Also, about 50% of moment-resisting frame specimens and about 80% of specimens with in-plane lateral support are contributed to lateral displacement by the flexural behavior of the wall. In the moment-resisting frame specimens, the sum of $\Delta_{B,net}$ and $\Delta_{pz,net}$ is relatively small, within about 15%. In Figure 5-36, most of the lateral displacement participation is the flexural behavior of the wall. However, the lateral displacement of about 10% with in-plane lateral support significantly affects the transfer column in the failure mode. Therefore, it is analyzed that the lateral displacement by diaphragm behavior in the transfer floor must be reflected in the transfer structure design.

5.8 Summary

Table 5-12 shows the summary of test results according to the strength, yielding of the member, and the failure mode.

Table 5-12 Summary of specimen results

Specimen	Target Strength (V_{target})	Ultimate Strength (V_{Peak})		V_{Peak}/V_{target}		Yielding	Location of plastic hinge	Failure mode
		Pos (+)	Neg (-)	Pos (+)	Neg (-)			
W-R40-BR	145	171	-132	1.2	0.9	Wall	Bottom of the wall	Flexural Tension
WB-R40-BR		177	-141	1.2	1.0	Wall, Beam, Column	Bottom of the wall	Flexural Tension
W-R25-BL		162	-154	1.1	1.1	Wall	Bottom of the wall	Flexural Tension
W-R40-BL		130	-106	0.9	0.7	Wall Column	Top of the column	Flexural compression

Except for the W-R40-BL specimen, the strength meets and exceeds the target strength through the flexural yielding of a wall. In the W-R40-BL specimen, cantilever behavior is added to the wall and column according to allowing the lateral displacement. As a result, flexural compression failure occurred in the column at a high lateral drift ratio, so that a plastic hinge could not be placed on the wall. However, flexural behavior of wall occurred, and brittle failure did not occur.

The specimen where flexural yielding of the wall occurred is defined within the ductility range of 2.2 to 2.8. On the other hand, the specimen where the column is dominant behavior represents a ductility of 1.7. Through this, it is reasonable to induce ductile behavior through flexural yielding of the wall.

As a result of the participation of lateral displacement, the most behavior of all specimens was the flexural behavior of the wall. The moment-resisting frame specimens showed more than 50%, and the specimens with in-plane lateral support showed more than 80% for the flexural behavior of the wall. However, the lateral displacement of about 10% with in-plane lateral support significantly affects the transfer structure considering the failure mode.

The ultimate strength in the negative direction was relatively lower than in the positive direction because the tensile re-bar in the discontinuous section did not occur plastic deformation. In the specimen(R40) with a large reduction in width, the target strength is not met in the negative direction. On the other hand, only a difference in the overstrength occurred in the specimen(R25) with a small reduction in width. Therefore, reflecting the above results, additional re-bars in the discontinuous section must be increased to satisfy the required strength in the wall-column transfer structure with a reduction ratio of over 25%.

The comparison through the moment-resisting frame specimens is as follows. WB-R40-BR specimen showed better structural performance in the evaluation of energy dissipation and ductility. However, at the ultimate strength, the spandrel beam and column yield and the flexural yielding of the spandrel beam affect the cracks up to the column. This can cause significant risks (torsional behavior, weak story, etc.) to the entire RC structure.

The comparison through the specimen with in-plane lateral support is as follows. When the lateral displacement is limited, the result as the induced design concept is obtained through the W-R25-BL specimen. Whereas, in case of allowing lateral displacement, the cantilever behavior according to the lateral displacement is added, and a large flexural moment and stress concentration acts on the column. Also, the behavior of column is dominant.

Therefore, it is appropriate to occur a plastic hinge only on the wall, and the overstrength factor (1.25) should be applied to the members in transfer floor. Additionally, if the cantilever behavior is dominant in the column due to the large lateral displacement of the transfer floor, the concrete strength should be determined by considering the compressive stress concentration.

Chapter 6. Proposal of Design Guidelines

6.1 Design process

Based on test results, this study proposes a design method and recommendations according to the resisting seismic load that may occur in the wall-column transfer structure. According to the current design codes, special seismic loads are applied to vulnerable earthquake-resistant members such as transfer structures. A bearing wall structure such as an apartment has an overstrength factor (Ω_0) of 2.5 applied under a special earthquake load, so the member must be designed by a high required strength. But, instead of applying special seismic load, capacity design through the other seismic-force-resisting elements is possible.

So, this study proposes a seismic design method based on the strut-tie model. This is because the transfer structure is D-region where stress concentration can occur due to sectional changes. The purpose of the capacity design is to secure the ductile behavior of the system through flexural yielding of the wall by using the concept of capacity design. Also, the risk of brittle failure of members in transfer floor that may cause significant damage to the entire RC structure should be prevented. Based on this capacity design concept, the process of the design method considering the RC structure design is presented as shown in Figure 6-1.

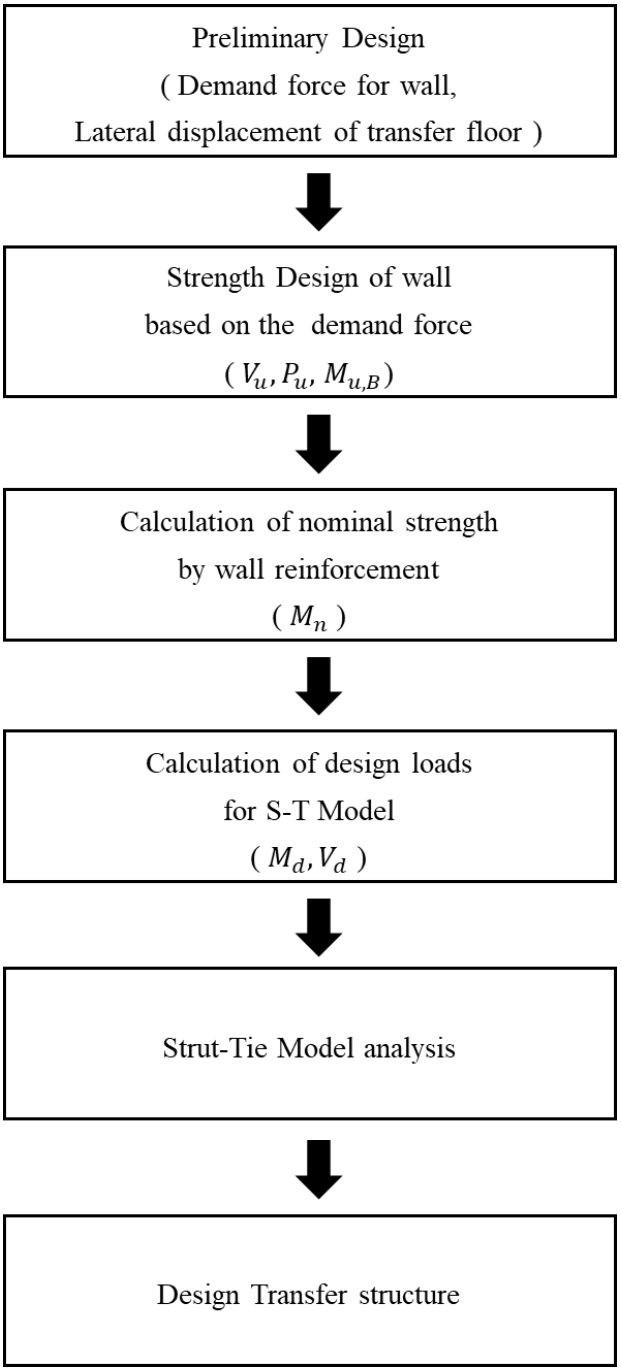

Figure 6-1 Design Process for wall-column transfer structures

6.1.1 Preliminary design

The entire structure analysis of the RC building is performed based on elastic analysis. Through the analysis, the preliminary design is performed for the members of the regions where the wall-column transfer structure is required. In this case, the design of the wall-column transfer structure recommends the following (materials, dimensions and etc.).

- The concrete material strength of the members in transfer floors is designed to be 30 MPa or higher.

- The vertical re-bars of the wall should be used for the seismic-resistant steel deformed bar under the KDS standard to secure overstrength for the wall-column transfer structure.

- The width of the section in the column should be at least 60% of the length of the wall.

- The area of the column must be the same as the area of the upper wall.

- The size of the member on the transfer floor is designed without considering the special seismic load.

Based on this preliminary design, the required strength (axial force, bending moment, shear force) acting on the wall using the wall-column transfer structure and the lateral displacement of the transfer floor are derived through the elastic analysis.

6.1.2 Strength design of wall based on demand force

Based on the required strength acting on the upper wall through elastic analysis, the maximum internal force is derived and the wall is designed by the structural design standard.

The wall's design with a width reduction of more than 25% reflects the test results. When the discontinuous section is received to tensile force, the internal force of the wall is reduced by up to 10% against the required strength. Thus, the vertical re-bars in discontinuous section are increased to 1.1 times the demand (required rebars by $M_{u.B}$) considering the test result.

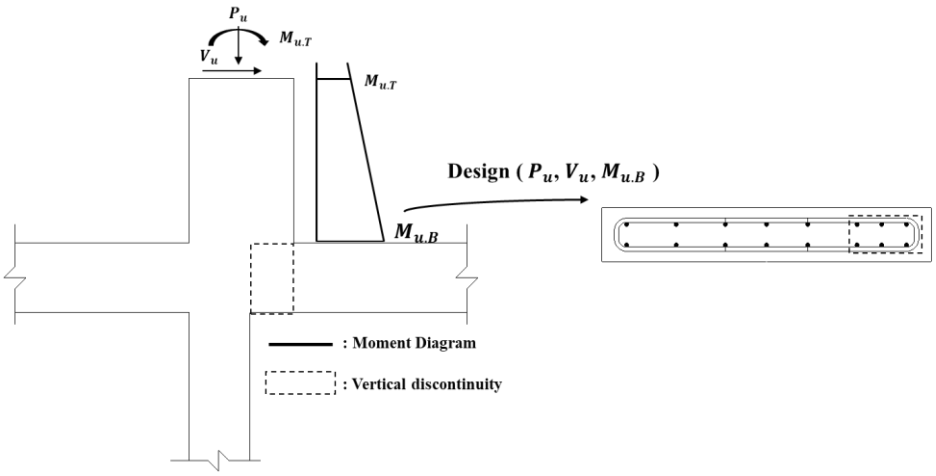

Figure 6-2 Strength Design of wall

6.1.3 Calculation of nominal strength & design loads

Based on the reinforcement according to the demand, make a P-M interaction diagram as shown in Fig. 6-3. The nominal flexural moment of the wall is calculated based on the axial force acting on the wall according to the seismic load.

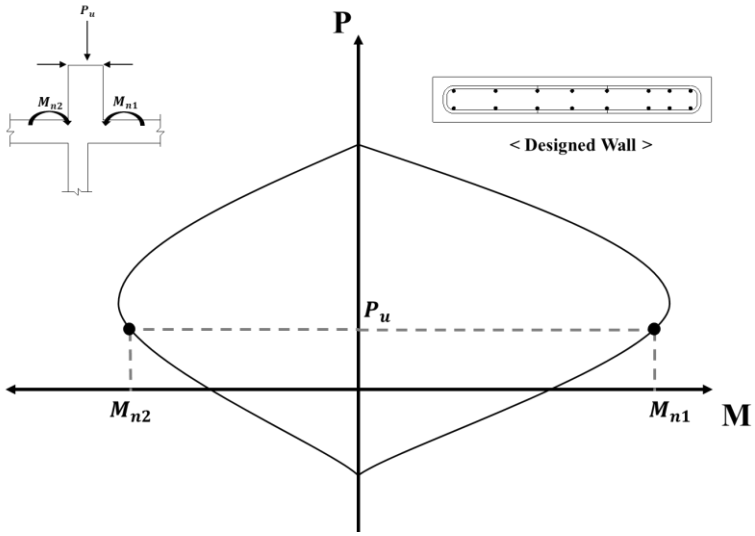

Figure 6-3 P-M interaction diagram of designed wall

After this process, the design load amplification factor (α) that reflects the property of the nominal strength in the wall is obtained. The design loads of the strut-tie model are calculated by applying the design load amplification factor to the demand loads (V_d, M_d) of the wall from the elastic analysis. The equation for calculating this process is as follows.

$$\alpha \text{ (Design load amplification factor)} = M_n / M_{u,B} \tag{6-1}$$

$$M_d = \alpha \times M_{n,T} \tag{6-2}$$

$$V_d = \alpha \times V_u \tag{6-3}$$

6.1.4 Strut-Tie Model analysis

In the strut-tie model of the wall-column transfer structure, it is constied of struts, nodal zones and ties. The ties are configured in the same direction as the arrangement of each re-bar, and the struts and nodal zones are placed in vertical, horizontal, and diagonal directions. The strut-tie model is composed of the inflection point of the spandrel beam.

Based on the test result for the ultimate behavior of each boundary condition, the strut-tie model makes up a comprehensive design model, as shown in Figure 6-4. In general, the behavior of the moment-resisting frame and in-plane lateral support of the diaphragm effect is simultaneously resisted by a seismic load in the transfer floor. So, a design model has complex boundary conditions in which the lateral displacement is allowed at the end of the spandrel beam.

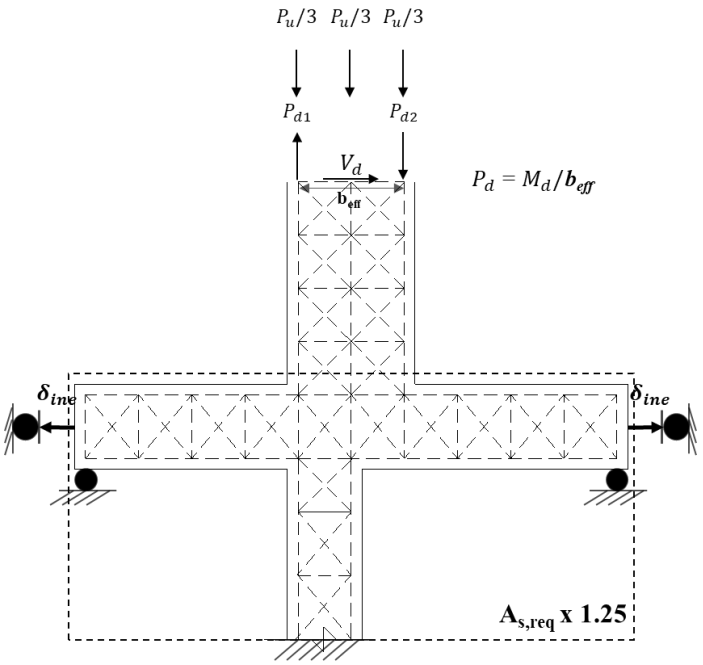

Figure 6-4 Strut-tie model for wall-column transfer structure

Based on the test results, the lateral displacement that can occur with in-plane lateral supports have a great effect on the structure behavior. So, it must be considered in the boundary condition. In addition, the inelastic displacement (δ_{ine}) that can actually occur during an earthquake should be applied to the boundary condition. Therefore, the elastic displacement (δ_e) in transfer floor should be converted into inelastic displacement and applied in accordance with design code (Refer to KDS 41 17 00 7.2.8.1).

$$\delta_{ine} = \frac{C_d \delta_e}{I_E} \tag{6-4}$$

Where, C_d = displacement amplification factor (to consider the inelastic deformation), δ_e = lateral displacement determined by an elastic analysis, I_e = Important factor

6.1.5 Design transfer structure

Then, the design loads (P_u, V_d, M_d) are applied to the strut-tie model, as shown in Figure 6-4. The moments in Figure 6-4 assume a linearly distributed load. Based on the required strength on each member, the following design requirements are recommended.

- Reinforcement of spandrel beam and column = 1.25 × $A_{s,req}$ (required amounts of re-bar)
- The coefficient factor (β_s, β_n) for each strut and nodal zone is applied according to the design standard for concrete structures.

- If only the required strength of a diagonal strut is greater, it is recommended to lower the reduction in width rather than to increase the concrete material strength.

- If the behavior of the column is dominant due to inelastic displacement occurring in the transfer floor, HPC (High-Performance Concrete, 40 MPa or more) is recommended for the wall-column transfer structure.

- The transverse reinforcement of spandrel beam is designed to satisfy the design code for intermediate moment frame. Also, the transverse reinforcement of the column and joint are designed to satisfy the design code for the piloti.

6.2 Rebar details for wall-column transfer structure

Based on this test, this study proposes the rebar details by the performance verification for the seismic design of the wall-column transfer structure, as shown in Figure 6-5.

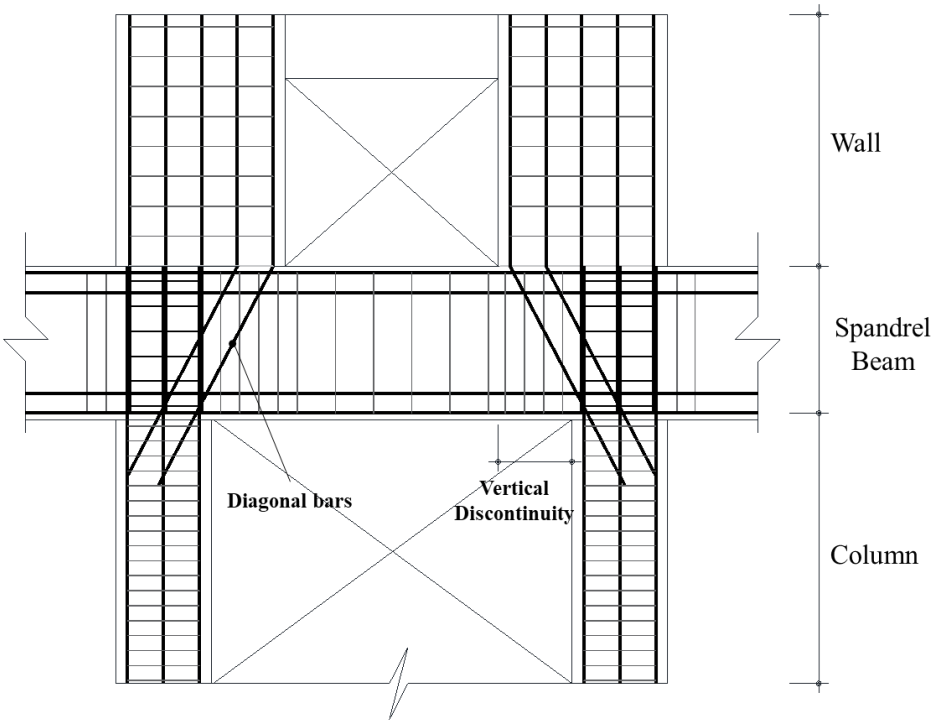

Figure 6-5 Example of reinforcement in wall-column transfer structure

The recommendations of rebar details for wall are as follows.

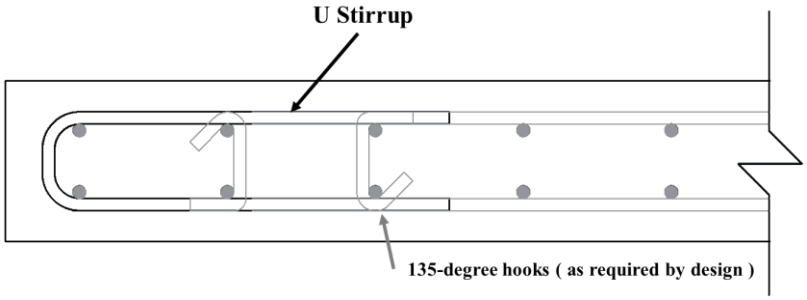

Figure 6-6 Example of boundary transverse reinforcement in wall

In order to improve the structural performance of the wall-column transfer structure, the vertical re-bars of the wall should be used U-shaped bars. The hooks are used as necessary. Development and splices of reinforcement follow design codes for concrete structure.

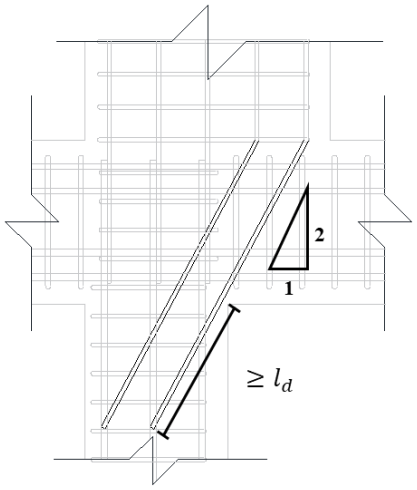

Figure 6-7 Example of diagonal bars in wall

Diagonal re-bars are applied from wall to column to serve as a compression reinforcement and as a role of connecting the tension force of the wall to the column in cyclic loading. In addition, if the width of the spandrel beam is small,

it is also possible to secure the development length of the re-bars in the discontinuous section. The development length of the diagonal rebars should extend to the vertical re-bars of the column beyond the design code, as shown in Figure 6-7. Also, the strut slope confirmed from the tests is applied to the diagonal rebars.

The recommendations of rebar details for joint and spandrel beam are as follows. The joint details are applied to prevent brittle failure of the diagonal strut in the discontinuous section due to the plastic hinge of a wall, as shown in Figure 6-8. Therefore, the detail of the shear reinforcement in the spandrel beam is applied, and cross-ties are added only to the discontinuous section, as shown in Figure 6-9.

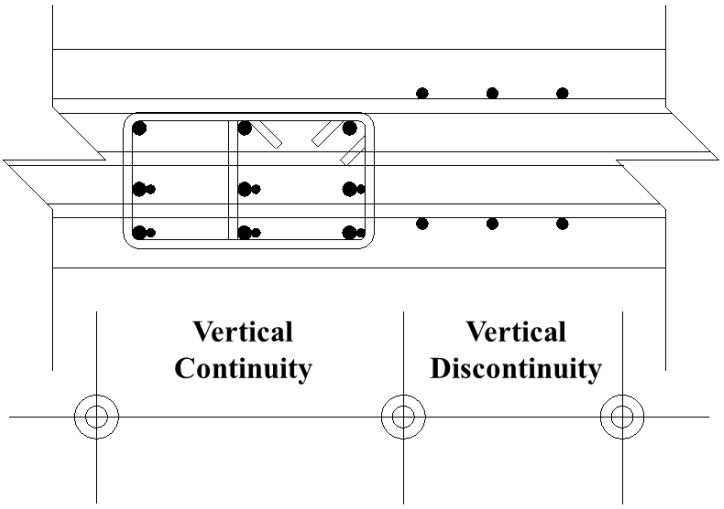

Figure 6-8 Example of joint including vertical discontinuity

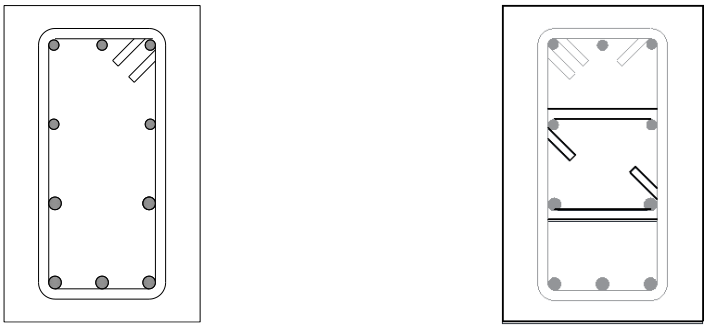

(a) Except for vertical discontinuity (b) Vertical discontinuity

Figure 6-9 Cross-section of spandrel beam

The details of the joint use hoops, including both vertical rebars of the wall and column in the continuous section. Also, vertical rebars of the wall and column extend to the joint. The transverse reinforcement in the joint is equal to the column spacing following the design code in the piloti.

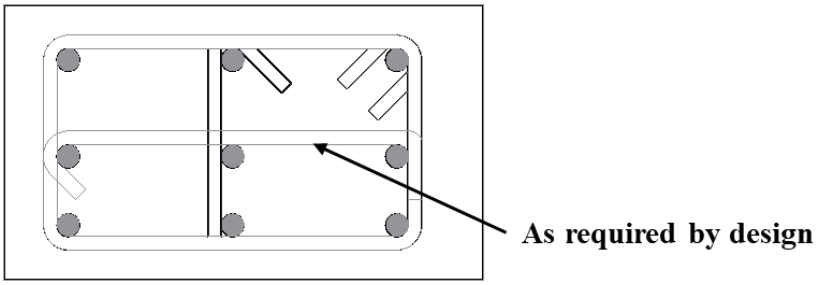

Figure 6-10 Example of column

The recommendations of rebar detail for column are as follows. If the depth of the spandrel beam is larger than the column, a cross-ties should be placed in the vertical re-bar of the column as in the design code for the transverse reinforcement for the piloti. The details applied to the column in wall-column transfer structure are shown in Figure 6-10.

6.3 Summary

In this chapter, the economical design method for the wall-column transfer structure were developed based on the test results. This design method used the capacity design concept and strut-and-tie model. The design procedure was proposed considering the design process of high-rise RC structure. The major conclusions are summarized as follows:

The design method for the upper wall is separately presented in the wall-column transfer structure. Based on the strength degradation for the test result, the vertical re-bars for the discontinuous section are increased by 1.1 times the $A_{s,req}$ in the vertical reduction ratio over the 25%. For the detailed design of strut-and-tie model, the design loads reflect the nominal strength for the designed upper wall.

The detailed design of strut-and-tie model reflects the test results. Since the lateral displacement in the transfer floor can greatly affect the transfer column, the lateral displacement reflects the inelastic displacement through the elastic analysis. Also, the reinforcement of the spandrel beam and column is designed by applying the overstrength factor for the upper wall. In addition, recommendations for materials, transverse reinforcement, and section reduction were provided.

The re-bar details prevent the local failure due to the stress concentration and ensure the ductile behavior. For the re-bar details, the transverse reinforcement of wall, transfer column, and spandrel beam, details of joints different from the design code, and diagonal re-bar were presented.

Chapter 7. Conclusion

In the present study, a seismic design and the re-bar details were studied for the safe and economical design of the Wall-column transfer structure in an RC building. So, a capacity design was used to prevent brittle failure of the members in the transfer floor before the flexural yielding of the upper wall. Therefore, the member on the transfer floor was designed to have sufficient internal force by applying an overstrength factor. Also, since the wall-column transfer structure is the D-regions where stress concentration occurs, the capacity design of the specimen was conducted through the strut-and-tie model analysis.

The structural performance was verified through a cyclic loading test with a nominal constant compression load of 0.2 $f_c^{'}A_g$. In the test, the specimen's size was the as reduced size of 1/2 the width, thickness, and 1/3 the height of the prototype structure. The test parameters include boundary conditions, re-bar ratio, reduction in width, allowable lateral displacement according to lateral support, and use of an overstrength factor. In the case of the W-R40-BR and WB-R40-BR specimens, it is assumed that the moment-resisting frame with a similar stiffness is continuous to support lateral force. On the other hand, the W-R25-BL and W-R40-BL specimens are assumed that it was laterally supported due to the rigid structure. However, in this situation, it was assumed that the W-R25-BL specimen limited lateral displacement, and the W-R40-BL specimen allowed lateral displacement.

The test results showed that ductile behavior occurred without premature brittle failure of the member in transfer floor. Seismic performance intended for capacity design was verified through the strain of the re-bar, yielding of the member, and failure mode results. However, some damage occurred to the members where the overstrength factor was not applied. The flexural yielding of the spandrel beam was confirmed to have higher performance in terms of strength and ductility due to the effect of moment redistribution. However, the yielding and damage of the column in ultimate behavior can cause significant damage to the entire RC structure. Also, the yielding of the column caused the dominant behavior than the yielding of the wall. Therefore, it is appropriate to apply the overstrength factor to the member in the transfer floor and induce the flexural yielding of the upper wall. The effectiveness of re-bar details used to prevent the local failure of the transfer structure was also confirmed. In particular, the details of the joint applied in the design to lower the diagonal strut on the discontinuous section to prevent brittle failure of the system. Diagonal re-bars are applied from wall to column to serve as a compression reinforcement and as a role of connecting the tension force of the wall to the column. However, when the diagonal re-bars are received to flexural tensile force, the capacity of the wall is relatively lower than the target strength. This result indicates that the flexural tensile rebars in the discontinuous section should be increased by 10% in the design proposal process.

Based on the test results, an economical design method using the strut-and-tie model was proposed for the actual design. The capacity design procedure was proposed considering the design process of high-rise RC structure. The proposed procedure is as follows. The procedures are preliminary design,

strength design of the wall, calculation of nominal strength and design loads for analysis, strut-and-tie model analysis, and design transfer structure. In the preliminary design, recommendations such as material strength and member sizes were presented for the wall-column transfer structure. After this preliminary design, a design method for the upper wall and a design model based on the strut-and-tie method was presented. In addition, details of the re-bar to be applied to the wall-column transfer structure are included to secure the ductile behavior.

The proposed seismic design method and details should be applied only to the wall-column transfer structure of a single-frame system. If the wall-column transfer structure exists symmetrically, the members in the transfer floor could be strengthened further, considering a coupling effect.

References

[1] Korean Design Standard. (2019). “Seismic Design Code of Buildings (KDS 41 17 00).” Korean Design Standard.

[2] Korean Building code. (2016) “Korean Building code and commentary (KBC 2016).” Korean Building code.

[3] ACI Committee 318. (2019). “Building Code Requirment for Structural Concrete (ACI 318-19) and Commentary.” American Concrete Institue.

[4] CEN. (2005). “Eurocode 8: Design of Structures for Earthquake Resistance Part 1: General rules, seismic actions and rules for buildings.” British Standards Institution

[5] AIK (2021). “Guidelines for Performance-Based Seismic Design of Reinforced Concrete Buildings.” Architectural Institute of Korea.

[6] Nist. (2014) “Recommendations for Seismic Design of Reinforced Concrete Wall Buildings Based on Studies of the 2010 Maule, Chile Earthquake.” National Institute of Standards and Technology.

[7] ATC. (1998) “EVALUATION OF EARTHQUAKE DAMAGED CONCRETE AND MASONRY WALL BUILDINGS.” FEMA 306 Report, Federal Emergency Management Agency

[8] AIK. (2018) “A Study on Earthquake Prevention Measures for

Earthquake Vulnerable Buildings such as Piloti.” Architectural Institute of Korea.

[9] H.G. Park, C.G. Kim. (2018). “Building Damage in Pohang EQ and the Lessons”, Review of Architecture and Building Science, 62(12)

[10] S.H. Kim, H.G. Park, H.J. Hwang. (2019). “Load-Transfer Design of Wall-Piloti Structure with Lateral Support.” ACI Structural Journal

[11] H.J. Hwang, Kim, H.G. Park, C.H. Lee, C.H. Park, H.S. Kim, S.B. Kim. (2011). “Seismic Resistance of Concrete-filled U-shaped Steel Beam-to- RC Column Connections.” KOREAN SOCIETY OF STEEL CONSTRUCTION, 23(1)

[12] J.J. Han, H.J. Son, D.J. Kim. (2022). “Structural Performance of the RC Boundary Beam–Wall System Subjected to Axial Loads.” J. Comput. Struct. Eng. Inst. Korea, 35(1) pp.57～64

[13] Leonardo M. Massone, et al. (2019). “Understanding the cyclic response of RC walls with setback discontinuities through a fnite element model and a strut-and-tie model.” Bulletin of Earthquake Engineering

[14] H.J. Hwang, Kim, H.G. Park. (2019). “Requirements of Shear Strength and Hoops for Performance-Based Design of Interior Beam-Column Joints.” ACI Structural Journal, 116(2)

[15] H.J. Hwang, Kim, H.G. Park, W.S. Choi, J.K. Kim, L. Chung. (2014). “Cyclic Loading Test for Beam-Column Connections with

600 MPa (87 ksi) Beam Flexural Re-bars.” ACI Structural Journal, 111(4)

[16] R. Park. (1989). “EVALUATION OF DUCTILITY OF STRUCTURES AND STRUCTURAL ASSEMBLAGES FROM LABORATORY TESTING.” BULLETIN OF THE NEW ZEALAND NATIONAL SOCIETY FOR EARTHQUAKE ENGINEERING, 22(3)

[17] ACI Committee 374. (2013). “Guide for Testing Reinforced Concrete Structural Elements under Slowly Applied Simulated Seismic Loads.” American Concrete Institue.

[18] ACI Committee 374. (2014). “Acceptance Criteria for Moment Frames Based on Structural Testing and Commentary.” American Concrete Institue.

[19] MOLIT. (2018). “Structural Design Guidelines for Piloti Buildings.” Ministry of Land, Infrastructure and Transport.

Appendix : Measured Reaction Force of Loadcell

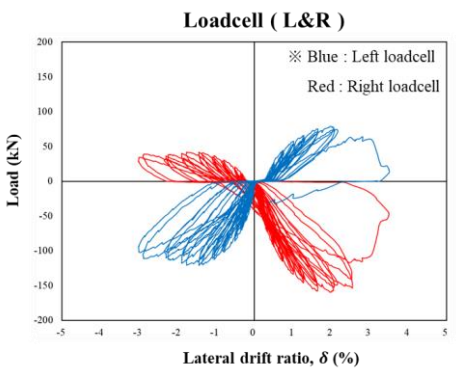

(a) W-R40-BR

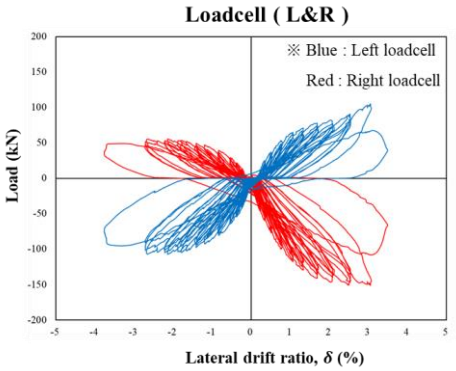

(b) WB-R40-BR

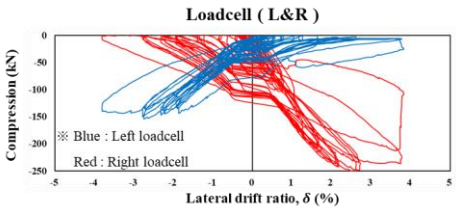

(c) W-R25-BL

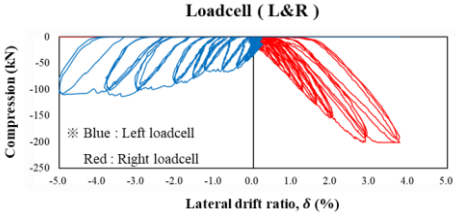

(d) W-R40-BL

Figure. Measured reaction of loadcell

초 록

철근콘크리트 구조물의 벽기둥 전이구조 내진설계

구 자 형

서울대학교 건축학과 대학원

국내 RC 고층 건물에서는 개방감 및 공용공간 확보를 위해 전이구조를 활용한다. 기존의 전이구조는 대형 단면의 전이부재를 많이 활용하였지만, 최근 시공성과 경제성을 고려하여 간략화된 전이구조를 개발한다. 간략화된 전이구조 중 하나의 방법으로 벽체에서 기둥으로 하중이 바로 전이되는 전이구조가 개발되었다. 하지만 벽기둥 전이구조에 대한 경제적인 내진설계방법이 없기에, 이에 대한 설계법 개발 및 실험적 검증을 통해 내진설계 지침을 제시하고자 한다.

전이구조에 대한 성능설계은 지진하중에 대하여 벽체의 휨연성거동을 유도하고 연성능력이 취약할 것으로 판단되는 하부의 전이부재(기둥, 벽보)는 초과강도를 고려하여 손상을 억제하도록 하는 것을 목적으로 한다. 따라서 전이구조에 대한 지진하중은 실제 벽체의 철근배근에 근거한 벽체의 휨강도를 계산하며, 이

지진하중을 안전하게 전이구조가 지지하기 위하여 전이부재는 초과강도계수(1.25)를 적용하여 충분한 강도를 보유하도록 설계해야한다. 또한 전이구간은 응력집중이 발생하는 'D' 영역이므로, 스트럿-타이 모델을 기반으로 해석과 설계를 하였다.

반복가력 실험은 일정한 축력하에서 주기 횡하중을 가력하여 지진하중에 대한 강도와 변형능력을 검증하는 것을 목적으로 하였다. 실험체의 경계조건은 실제 전이층에서 발생할 수 있는 두 가지 극단적인 횡지지조건을 고려하였다. 첫 번째는 동일한 전이구조의 골조가 연속되어 전이골조 자체의 모멘트 저항능력으로 횡력을 지지하는 경우, 두 번째는 전이층에 강성이 큰 횡력지지구조가 존재하여 전이구조가 횡력지지구조에 의하여 횡지지되는 경우를 고려하였다. 실험체는 실험체는 실제 공동주택 전이구조의 축소된 크기이며, 실험 변수로는 경계조건, 철근비, 단면감소율, 횡지지에 따른 허용 횡변위, 초과하중 계수 적용 등으로 하였다. 벽체로부터 기둥으로 전이되는 단면변화에 따른 응력집중완화를 위한 횡철근 상세, 수직철근절곡 상세 등을 적용하였다.

실험 결과는 경계조건과 관계없이 모든 실험체가 연성거동을 나타냈으며, 전이기둥을 비롯한 전이부재의 손상은 억제되어, 성능설계에서 의도하였던 내진성능을 만족하였다. 다만, 초과강도를

적용하지 않은 전이 기둥과 벽보에는 휨균열 등 일부 손상이 발생하였다. 따라서 전이구조에 대한 초과강도계수 적용의 타당성을 검증하였다. 또한 단면이 축소되는 구간(철근이 절곡되는 위치)에서 휨인장력을 받는 경우, 벽체의 설계휨강도를 만족하지 못하였기에, 이에 대한 고려사항을 설계방법에서 반영하였다. 이외에도 전이구조의 국부파괴를 방지하기 위하여 제안한 철근상세의 유효성도 확인하였다.

실험결과를 바탕으로, 전이구조에 적용할 수 있는 성능설계방법을 제안하였다. 성능설계방법은 고층 RC 구조물의 일반적인 설계방법을 고려하였다. 성능설계의 절차는 전체골조해석, 벽체설계, 성능설계를 위한 하중계산, 스트럿-타이 모델 구성방법 및 해석, 초과강도계수를 고려한 전이부재의 설계, 철근상세 지침 순서로 제안한다. 이러한 절차 안에는 설계법 적용을 위한 제한조건(단면폭 축소율, 단면의 크기, 재료강도 등), 전이구조의 벽체설계, 전이층 해석모델 및 설계하중 산정, 철근 상세 등이 제시되어있다.

주요어 : 고층공동주택, 벽기둥 전이구조, 성능설계, 스트럿-타이 모델, 반복가력실험

학 번 : 2021-27166